THE COMMUNICATIONS TECHNOLOGY SATELLITE AND ITS 14/12 GHZ FREQUENCY TRANSLATOR

by

John A. Tzevelekos

MAJOR TECHNICAL REPORT

IN

THE FACULTY

OF

ENGINEERING

Presented in Partial Fulfillment of the Requirements for
the Degree of Master of Engineering at
Concordia University
Montreal, Canada

MARCH 1976

ABSTRACT

JOHN A. TZEVELEKOS

THE COMMUNICATIONS TECHNOLOGY SATELLITE AND ITS 14/12 GHZ FREQUENCY TRANSLATOR.

The purpose of the present study is to present the Communications Technology Satellite (CTS) and its 14/12 GHZ frequency translator (mixer) which is one of the advanced technology units of the experimental high powered spacecraft.

By presenting this study on the above subject the author's intention is to fulfil two objectives. Namely, to convey to a person of little engineering background in the satellite communications field the general concept of the CTS system, and secondly to provide a reader who has a deeper satellite engineering knowledge, with a brief of valuable information concerning the performance of the frequency translator of the CTS Transponder.

To fulfil the above objectives the subject is treated as follows: Chapter I presents a brief history of communication satellites and the needs that led to the development of the CTS satellite system. The capabilities of the CTS and its Super High Frequency (SHF) Transponder (radio repeater), are described in Chapter II and III respectively. Chapter IV presents the theory of frequency translation and different microwave mixing systems to prepare the reader for the subsequent analysis of the CTS Transponder's frequency translator. This analysis is presented in Chapter V. The study ends with the presentation of conclusions and recommendations of the present system's performance relative to possible future attainable performances.

ACKNOWLEDGEMENTS

The author wishes to express his gratitude to Dr. K. Feher, for suggesting this project and for supervising this study.

In addition, I would like to thank RCA Ltd. and the Communications Research Centre (CRC) for their permission to use this report as a Major Technical Report to be submitted to Concordia University in partial fulfilment of the requirements for the degree of Master of Engineering.

Thanks are also due to my wife, Olga, for putting up with me during the preparation and writing of this report.

I would like to take the opportunity to thank my parents, Andreas and Evangelia, for the encouragement they have given me throughout my studies.

March 1976

John A. Tzévelekos

TABLE OF CONTENTS

LIST OF FIGURES

LIST OF TABLES

GLOSSARY

AM	-	Amplitude Modulation
ATS	-	Applications Technology Satellite
BP	-	Band Pass Filter
CTS	-	Communications Technology Satellite
CW	-	Continuous Wave
C_j	-	Junction Capacitance of a Diode
DC	-	Direct Current
DUT	-	Device under Test
dB	-	$10\log_{10} \frac{\text{Power } P_1}{\text{Power } P_2}$
dBw	-	$10\log_{10} \frac{P_1 \text{ in watts}}{P_2 = 1 \text{ watt}}$
dBm	-	$10\log_{10} \frac{P_1 \text{ in milliwatt } (10^{-3} \text{ watt})}{P_2 = 1 \text{ milliwatt } (10^{-3} \text{ watt})}$
EIRP	-	Effective Isotropic Radiated Power
FM	-	Frequency Modulation
FETA	-	Field Effect Transistor Amplifier
F_o	-	Noise Figure
FSK	-	Frequency Shift Keying
GHz	-	10^9 cycles/second
G_s	-	Antenna Gain
GFEC	-	Graphite Fiber Epoxy Composite
IMD	-	Intermodulation
KW	-	1000 watts
KHz	-	1000 cycles/second
LMSR	-	Liquid Metal Slip Ring

LP	-	Low Pass Filter
L_c	-	Conversion Loss of the Mixer
L.O	-	Local Oscillator
mW	-	10^{-3} watts
MHz	-	10^{6} cycles/second
mlb	-	millipound, 10^{-3} pounds
nsec	-	10^{-6} seconds
P_s	-	Transmitter Power Output
PCM	-	Pulse Code Modulation
PM	-	Primary Mode of the Transponder
RPM	-	Revolutions per Minute
RB_1	-	Receive Band 1
RB_2	-	Receive Band 2
RP_1	-	Receive Port 1 of the Transponder
RP_2	-	Receive Port 2 of the Transponder
RF	-	Radio Frequency
R_j	-	Junction Resistance of a Crystal Diode
R_s	-	Series Resistance of a Crystal Diode
SHF	-	Super High Frequency
SA	-	Spectrum Analyzer
SM	-	Secondary Mode of Operation of the Transponder
TWTA	-	Travelling Wave Tube Amplifier
TV	-	Television
TDMA	-	Time Division Multiple Access
TB_1	-	Transmit Band 1
TB_2	-	Transmit Band 2
TP_1	-	Transmit Port 1 of the Transponder
TP_2	-	Transmit Port 2 of the Transponder

TDA	-	Tunnel Diode Amplifier
t_{gr}	-	Group Delay
t_{ph}	-	Phase Delay
UHF	-	Ultra High Frequency
VSWR	-	Voltage Standing Wave Ratio
ω_{IF}	-	Intermediate Frequency or IF
ω_o	-	Local Oscillator Frequency
ω_s	-	RF (Radio Frequency) Signal Frequency

CHAPTER I

INTRODUCTION

In the last few years the art of telecommunications has made great advances which were previously considered impossible. The main credit rightfully belongs to the advances in the field of science and technology. But if a single factor could be selected as having made the greatest contribution to these advances, it would be the art of satellite communications which is the outgrowth of developments in two main areas: space technology and communications technology.

Communication satellites are described as radio relay stations in the space. This description is a simplification and does not give the major characteristics of satellite systems and the main differences between satellite and terrestrial systems. A satellite system comprises both a satellite and associated earth stations. The system design must be based upon optimization of the overall technical and economical factors. Some of the main characteristics of a satellite communication system are: capacity, flexibility and the capability of providing interconnections over very large distances, and to cover wide areas of the surface of the earth at a low cost. Through a single satellite communications system it is possible to serve multiple routes, in addition to point-to-point communication, and reallocating channel capacity among these routes. This is not

possible with terrestrial links which interconnect only two points.

The satellite systems provide capacity not only for the simultaneous use of many channels for traditional services like telephony, telegraphy, etc., but also can provide broadband services. This has been proven by overseas television transmissions previously impossible, because they could not be handled through terrestrial systems. Note that one voice circuit theoretically requires 4 kc/s of bandwidth, while television transmission requires 6 Mc/s of bandwidth. The limited operational life-time of satellites which ranges from five to ten years is one of the disadvantages compared with terrestrial systems. The situation will change in the future if repairs on satellites in orbit become possible.

1.1 Brief History of Communication Satellites

The history of satellite communications starts with the suggestion, first made by an Englishman, Arthur C. Clarke, that an artificial satellite could be used to link distant points on the earth's surface, acting as a relay station at thousands-of-miles altitude. In October, 1945, Clarke pointed out that "radio towers" into a satellite orbit would make available the use of centimetric waves, which with their enormous traffic-handling capacity will lead to the possibility of global television services. He also suggested that three such stations, if established 22,300 miles (35,000 km) above the equator with 120° spacing, could cover about 90% of the earth's surface.

Starting with the remarkably precise forecast by A. C. Clarke, the communications satellite technology can be acquired through the identification of three distinct periods of its development. In the first period, which lasted some twelve years, nothing really happened, except

that the first attempts at space communication were made, not with man-made objects but with the moon as a reflector (passive communication satellite). The historic demonstration took place on May 15, 1959 when special radio transmissions were transmitted from England and received clearly at the United States about 2.6 seconds later. Only in the second period, from 1957 to 1964, were man-made satellites actually used for communication purposes. This period was characterized by many launches of space vehicles among which a variety of communication satellites like ECHO I (August 1960), TELSTAR (July 62), RELAY (December 62), etc.. ECHO I, a 100-foot balloon of aluminised mylar polyester, is a so called passive satellite. It was designed to provide radio-wave reflectivity of at least 98% with frequencies of up to 20,000 MHZ. TELSTAR and RELAY are both active repeater satellites for reception, amplification and retransmission of messages received from earth. Both were used for international wideband communications, including television transmissions.

The launches of the INTELSAT I, Early Bird, in 1965 (240 telephone circuits) and the first MOLNIYA satellites started the third period, which can be called the operational phase of satellite communications. While the western world used satellites for international, world-wide communications, the U.S.S.R. was first in using them extensively and effectively for domestic purposes. Between the recent major events are the launchings of INTELSAT II in 1967 (240 circuits), INTELSAT III in 1968 (1,200 circuits), INTELSAT IV, IV-A in 1971 and 1975 with 3,000 and 6,000 circuits respectively; also the launchings of the Canadian ANIK I, II, III satellites in Nov. 1972, April 1973 and 1975 respectively and the RCA domestic satellite in December 1975 which contains 24 channels operating in the 4/6 GHZ band, each with a bandwidth of 36 MHZ.

There are at present, two different types of systems by which satellites are so positioned: 'Synchronous or stationary or the 24-hour orbit' and 'random orbit'. A satellite placed in synchronous orbit will appear to hang motionless in the sky. The major characteristic and advantage of the synchronous satellite is that it is relatively simple to keep the antennas at the sending and receiving earth stations properly pointed at the satellite. Satellite in random orbit will be simultaneously visible to any given pair of earth stations for only a portion of each day and to provide continuous communications more than one satellite would be required, and the earth stations have to be equipped with very advanced electronic and mechanical equipment in order to keep the antennas constantly pointed in the direction of the satellite.

1.2 The Future of Satellite Communications

Satellites in existing systems generate relatively low effective power, in part because of payload limitations of launch vehicles and in part because their power is not focusing in a single direction. Because of that, costly earth stations are needed and as a result the early satellite systems have been point-to-point communication systems. Another system, called distribution satellite system, provides stronger signal to a smaller region of the earth than in the previous case. Quite a different pattern of use will be introduced with the broadcast satellite systems. In this case, radio and especially television programmes transmitted from an earth station to a powerful satellite would be broadcasted from the sattellite for direct reception by individual modified or ordinary home receivers. Such broadcasting would require a high on-board satellite power which

poses certain technical difficulties, and the satellite would be so heavy as to require powerful expensive boosters, better power sources in the satellite, extended life time, stabilized position control, greater antenna directivity, and greater channel capacity. Of course, the direct broadcasting into home receivers on an operational basis is not foreseen for the next decade.

The single channel per carrier (SCPC) system is one of the optimum satellite communication systems between many small earth stations. Its ability to provide facsimile, high-speed data, and voice circuits of good quality is expected to result in increasingly rapid growth in the number of applications.

The next most significant change in communication satellites will occur when they will change from functioning as mere repeaters to functioning as orbital switchboards. On board satellite switching coupled with time division multiplexing (TDM), and time domain multiple access (TDMA), will result in further substantial increases of satellite capacity by utilizing the bandwidth more efficiently. The use of spectral regions above 10 GHZ, the frequency reuse, and advanced modulation schemes will lead to communication capacities progressively higher than those presently available.

Since there is a direct relation between the satellite and earth station the more powerful the satellite, the simpler, smaller and less expensive the earth stations. This, in part, led to the development of the present experimental high-powered CTS system operating in the new 14/12 GHZ frequency band allocated for the next generation of communication satellites. The CTS is the world's most powerful technology satellite and it is the forerunner of a new series of high-powered orbiting transmitters.

It will be able to provide medical information to doctors and nurses in remote areas, long distance teaching, television and radio signals to small portable ground stations and a range of other sophisticated services. It will also be used for space communication experiments to be undertaken jointly by Canadian and American scientists.

1.3 The Frequency Translator (Mixer)

To convey intelligence, the transmitted electromagnetic energy at microwave frequencies must be modulated. The intelligence is extracted at the receiving end by a process of demodulation. The mixer or frequency translator is part of the receiver front end for every communication system in existence that transmits intelligence from one point in space to another.

In the early days of microwaves, when no low noise amplifiers at those frequencies were available, it was necessary to receive signals either by direct detection or by mixing. Since direct detection was so insensitive, very early in the development of the radio communications, the superheterodyne concept was invented. With this concept we shift or translate the modulation, from all desired incoming signals to this new, fixed "Intermediate frequency" or IF.

Conventional microwave mixers operate with a local oscillator frequency which differs from the signal frequency by approximately 30 to 60 MHz. With the IF frequency in the 30 to 60 MHz region, low noise amplification, by means of conventional methods, is possible. By maintaining the IF frequency and bandwidth constant, it is much easier to achieve good selectivity over a relatively wide input frequency range.

In addition to the conventional low frequency IF mixers, there are devices where the signal and local oscillator frequencies combine to generate a resultant frequency in the microwave region of the spectrum. These mixers are characterized by high input return loss (low input VSWR), low overall noise figure, and low conversion loss.

The frequency translator of the CTS transponder, which in part is the subject of this report, translates the uplink 14GHz signal frequencies to the downlink 12GHz signal, using a local oscillator frequency of 2.1667 GHz, and it has the above characteristics.

CHAPTER II

COMMUNICATIONS TECHNOLOGY SATELLITE (CTS)

2.1 INTRODUCTION

The Communications Technology Satellite (CTS) is an experimental high-power satellite. The CTS is part of a joint Canada/United States space technology project. The prime goal of the high-power CTS is the advancement of technology for future generations of high power communication satellites.

Efficient utilization of satellites for communication systems requires the generation of high signal levels in the satellite in order that ground terminals can be made as small and simple as possible. By making the earth terminals small and simple the cost is low and this is a very important factor when a large number of earth terminals access or use a given satellite. Output power of the present generation of communication satellites is in the range of 5 to 20 watts per channel. High powered satellites, greater than 0.5 kw, require accurate 3-axis stabilization and station-keeping, use of large deployable solar cell arrays, and the development of travelling wave tube amplifiers (TWTA's) of significantly greater output power and efficiency than those currently space proven.

The generation of high signal power in the CTS is accomplished

through the use of large solar cell arrays, as the source of prime power, a 12 GHz TWTA having greater than 50 per cent efficiency at a power output of 200 watts and narrow beam antennas.

The CTS is expected to produce advances in the field of spacecraft communication systems by operating at the newly allocated broadcast frequencies of 12 and 14 GHz, and by significantly increasing radiated power levels over those provided by existing or project approved spacecraft. The frequency range of 12 and 14 GHz was selected because it is not crowded and large bandwidth is available. The increased power capability of the CTS is illustrated in Figure 2.1 which shows the historical growth of the Effective Isotropic Radiated Power (EIRP) with time.[1] EIRP is a term that has been found convenient for use in describing the power radiated from a terminal and is given by the product of the transmitter power output P_s and the antenna gain G_s, $EIRP = P_s \cdot G_s$, or in decibels $EIRP = P_s + G_s$. For example, a satellite transponder with a 20 watt final amplifier and an antenna with a gain of 10 dB would have an EIRP of 200 watts or 23 dBW. For the CTS transponder with 200 watt amplifier and an antenna gain of 37 dB, has an EIRP of 1,000,000 watts or 60 dBW.

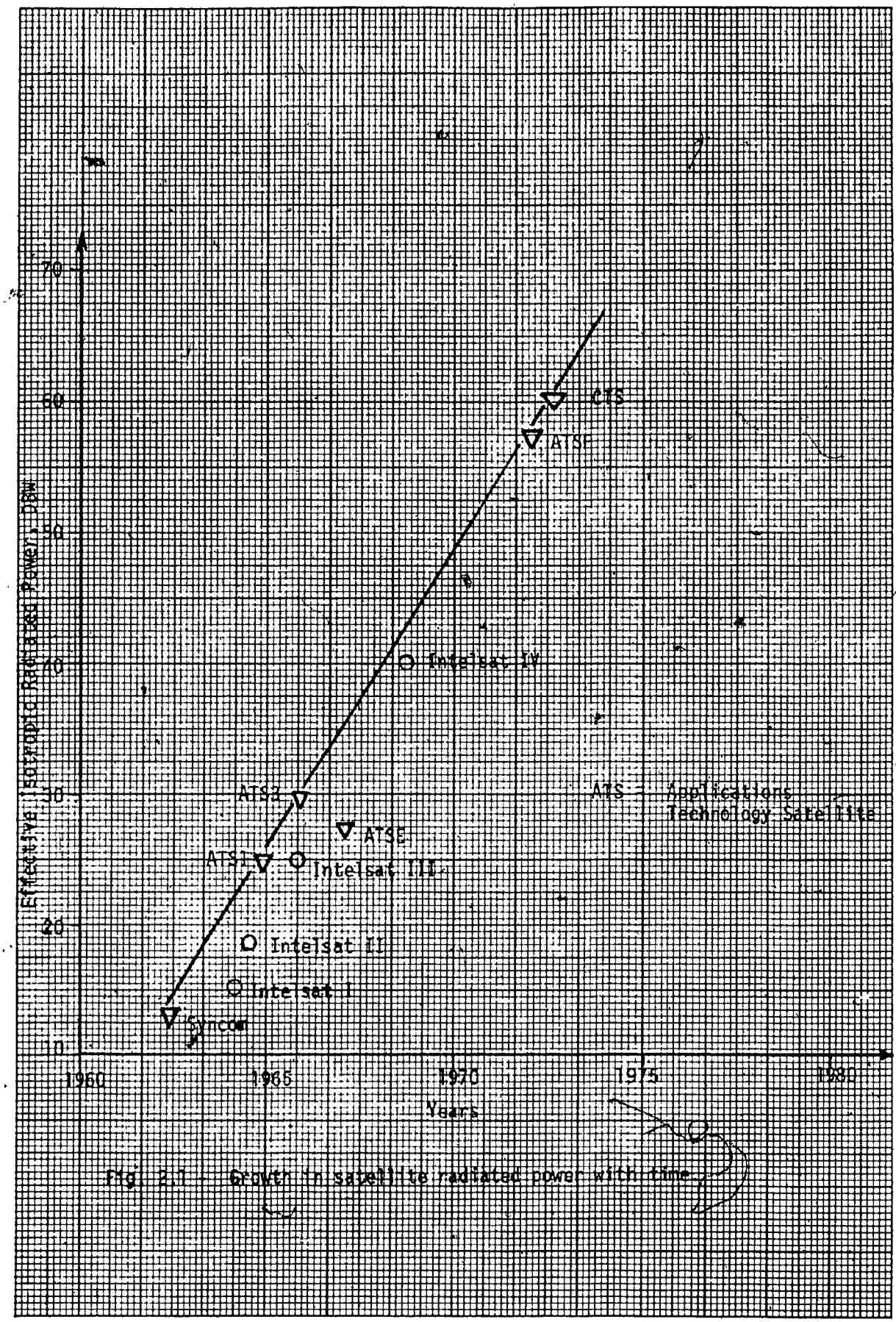

Fig. 2.1 - Growth in satellite radiated power with time

2.2 Launch of the CTS and Technology Experiments

The CTS began its planned two-year mission on January 17, 1976, when a Delta 2914 launch vehicle launched it into synchronous orbit at an altitude of 22,000 status miles. The period T, which is the time required for a complete revolution of a satellite around the earth in synchronous orbit, is 24 hours and from the earth the satellite looks stationary. The launch procedure involves two phases as shown in Figs, 2.2 and 2.3.[2]

After the CTS arrives on station and is three-axis stabilized, a flexible, lightweight solar array which is a special feature of the satellite will extend. The array consists of two sails, each about 21 feet by 4 feet. The sails are stored upon the body of the spacecraft and then deployed concertina style upon ground command as shown in Figure 2.4.[2] The array will deliver a beginning of life power of more than 1000 watts at 67 volts for the experiments, and 220 watts at 29 volts for housekeeping. Sensors, mounted on the sails, will automatically control the array steering mechanisms so that the sails will always face the sun. Two nickel-cadmium batteries will provide power during eclipse periods.

Two technology experiments, that have general application to possible future generations of high-power 3-axis stabilized communication satellites, will be conducted: one concerned with the high-power flexible solar array and the other with attitude control. The solar array experiment is designed to study the behaviour of the array during deployment, and to determine its characteristics when in sunlight and when entering and leaving the eclipse period. This experiment is also concerned with the thermal characteristics of the array, its solar cell performance, and the behavior of the deployed array under specific dynamic excitation.

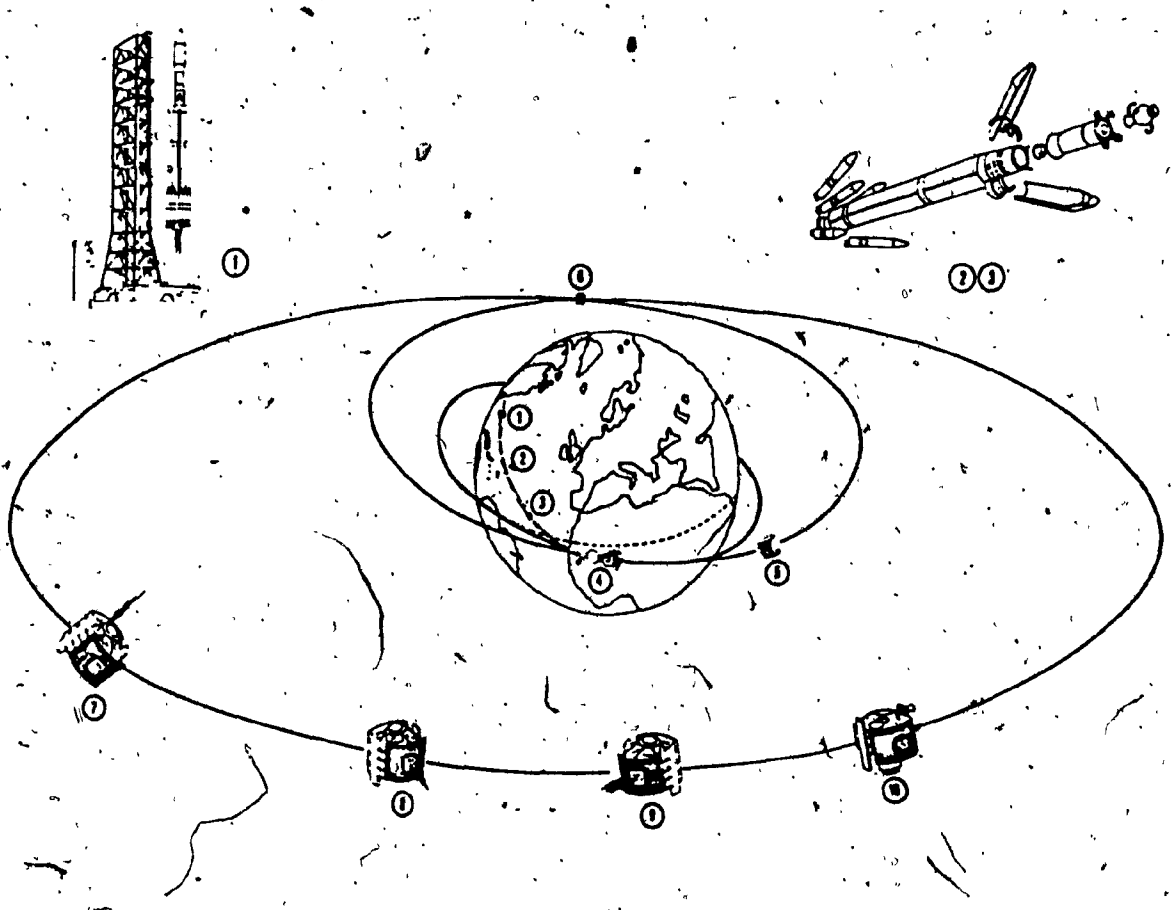

Fig. 2.2 - Launch Procedure of the CTS

(From CRC Serial Document 06-RI & PS-1, May 1973)

1 - Lift off from eastern test range (Cape Canaveral)
2 - Second stage ignition
3 - Spin-up to 60 rpm
4 - Third stage ignition
5 - Alignment of spacecraft for apogee burn
6 - Apogee Motor firing
7 - Alignment of spacecraft for positioning maneuvres
8 - Positioning of spacecraft
9 - On station
10 - Spacecraft correctly oriented.

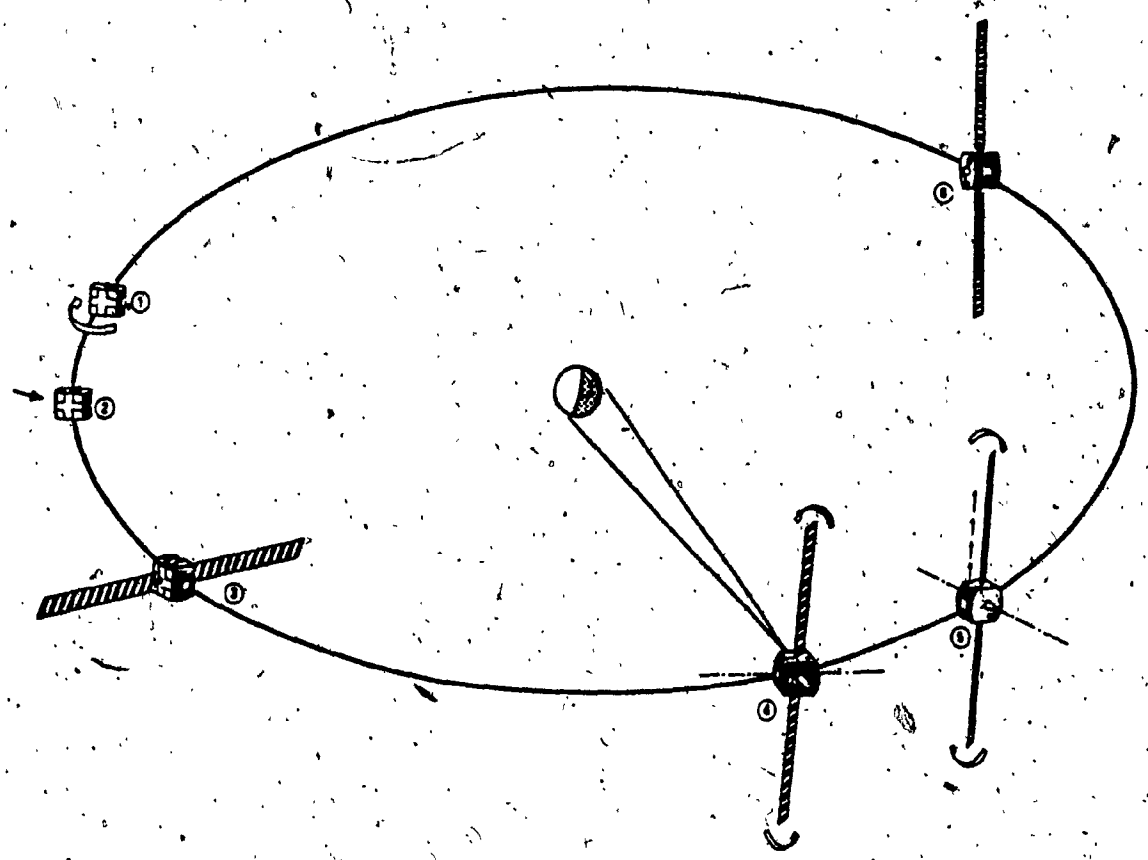

Fig. 2.3 - Attitude Control Procedure of the CTS.
(From CRC Serial Document 06-RI & PS-1, May 1973)

1 - Despin from 60 rpm

2 - Stop rotating with sun sensor pointing to sun

3 - Deploy solar arrays to supply power

4 - Roll about spacecraft sun-line to lock on earth with non-spinning earth sensor

5 - YAW manoeuvre about spacecraft earth-line using sun sensor data to align roll axis with orbited velocity vector

6 - Spacecraft operational; attitude determined by earth sensor and sun sensor.

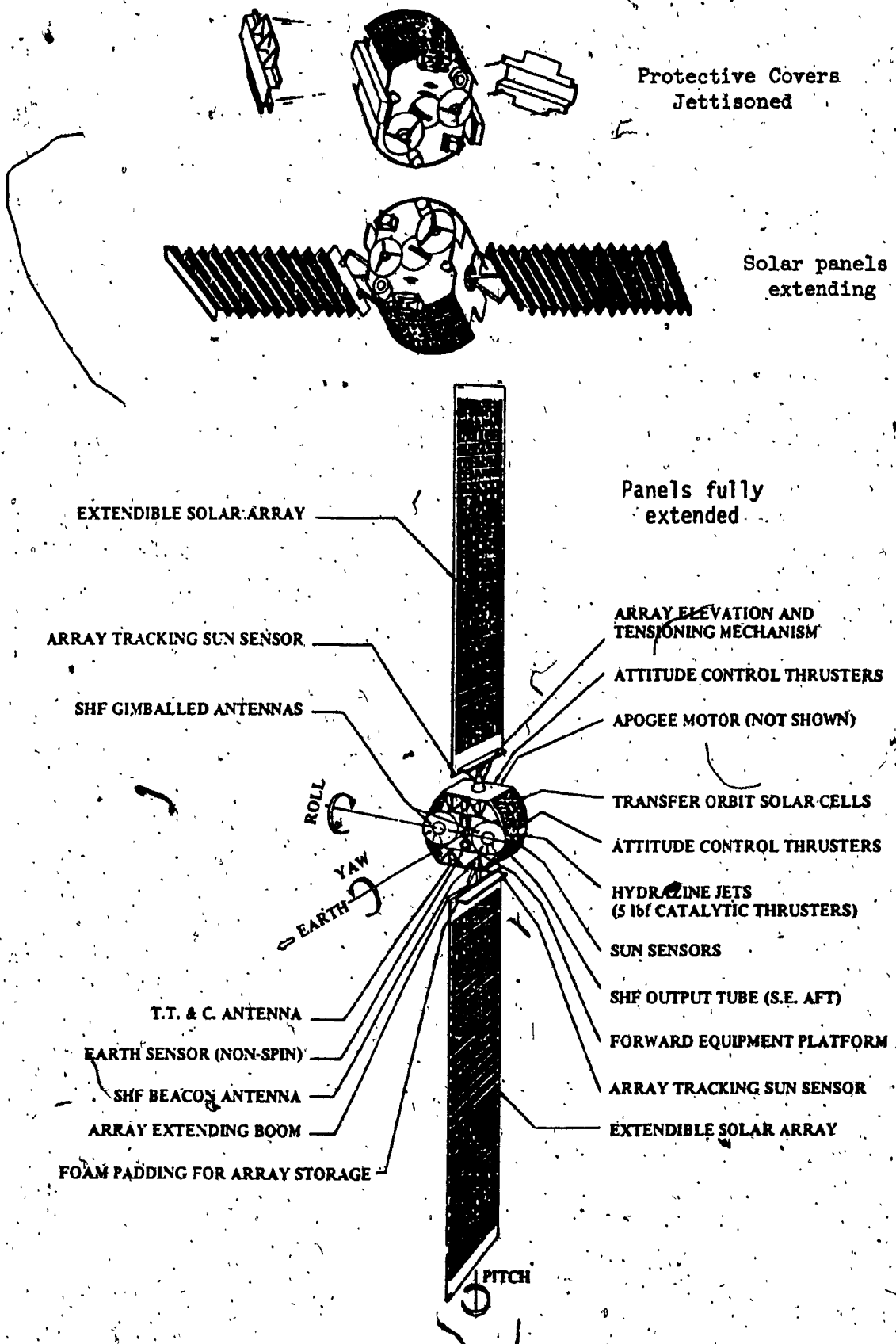

Fig. 2.4 - Array deployment and spacecraft details on station. (From CRC Serial Document 06-RI & PS-1, May 1973).

Sensors, mounted on the array, will measure acceleration, deflection, tension and temperature. The attitude control experiment will provide telemetered data on spacecraft stabilization and control during the attitude acquisition and on-station phases of the mission. This experiment includes studies to determine the solar-torque magnitude and the effects of the space-craft flexibility on the operation of the attitude control.

Other experiments, where failure is not detrimental to the planned mission, are: a) a 0.4 mlb 5-cm mercury bombardment ion thruster (engine) for north-south stationkeeping and attitude control experiment and b) a liquid metal slip ring (LMSR) experiment. The LMSR experiment involves the investigation of the characteristics of low friction liquid metal slip rings with features that permit the study of both high-voltage effects in excess of 2,000 volts, and high-current effects at greater than 4 amperes per ring. The liquid metal to be uses is Gallium.

The command signals will be in a PCM/FSK/AM format. The command code bit rate will be 700 bits per second and the synchronization is accomplished by amplitude modulating the subcarrier at the bit rate frequency. The telemetry system is specified as PCM/FM/PM in which pulse code modulation (PCM) frequency modulates an FM subcarrier oscillator which, in turn, phase modulates the transmitter. The PCM bit rate is 1536 bits per second with 192 eight bit words per frame. Two sampling rates are provided; one sample per second, and one sample per 32 seconds.

2.3 Communications Capability of the CTS

Two 28 inch diameter antennas with paraboloid reflectors will be gimbal-mounted on the forward (earth-oriented) deck. The 3-axis stab-

bilization system will maintain antenna boresight pointing accuracy to 0.1^{o} in PITCH and ROLL, and 1.1^{o} in YAW on a spacecraft with flexible appendages. As shown in Fig. 2.5 each antenna provides a single 2.5^{o} beamwidth of circular cross-section for the simultaneous transmission and reception of orthogonal linearly polarized signals. A wave is said to be linearly polarized if its electric field vector lies always in a given direction. Each antenna can be steered independently to cover different parts of Canada and United States (including Alaska and Hawaii) to support various CTS communication experiments.

Figure 2.6 shows the antenna coverage obtainable for various boresight positions of the antenna from a synchronous orbit position of 116^{o} west longitude. The inner contour shows the effect of coverage constraints resulting from positioning and pointing errors. The outer line of each pattern shows the nominal 3 dB antenna contour. With each antenna capable of being positioned on ground command with its boresight anywhere within a 15 degree cone, an EIRP capability of up to 60 dBW is to be provided as noted in Figure 2.1.

The CTS transponder, which is essentially a Radio Repeater, receives a signal at 14 GHz, amplifies and frequency translates it to 12 GHz and then broadcasts the processed signal. The communication capability is, of course, bounded by the combination of powers and bandwidths available. In the primary operating mode (see Chapter 3, para. 2 for operational modes), a mixture of an FM colour TV signal, an FM sound broadcast signal, and up to ten channels of duplex voice signals can be transmitted simultaneously from the main terminal to a variety of remote terminals. At the same time it is possible to transmit a colour TV signal from the remote transmission station to the main terminal via the transponder.

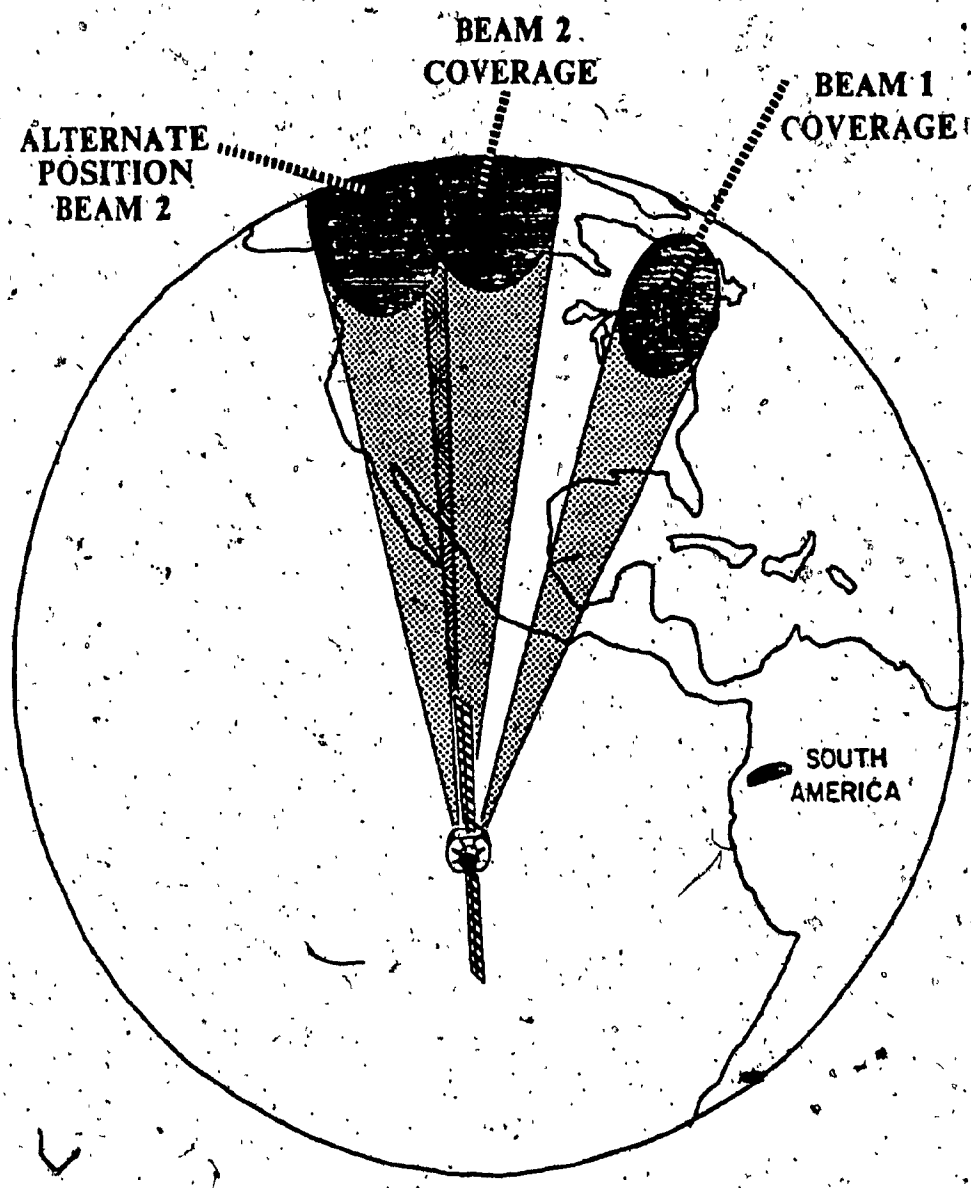

Fig. 2.5 - Typical Beam Coverage Areas

(From CRC Serial Document 06-RI & PS-1, May 1973)

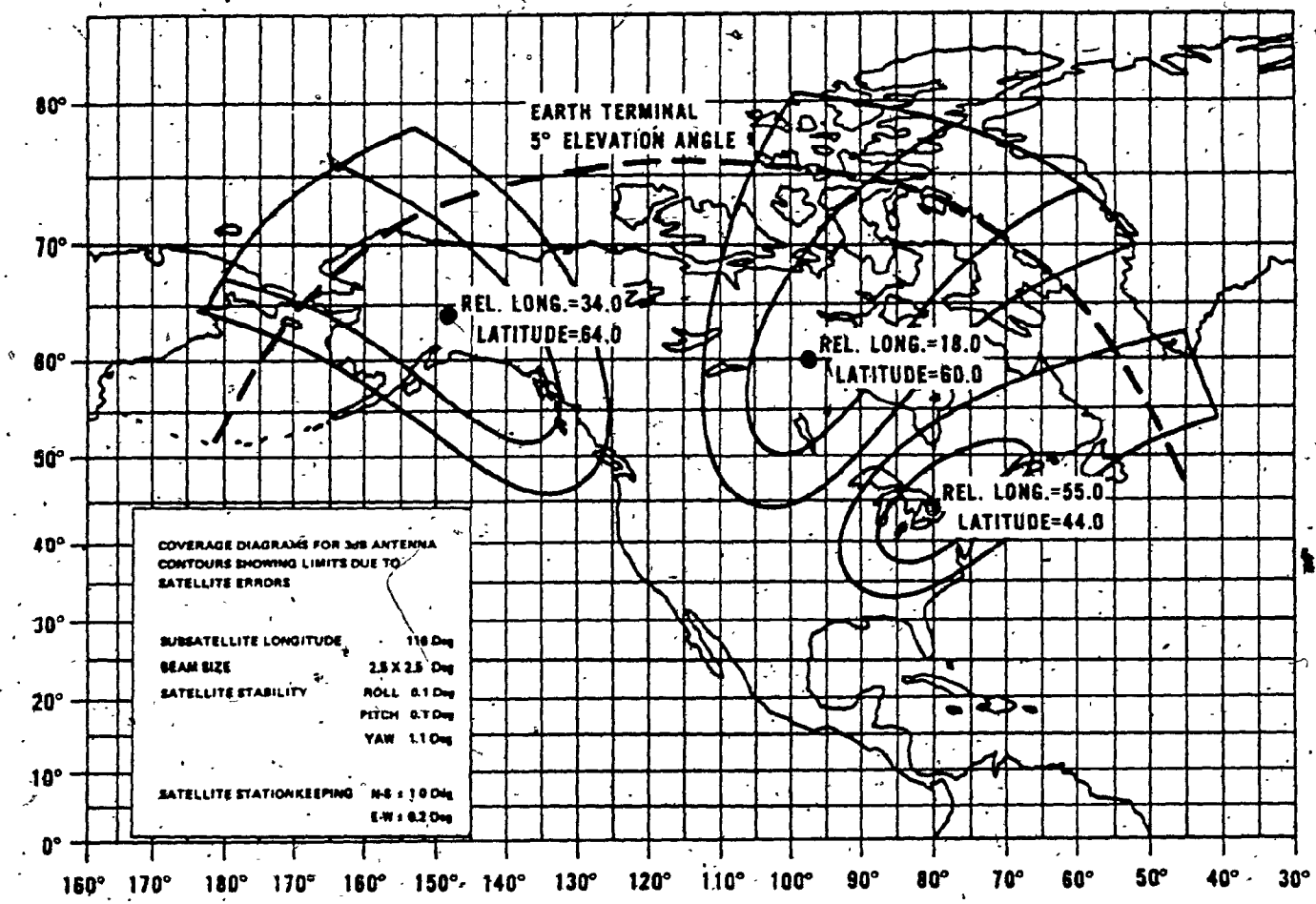

Fig. 2.6 - Super high frequency (SHF) antenna coverage patterns for CTS at 116° degree west longitude. Inner line for each pattern shows reduction in coverage due to spacecraft pointing errors.
(From CRC serial Document 06-RI&PS-1, May 1973).

As noted previously, the CTS will be capable of providing an EIRP of up to 60 dBW. Taking into account the attenuation for the combined effects of down-link precipitation, tropospheric fading and the path loss, the final received power at the receiver terminals of an 8 ft diameter antenna still will be capable of providing a very good colour TV video signal-to-noise (S/N) ratio. Also the power received by the Ottawa main station from the remote TV transmission terminal will provide a good network quality video S/N ratio.

2.4 Super High Frequency (SHF) Communication Experiments

Once the CTS is operational it will be used for experimental purposes equally by Canada and the United States. The major communication experiment is based on the 200 watts, 12 GHz TWTA, and one of the principle objectives of the CTS will be to demonstrate up-link TV transmission at 14 GHz from transportable terminals and TV transmission at 12 GHz from a satellite to low-cost ground terminals.

In Canada it is planned that most transmissions will take place between the main ground station at Ottawa, via a 30 foot diameter transmitting-receiving antenna, and remote terminals to the north. Terminals intended for television reception will use 8 foot diameter antennas which will allow for simultaneous reception of television and sound broadcast and multichannel voice transmission using the 200 watts channel of the transponder. System calculations showed that using all 200 watts for a single television broadcast carrier would permit the reception of a good quality picture at a receiving station using an antenna of only 4 feet in diameter.

A transportable ground terminal, using a 10 foot diameter

antenna, will be capable of transmitting television, of a quality suitable for subsequent broadcast use, from a remote site to the main Ottawa station via the 20 watts (low power) transponder channel. This will leave the main 200 watts (high power) channel available for transmission to remote terminals making possible two way television for teleconferencing applications. In addition other transportable terminals with 4 foot diameter antennas will be used for providing two-way voice communications between remote communities and other isolated parties and the main Ottawa station. In addition to the remote terminals already discussed small FM sound broadcast (receive only) terminals with fixed antennas of only 2 feet in diameter will be used.

In summary, the Canadian Communications experiments that will be carried out with the CTS are:

a) Colour TV broadcast from Ottawa to remote terminals to evaluate technical characteristics and socio-economic impact and viability

b) Colour TV transmission from remote terminals to Ottawa for network retransmission to observe impact of live TV from normally inaccessible places, or rare events.

c) Two-way voice operation to evaluate technical characteristics and utilization

d) Sound broadcast from Ottawa to 2 foot remote terminals to evaluate terminal costs, reliability, durability and assess user acceptance

e) Digital communications [Time Division Multiple Access (TDMA) and wideband data transmission] for access synchronization technique and TDMA technology; to evaluate error rates; interference effects and advances in digital modulation techniques.

Bit rate about 60 to 90 Mbits/sec are expected.

The United States' experiments are primarily aimed at testing the concept of low cost ground stations with small antennas, trading off small ground stations for high power on satellite. Most of the experiments are related to use, rather than technology. For example, the American Red Cross will test a small transportable ground station to set up emergency communications in disaster areas. The Veterans Administration will test video transmissions between hospitals, and the New York State Department of Education will test the transmission of documents to libraries throughout the United States. The only technological experiment will be run by NASA-Goddard, which will test propagation characteristics of the 12 to 14 GHz signals through rain.

CHAPTER III

SUPER HIGH FREQUENCY (SHF) TRANSPONDER OF THE CTS

This chapter deals with the transponder (radio repeater), a major subsystem of the CTS satellite. In section 3.1 a general description of the subsystem is given. The transponder gain, the output power per channel and the antenna port, to which each channel is connected, depends on the mode in which the transponder is operated. Section 3.2 presents those operational modes of the transponder. Section 3.3 presents the advanced technology units and the subsections describe the main units of the transponder.

3.1 Transponder Description

The transponder, receiver-transmitter combination, will provide amplification, frequency translation, and re-transmission of received SHF signals. The communications transponder is a multiport microwave subsystem capable of performing communication functions. The four major ports have been named as:

Receive Port 1 (RP1)
Receive Port 2 (RP2)
Transmit Port 1 (TP1)
Transmit Port 2 (TP2)

In addition, there is a secondary port, the beacon port, which interfaces with the SHF beacon subsystem. RP1 and TP1 are connected to a single

communication antenna (antenna No. 1) via an orthomode coupler to allow simultaneous reception and transmission of orthogonal, linearly polarized waves. Similarly RP2 and TP2 are connected to an identical antenna, antenna No. 2. Orthogonal, linearly polarized waves are used for better discrimination of different signals.

A block schematic diagram of the SHF transponder switched to its different operating modes is shown in Figure 3.1 a,b,c,d and is described in section 3.2. To improve subsystem reliability, all active elements in the receiver and driver stages of the transponder are redundant. In addition to this redundancy the TWTA's are configured so that failure of any one will not jeopardize the transponder operation.

The transponder has four 85 MHz pass bands, two for transmitting in the 11.7 to 12.2 GHz band, and two for receiving in the 14.0 to 14.3 GHz band as shown in Fig. 3.2. The frequency bands of the two receive channels are combined in the input multiplexer, amplified in a low noise amplifier and frequency translated to the transmit bands. Additional amplification is provided in the driver and output stages of the transponder. A signal of the proper frequency and amplitude received in port RP1 will be translated in frequency without inversion, amplified, and sent out through the port TP2. A similar process will occur for signals received in port RP2. Information received by the transponder within the receive band 1 (RB1) will be re-transmitted within the transmit band 1 (TB1) without frequency inversion. A similar process will occur for the receive band 2 (RB2) to transmit band 2 (TB2). The term "without frequency inversion" means that the received band of frequencies is above the local oscillator frequency, and an increase in the signal frequency causes an increase in the intermediate frequency.

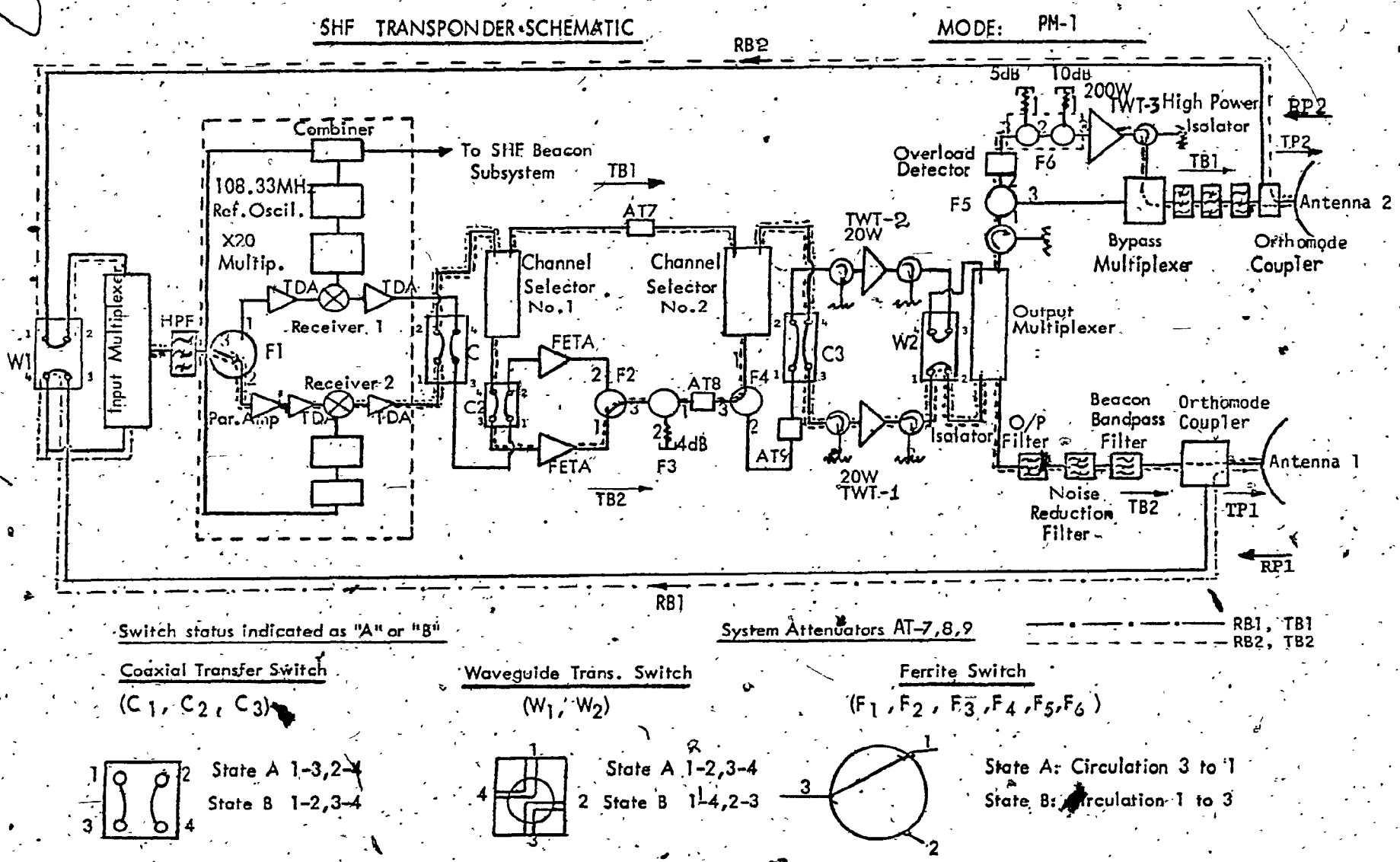

Fig. 3.1a - SHF Transponder Schematic Switched to its Primary Operating Mode 1.

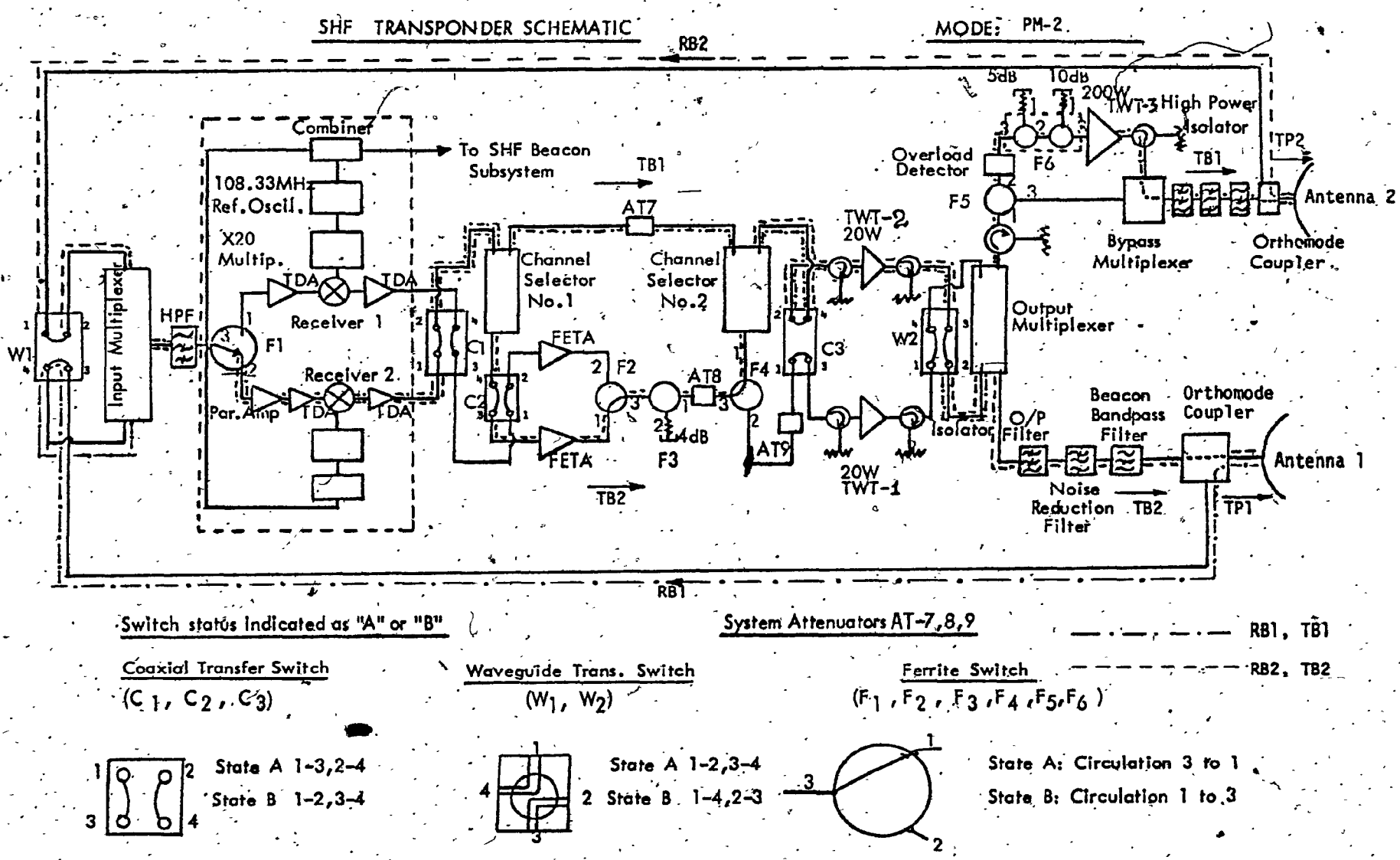

Fig. 3.1b - SHF Transponder Schematic Switched to its Primary Operating Mode 2.

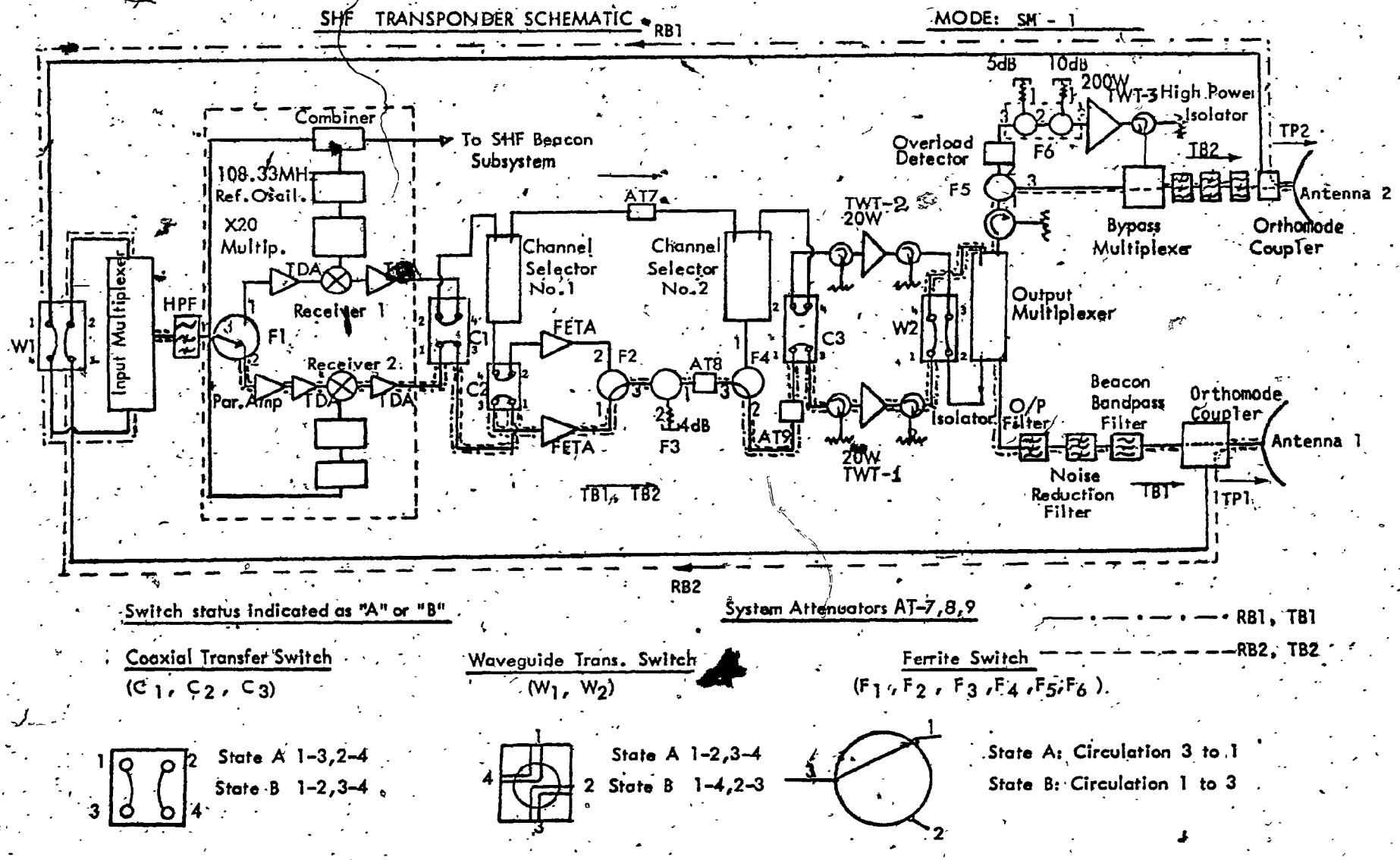

Fig. 3.1c - SHF Transponder Schematic Switched to its Secondary Operating Mode 1.

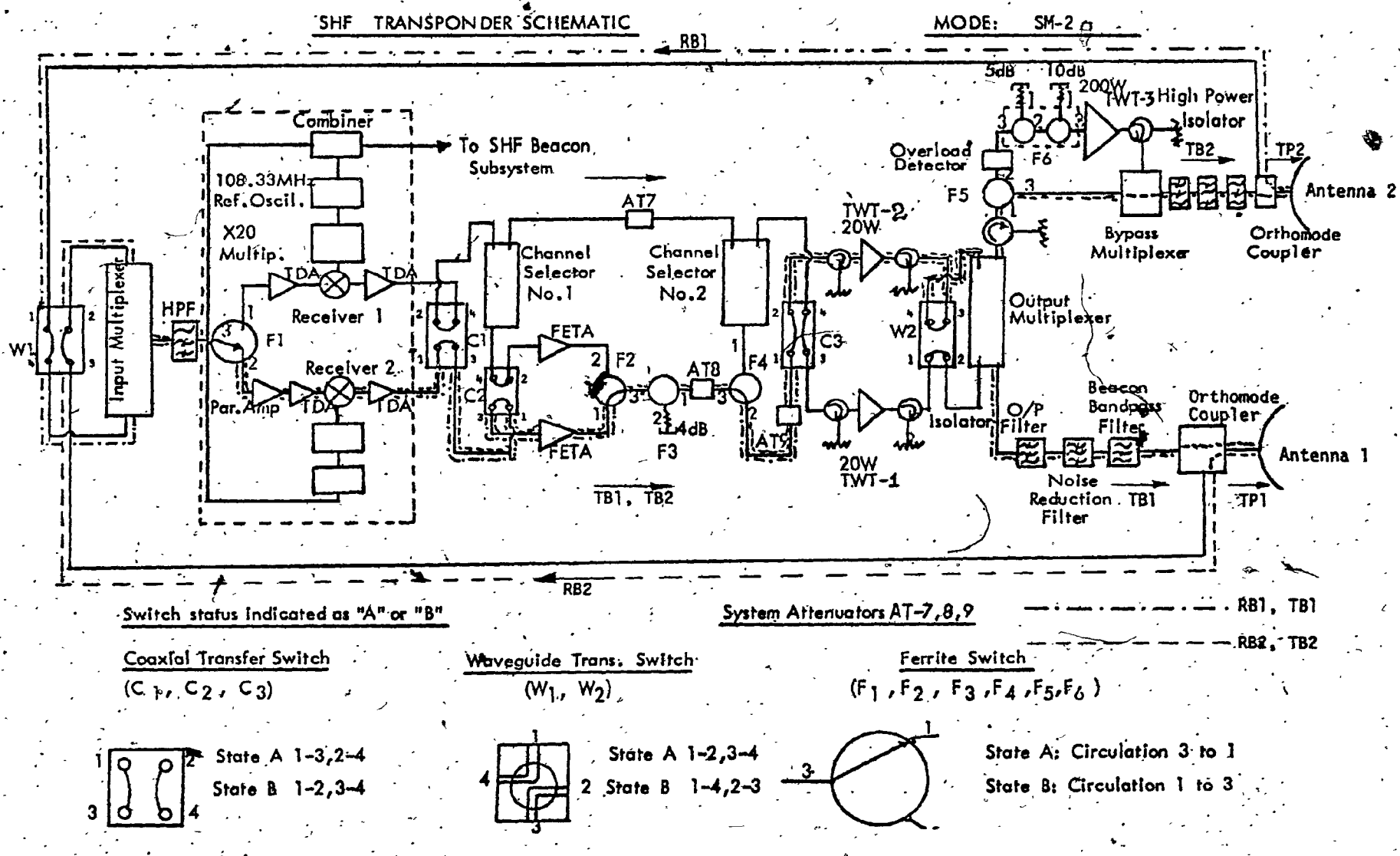

Fig. 3.1d - SHF Transponder Schematic Switched to its Secondary Operating Mode 2.

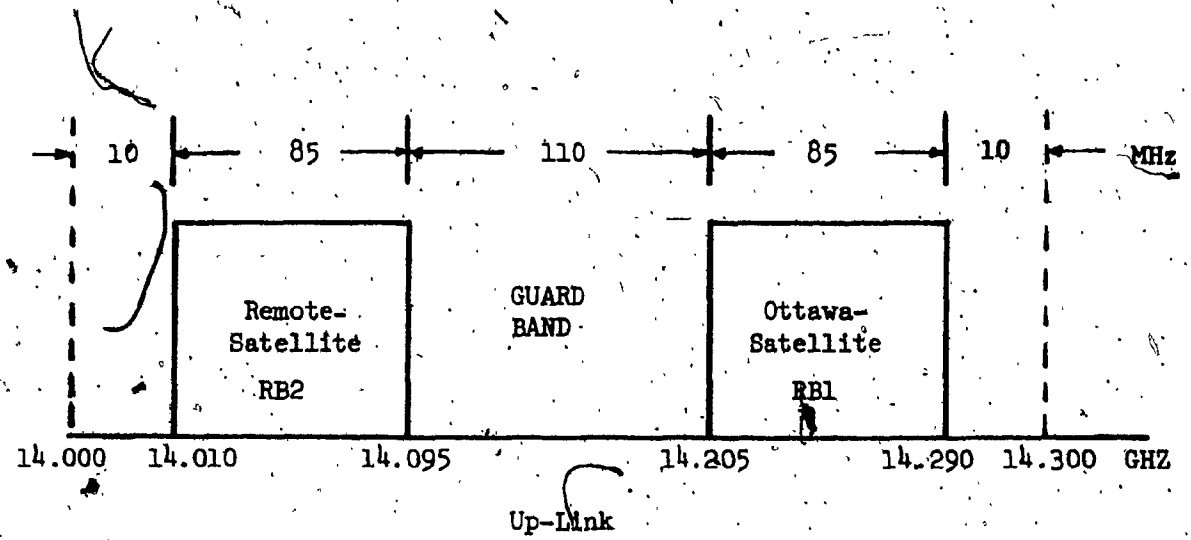

Location of Receive Bands RB1 and RB2

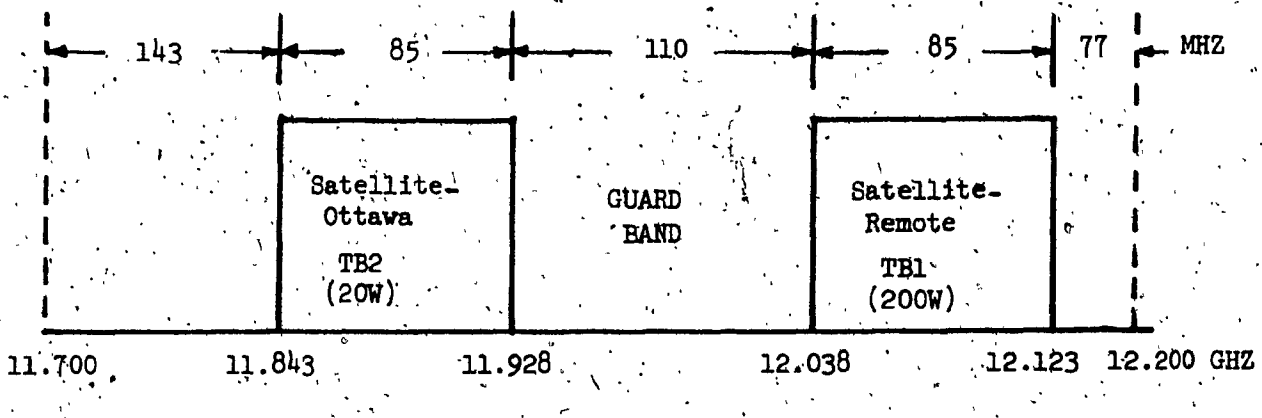

Location of Transmit Bands TB1 and TB2

Fig. 3.2 - SHF Frequency Plan

3.2 Operational Modes of the CTS Transponder

A number of microwave logic functions are included in the design of the transponder to enable experiments to be undertaken with different gains and output power levels. The mode in which the transponder is switched determines the gain, the output power per channel, and the antenna port to which each channel is connected. The transponder has two basic operating modes:

a) The primary, or normal operating mode (PM)

b) The secondary, or back-up operating mode (SM)

The PM mode will be denoted PM1 when TWTA-1 is used, and PM2 when TWTA-2 is used. Similarly for the SM mode, it is denoted SM1 and SM2. Each one of the four operational modes is described below.[3,5]

(i) Primary Operational Mode 1, Figure 3.1a: This is a bidirectional mode in which the 200 watt TWTA-3 is the output amplifier for one channel, and the 20 watt TWTA-1 is the output amplifer for the second channel. In this mode the 20 watt TWTA-1 is also used as a lower power driver amplifier for the high power channel. The Field-Effect Transistor Amplifier (FETA) is used as a driver for the lower power channel. The saturated gain for signals converted from band RB1 to band TB1, that is the high power channel, is 122 ± 4 dB. The small signal gain (-10 dB from saturation) for signals converted from RB2 to TB2, that is the low power channel, is 114±4dB.

(ii) Primary Operational Mode 2, Figure 3.1b: In this operational mode only the 20 watt TWTA-1 is replaced by the 20 watt TWTA-2, the rest is the same as in PM1 mode.

(III) Secondary Operational Mode 1, Figure 3.1c: This is a bidirectional mode in which the 200 watt TWTA-3 is switched off, and the 20

watt TWTA-1 is used as the output amplifier. In this mode the FETA acts as a driver amplifier for both channels. The TB2 band is directed to the antenna normally used by the 200 watt TWTA-3 via the bypass multiplexer. The small signal gain for signals converted from band RB1 to TB1 and from RB2 to TB2 is 114± 4 dB.

(iv) Secondary Operational Mode 2, Figure 3.1d: In this operational mode only the 20 watt TWTA-1 is replaced by the 20 watt TWTA-2, the rest is the same as in SM1 mode.

The microwave logic, necessary to ensure that the individual channels are combined and separated at appropriate points within the transponder, is provided by microwave switchers and channel selector units, as shown in Figure 3.1 a,b,c,d.

3.3 Description of the Main Units of the CTS Transponder

The transponder is designed to fulfil two basic functions:

(i) It will be used to perform a number of experiments to determine the feasibility of establishing economic, reliable communication links with very small earth terminals.

(ii) It will serve as a test bench for a number of microwave devices which represent an advance in technology over already flight proven units. The potential advantages of these units would increase from their inclusion in the next generation of communication satellites. These units are listed in Table 3.1.[3]

TABLE 3.1

ADVANCED TECHNOLOGY UNIT DESIGNS

UNIT		KEY FEATURES
1	200 watt TWTA	Direct Current (DC) to Radio frequency (RF) efficiency 50 percent
2	20 watt TWTA	Lightweight, high gain, high efficiency
3	Parametric Amplifier	Solid state pump, 300^{0}k noise temperature
4	Field-Effect Transistor Amplifier (FETA)	Low power consumption, solid state (Lightweight replacement of a TWTA driver)
5	High Power Multiplexing network	Low insertion loss, 250 watt continuous wave (CW) power handling capability
6	Wideband Frequency Translator	Low noise design with integrated low profile input and output filters
7	Graphite Fiber Epoxy Composite (GFEC) Wareguide Filters	Ultra lightweight (density = 0.053 lbs/cm^{3}) with coefficient of thermal expansion equivalent of invar

3.3.1 Input Multiplexer

The input multiplexer is a three-port device in the input microwave circuitry of the transponder. The two receive bands RB1 and RB2, which are defined in Figure 3.2, are multiplexed into one port to drive the front end of the transponder. In addition, the input multiplexer will also attenuate any leakage of the transmitted signal which is at a much higher power level than the received signal. Due to the fact that the unit is in front of the first amplifier stage of the receiver, the whole unit is constructed with waveguides to reduce insertion loss.

Two bandpass (BP) filters and a waveguide manifold form the multiplexing network for the receive bands. Schematically, the input multiplexer is as shown in Figure 3.3. An insolator is also shown in the schematic in the event it is necessary to damp out multiple reflections in this combination of units.

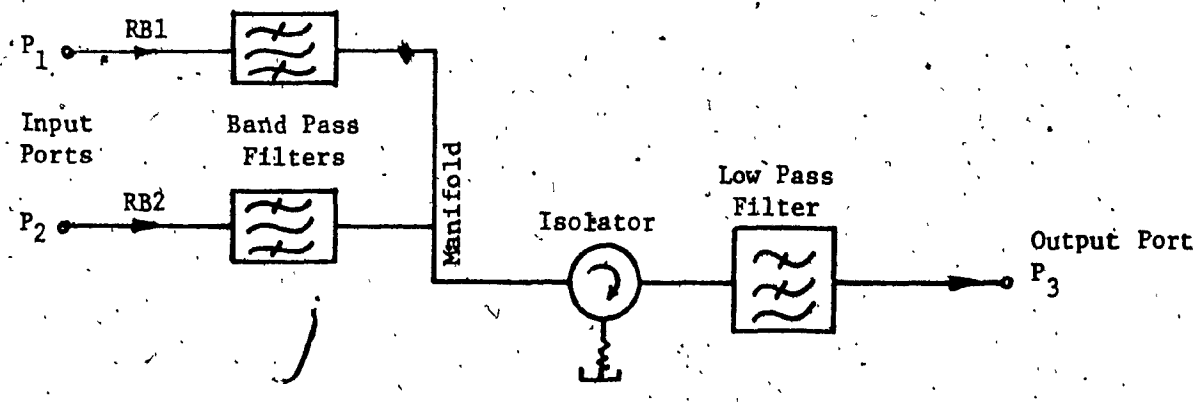

Fig. 3.3 - Schematic of the input multiplexer.

3.3.2 Low Noise Receiver

The receiver of the CTS transponder provides amplification and frequency translation of the received signals. The receiver as it is shown in Figure 3.1, consists of an input 14 GHz Tunnel Diode Amplifier

(TDA), a translation oscillator, a frequency translator and an output 12 GHz TDA. A similar redundant receiver is provided which contains, in addition, a low noise (3.3 dB) parametric amplifier.

The translation oscillator consists of a crystal controlled oscillator operating at 108.333 MHz followed by a multiplier chain which multiplies the frequency by a factor of 20 to yield 2166.7 MHz. The long-term frequency stability is one part per million over any one month. The wideband frequency translator which is an integral part of the low noise receiver will be the subject of Chapter 5. The high pass waveguide filter in front of the receiver chain provides further isolation for the transmit frequencies.

A signal combiner circuit is included in the receiver to provide the Beacon reference signal of 108,333 MHz and power level of +18 dBm. The signal is available from the translation oscillator of whichever receiver is in operation. The SHF beacon operating at 11.7 GHz will serve as a tracking aid for propagation studies and will provide a check of transponder frequency stability.

The input signal to the receiver (14 GHz) is -73 dBm and the level of the output signal (12 GHz) is -31 dBm, that is, the overall gain of the receiver is 42 dB.

3.3.3 Channel Selector No 1

The channel selector No. 1 is a passive microwave device which takes the output signals from the receiver and diplexes the two transmit bands (TB1 and TB2) into two separate ports. The unit is therefore a three port device with one input port and two output ports. The two transmit bands TB1 and TB2 are defined in Figure 3.2. Schematically, the

channel selector is shown in Figure 3.4. Three basic sub-units of one BP filter and two circulators are required to realize the device.*

3.3.4 CHANNEL SELECTOR NO 2

The two transmit bands TB2 and TB1 are to be multiplexed together to drive two TWTA's in the transponder. The diplexing of these two transmit frequency bands is accomplished in the channel selector No. 2. Thus, the channel selector No. 2 has two inputs and two outputs. One BP filter and two circulators are required to realize the device as shown in Figure 3.5.* The input port P_1 carries TB1 band only, but the input port P_4 may receive both TB1 and TB2 bands. The output port P_2 can transmit both bands TB1 and TB2 but output port P_3 can only transmit TB1 band.

3.3.5 OUTPUT MULTIPLEXER

The output multiplexer or medium power channel selector is a low loss waveguide diplexer at the output circuit of the transponder. The two transmit bands involved are again TB1 and TB2. Due to the different mode requirements of the transponder, it is necessary to have two input ports (P_1 and P_4) and two output ports (P_2 and P_3) as shown in Figure 3.6.* Either input port is capable of accepting frequencies in the two transmit bands. Deplexing is achieved within the multiplexer with the result that TB1 and TB2 are separated into the two output ports. For reasons of achieving a lower insertion loss in one of the transmit bands, the double filter passes frequencies in the TB1 band only.

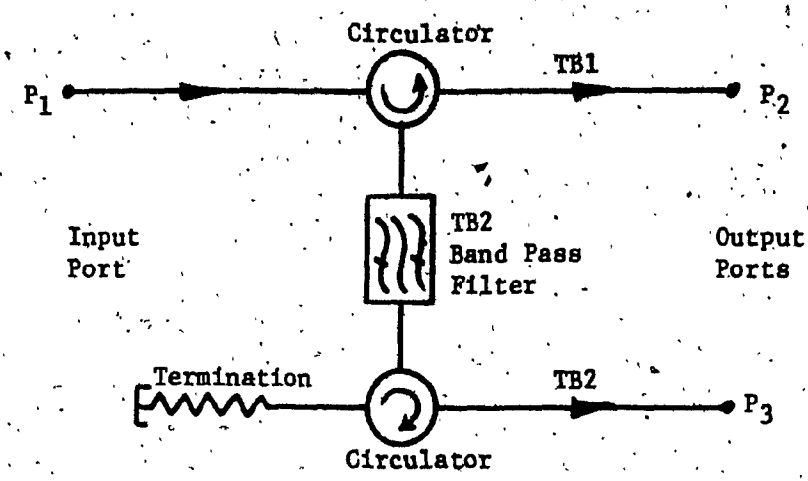

Fig. 3.4 - Schematic of Channel Selector N° 1.

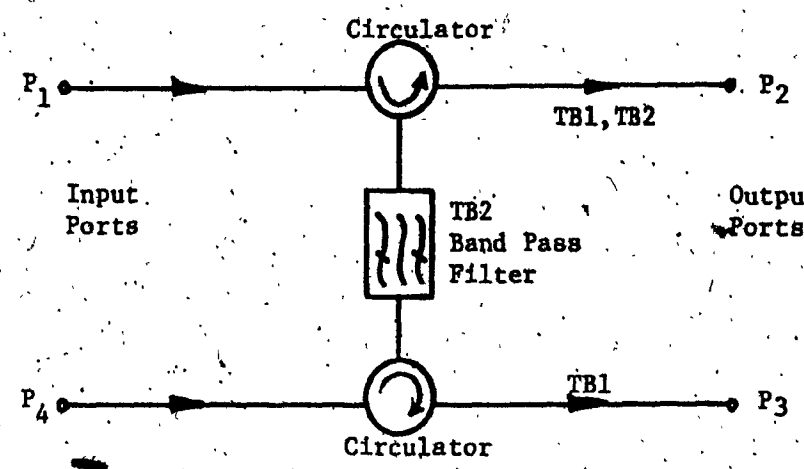

Fig. 3.5 - Schematic of Channel Selector N° 2.

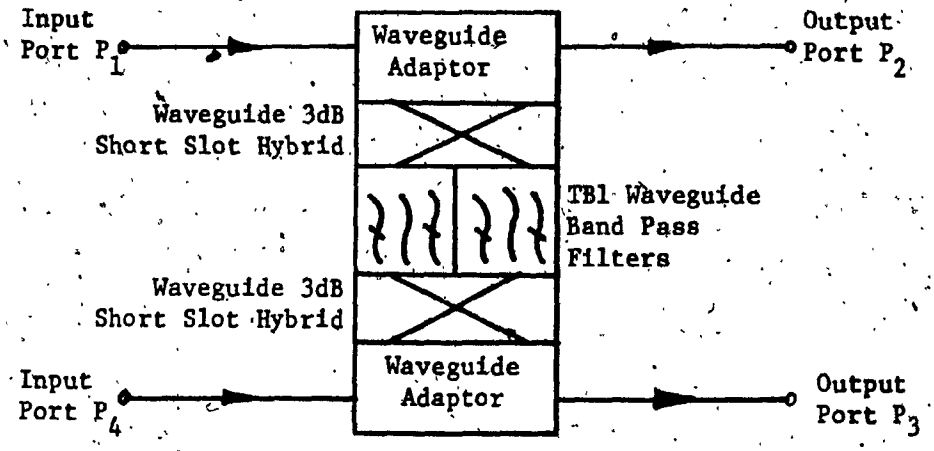

Fig. 3.6 - Schematic of the Output Multiplexer.

3.3.6 High Power Output Circuit

The high power output circuit is required to fulfil three functions:

(i) It must isolate the output port of the 200 watt TWTA from reflected power resulting from mismatches within the output circuit or at the antenna. This function is performed by the 3 port waveguide circulator with the third port terminated.

(ii) It must suppress both second harmonic power and noise power in the transponder receive band (14.0 - 14.3 GHz) generated by the 200 watt TWTA. This function is performed by the wide band output filter.

(iii) In the event of a 200 watt TWTA failure it must provide an alternate low loss path within the operating frequency band of the low power TWTA. This function is performed by the bypass diplexer.

The bypass diplexer is a three port device with two input ports and one output port as shown in Figure 3.7. The bypass diplexer enables the two transmit channels to be combined in such a manner that the insertion loss between ports 3 and 4 is less than 0.1 dB and between ports 1 and 4 is less than 0.7 dB. To achieve a lower insertion loss in one of the transmit bands (TB2) the double filter passes frequencies in the TB1 band only. The minimization of insertion loss was an important criterion in arriving at the design configuration of Figure 3.7.

Low pass-band loss and high power capability are the major design constraints used in the development of the circulator, bypass diplexer and wideband output filter.

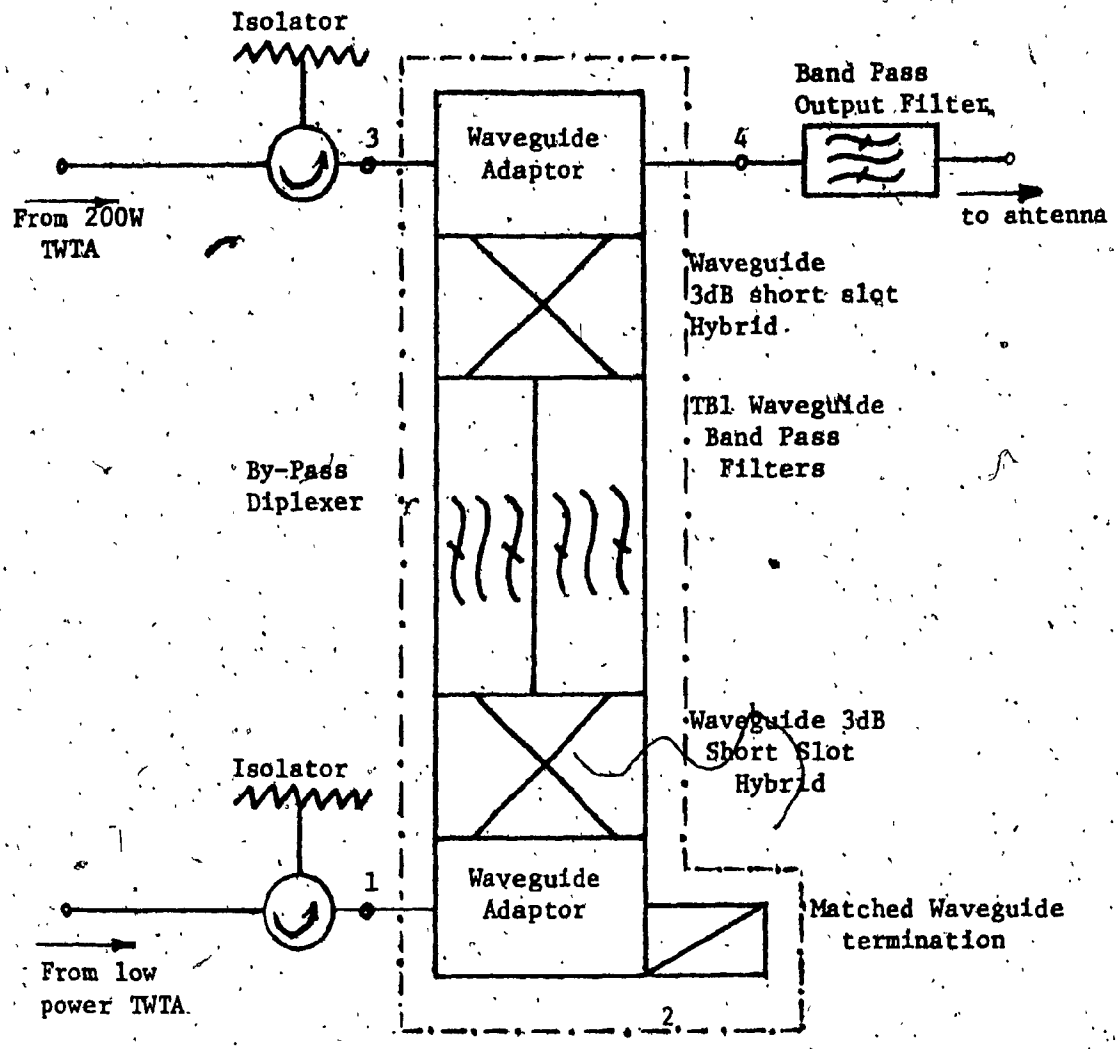

Figure 3.7 - Schematic Diagram of High Power Output Circuit.

A new lightweight, non-metalic material is used for the fabrication of the waveguide filters. This material is known as Graphite Fiber Epoxy Composite (GFEC). GFEC has about the same thermal expansion coefficient as Invar (usually used in communication satellites) but the density is 0.053 lbs/cm^3 compared to Invar which is 0.291 lbs/cm^3. Using GFEC to fabricate the filters of a multichannel transponder, the weight which is a critical factor is considerably reduced.

CHAPTER IV

THE MICROWAVE NONLINEAR FREQUENCY TRANSLATOR

This chapter provides the reader with background material in the field of frequency translation. This material is necessary for understanding the operation and performance of the CTS frequency translator (mixer) which is the subject of the next chapter. Section 4.1 presents the basic theory of frequency translation. In Section 4.2 a justification for the theory of Section 4.1 is given by using a crystal diode as the non linear element. Section 4.3 deals with the characteristics of a mixer crystal diode. In Section 4.4 the various diode parameters affecting conversion loss are discussed. The conversion loss is defined as the ratio of the available RF signal power at the input of the mixer to the available intermediate frequency output power of the mixer. Section 4.5 presents some of the diode packages which make the diode compatible with microwave circuits. Finally, incorporating the crystal diode into a circuit, it is shown that it can operate as a frequency translator. This is the subject of Section 4.6. Sub-sections 4.6.1 and 4.6.2 deal with the single diode and double diode (balanced) frequency translator respectively.

4.1 Frequency Translation

Many circumstances arise in which it is desired to translate a signal to another place in the frequency spectrum without disturbing the

relation of the sidebands to the carrier. This frequency translation is accomplished with the aid of a locally generated oscillation. The received signal together with the local oscillator (L.O) frequency is applied to a nonlinear element; for example, to a mixer diode to derive an intermediate frequency ω_{IF}, equal to the difference between the received RF signal and the L.O frequency. This ω_{IF} frequency can then be easily amplified and detected at a higher signal level.

The nonlinear device is essential in frequency translation, frequently called "mixing" process. As already stated, by the principle of superposition, the addition of two frequencies in a linear device never results in additional frequencies. If, however, the device is nonlinear, it will generate the sum and difference frequencies of the applied input signals. These new frequencies will, in turn, beat with each other and with the originally applied signals to create still more frequencies, etc., ad infinitum as shown in Section 4.2.

Let's consider a frequency translator as a three port network shown in Figure 4.1. The input RF signal power level is much lower than the L.O power level, and the generation of its harmonics is negligible. On the other hand, the mixer is nonlinear at the high L.O power (usually about 5 mW) and generates harmonics $n\omega_o (n = 2,3,\ldots)$ of the L.O frequency ω_o, which also may be important in the mixing process. In practice only the effect of the fundamental L.O frequency ω_o, and the second harmonic $2\omega_o$ are usually important since the power of the higher order harmonics is quite small.

The received signal frequency ω_s is mixed with ω_o and $2\omega_o$, producing the first and second order mixing products shown in Figure 4.2. For a very broadband circuit, a nonlinear resistor produces the sum (ω_Σ) and the intermediate frequency (ω_{IF}) with almost equal efficiency. The ω_{IF} is

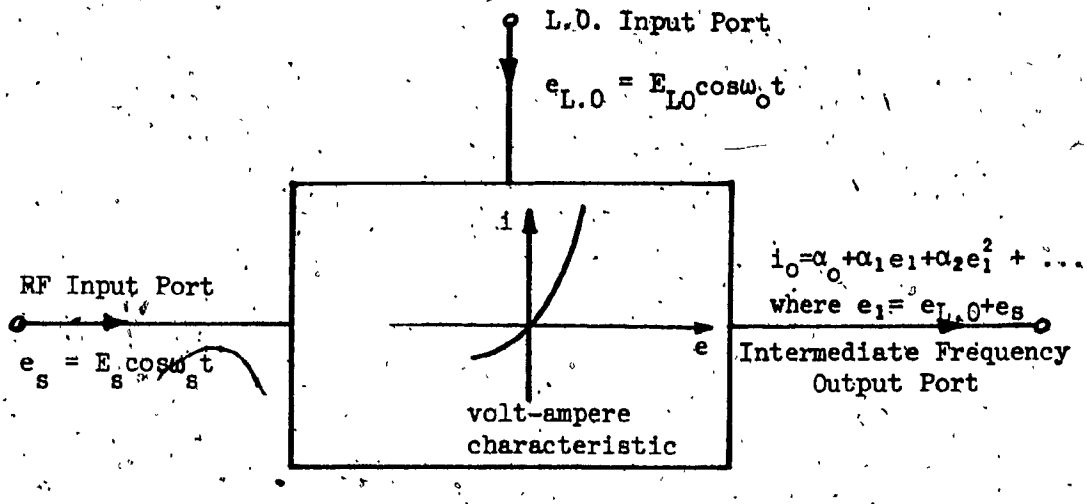

Fig. 4.1 - Block diagram of a frequency translator (Mixer).

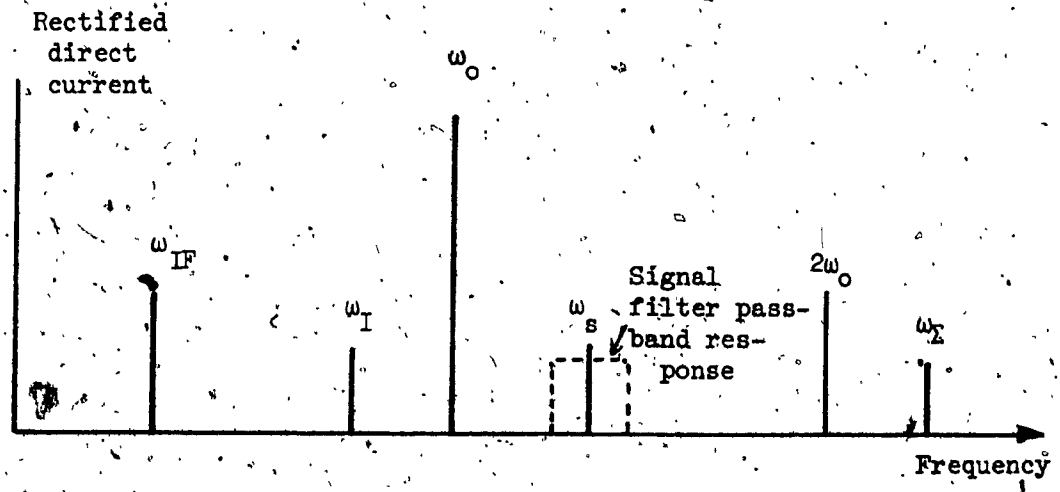

Fig. 4.2 - First and second order mixing products.

L.O frequency, ω_o

RF signal frequency, ω_s

Sum frequency, $\omega_\Sigma = \omega_s + \omega_o$

Intermediate frequency, $\omega_{IF} = \omega_s - \omega_o = \omega_o - \omega_I = \omega_\Sigma - 2\omega_o$

Image frequency, $\omega_I = 2\omega_o - \omega_s$

usually chosen to be sufficiently high so that the excess 1/f noise of the mixer diode is negligible. The image frequency ω_I is of special importance in the mixing process. The power consumed at the image and harmonic sidebands is taken from the RF signal power and the result is to increase the conversion loss of the signal to the desired output frequency ω_{IF}. By terminating these frequency components reactively, we can reduce to a minimum their power dissipation, and additional output power at ω_{IF} is obtained by the indirect path of beating them with the L.O frequency ω_o or its harmonics. In this case the conversion loss is decreased.

It can be shown[6] that the power available at ω_{IF} through the image frequency ω_I and the upper harmonic sideband ω_Σ is given by G^3P_s respectively, where P_s is the RF signal power and G is the reciprocal of the conversion loss. If we also do not consider the phase of the ω_{IF}, generated indirectly, we can say that ω_I and ω_Σ are of the same importance which is not true. The reason that makes ω_I more important is that the phase is controlled more effectively at the image frequency and that the impedance of the mixer at ω_{IF} frequency depends strongly on the termination of the ω_I but only weakly on that of ω_Σ. Hence, special attention should be paid to the image frequency and its termination in mixer design.

4.2 Crystal Diode as the Nonlinear Element of a Frequency Translator

In this section we will demonstrate the generation of all the frequencies discussed in Section 4.1, using the crystal diode as the nonlinear element. The principal characteristic of a metal-semiconductor interface of a crystal diode is that it acts as a nonlinear resistor or varistor. The resistance of a varistor is a function of the applied bias voltage across

the diode. The current i and voltage υ are related by equation (4.1) below[7].

$$I = I(\upsilon) = I_o \left[\exp q\upsilon/\eta kT - 1\right] = I_o \left[\exp a\upsilon - 1\right] \quad \ldots\ldots 4.1$$

where

$a = q/\eta kT \simeq 35\ V^{-1}$ at room temperature

I_o = diode saturation current

q = charge of an electron

T = absolute temperature ^oK

K = Boltzmann's constant

η = a constant slightly greater than unity

υ = voltage applied across the junction

For a small range about a DC bias voltage υ_o, the current-voltage characteristic given by equation (4.1) can be represented by Taylor expansion

$$i = I(\upsilon) = I(\upsilon_o) + \frac{1}{1!}\frac{dI(\upsilon_o)}{d\upsilon}(\upsilon-\upsilon_o) + \frac{1}{2!}\frac{d^2I(\upsilon_o)}{d\upsilon^2}(\upsilon-\upsilon_o)^2 + \ldots 4.2$$

Using equation (4.2) we can examine the basic mixing process using a microwave varistor. We will consider the mixing operation where the applied signal is either a single or double-side band modulated wave of very small amplitude that is mixed with a high level L.O voltage as shown in Fig. 4.1. Using the approximation given by equation (4.2) up to third power of voltage term and for zero DC bias voltage the output current becomes

$$i_o = \alpha_1\upsilon + \alpha_2\upsilon^2 + \alpha_3\upsilon^3 \quad \ldots\ldots\ldots\ldots\ldots\ldots 4.3$$

where $\alpha_1 = \frac{dI}{d\upsilon}$, $\alpha_2 = \frac{1}{2}\frac{d^2I}{d\upsilon^2}$, $\alpha_3 = \frac{1}{6}\frac{d^3I}{d\upsilon^3}$

$$\upsilon = e_s + e_{LO} = E_s\cos\omega_s t + E_{LO}\cos\omega_o t$$

e_s = RF input signal

e_{LO} = L.O voltage

Then from equation (4.3) we derive the following results:

$$i_o = \alpha_1(e_s + e_{LO}) + \alpha_2(e_s + e_{LO})^2 + \alpha_3(e_s + e_{LO})^3$$

$$= \alpha_1 e_s + \alpha_1 e_{LO} + \alpha_2 e_s^2 + \alpha_2 e_{LO}^2 + 2\alpha_2 e_s e_{LO} + \alpha_3 e_s^3 + \alpha_3 e_{LO}^3 +$$

$$\alpha_3 3 e_s^2 e_{LO} + \alpha_3 3 e_s e_{LO}^2$$

$$= \alpha_1 E_s \cos\omega_s T + \alpha_1 E_{LO}\cos\omega_o t + \alpha_2 E_s^2 \cos^2\omega_s t + \alpha_2 E_{LO}^2 \cos^2\omega_o t +$$

$$2\alpha_2 E_s E_{LO}\cos\omega_s t \cos\omega_o t + \alpha_3 E_s^3 \cos^3\omega_s t + \alpha_3 E_{LO}^3 \cos^3\omega_o t +$$

$$3\alpha_3 E_s^2 E_{LO}\cos^2\omega_s t \cos\omega_o t + 3\alpha_3 E_s E_{LO}^2 \cos^2\omega_o t \cos\omega_s t$$

Finally, rearranging terms we get:

$$i_o = (\alpha_1 E_s + \frac{3}{4}\alpha_3 E_s^3 + \frac{3}{2}\alpha_3 E_s E_{LO}^2)\cos\omega_s t + \ldots\ldots \text{Signal frequency}$$

$$+(\alpha_1 E_{LO} + \frac{3}{4}\alpha_3 E_{LO}^3 + \frac{3}{2}\alpha_3 E_s^2 E_{LO})\cos\omega_o t + \ldots\ldots \text{L.O frequency}$$

$$+ \frac{\alpha_2}{2}[E_s^2 + E_{LO}^2] + \ldots\ldots\ldots\ldots\ldots\ldots \text{DC component}$$

$$+ \alpha_2 E_s E_{LO}\cos(\omega_s - \omega_o)t + \ldots\ldots\ldots\ldots\ldots \text{Lower sideband frequency}$$

$$+ \alpha_2 E_s E_{LO}\cos(\omega_s + \omega_o)t + \ldots\ldots\ldots\ldots\ldots \text{Upper sideband frequency}$$

$$+ \frac{\alpha_2}{2} E_s^2 \cos 2\omega_s t + \ldots\ldots\ldots\ldots\ldots\ldots \text{Signal second harmonic}$$

$$+ \frac{\alpha_2}{2} E_{LO}^2 \cos 2\omega_o t + \ldots\ldots\ldots\ldots\ldots\ldots \text{LO second harmonic}$$

$$+ \frac{\alpha_3}{4} E_s^3 \cos 3\omega_s t + \ldots\ldots\ldots\ldots\ldots\ldots \text{Signal third harmonic}$$

$$+ \frac{\alpha_3}{4} E_{LO}^3 \cos 3\omega_o t + \ldots\ldots\ldots\ldots\ldots\ldots \text{LO third harmonic}$$

$$+ \frac{3}{4}\alpha_3 E_s E_{LO}^2 \cos(2\omega_o - \omega_s)t + \ldots\ldots\ldots\ldots \text{Image frequency}$$

$$+ \frac{3}{4}\alpha_3 E_S^2 E_{LO}\cos(2\omega_S - \omega_0)t + \ldots\ldots\ldots\ldots$$

$$+ \frac{3}{4}\alpha_3 E_S^2 E_{LO}\cos(2\omega_S + \omega_0)t + \ldots\ldots\ldots\ldots$$

$$+ \frac{3}{4}\alpha_3 E_S E_{LO}^2\cos(2\omega_0 + \omega_S)t + \ldots\ldots\ldots\ldots\ldots\ldots \quad 4.4$$

If more terms were included in the calculation there would be additional components. Some of these components will be added to those given by equation (4.4) and others will contribute new frequency terms up to infinity. Hence, the theory of Section 4.1 is justified.

The desired intermediate output frequency component, which is usually the difference of the RF signal and L.O frequencies, is given by the fourth term in equation (4.4). This intermediate frequency component is selected by using a bandpass filter in the output of the frequency translator. Since the factor $\frac{d^2I}{dv^2} = a^2I$ (from equation 4.1), in the fourth term, increases with forward bias applied across the diode, the output current at the intermediate frequency will also increase. This is one of the main objectives in attaining good mixer performance.

4.3 Characteristics of a Mixer Crystal Diode

In the analysis of the previous section a pure varistor behavior for the crystal diode was assumed. In fact, the signal frequency equivalent circuit shown in Figure 4.3 represents a practical microwave diode, operating as a mixer. Low minority-carrier injection (for no additional storage capacitance), low junction capacitance (C_j), and low series resistance (R_S) are required for good performance of a mixer crystal diode. Diodes having these characteristics usually make use of the nonlinear resistance of metal to semiconductor contact. Such devices are called Schottky-barrier diodes[8].

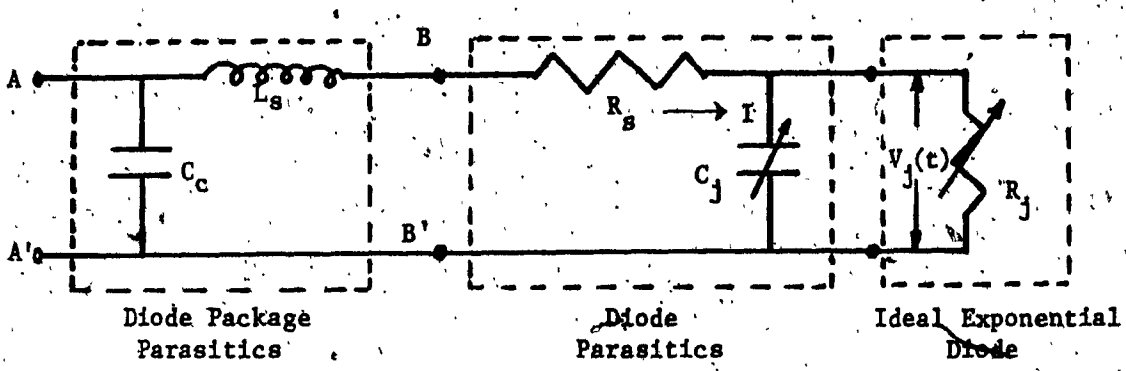

Fig. 4.3 - Equivalent circuit of a Microwave Mixer Diode.

R_j = junction resistance, C_j = junction capacitance

R_s = series spreading resistance, C_c = case capacitance

L_s = series package inductance

The current-voltage characteristic of a Schottky-barrier diode is qualitatively similar to that of a p-n junction but have a steeper forward slope, lower R_s, smaller forward turn-on voltage and lower breakdown voltage. The breakdown voltage must be sufficiently high to prevent large currents during the reverse swing of the L.O voltage.

Since the performance of a mixer diode is described in terms of the parameters R_j, C_j and R_s, we will now relate each of these elements to the physical properties of the semiconductor materials, geometry, and bias level for a Schottky-barrier diode, and in Section 4.4 we will discuss their contribution to the conversion loss.

(i) SERIES RESISTANCE (R_s)

The total resistance across a typical Schottky-barrier diode decreases rapidly with positive DC bias, until the forward-bias series resistance R_s dominates over the effect of the junction resistance R_j. The series resistance at forward bias V is given by equation (4.5) given below[8].

$$R_s = R_{so} + \frac{\varepsilon\rho}{C_{jo}}\left[1 - \left(1 - \frac{V}{\phi}\right)^{\gamma}\right] \quad \ldots\ldots\ldots\ldots\ldots\ldots\ldots\ldots\ldots\ldots 4.5$$

where

R_{so} = series resistance at zero bias

ε = permitivity of the semiconductor

ρ = average resistivity of the semiconductor epitaxial layer

C_{jo} = zero bias junction capacitance

ϕ = barrier voltage

V = forward bias

γ = exponent of the C-V (capacitance-voltage) relationship

The junction barrier voltage ϕ has to be low in order that significant current may flow without the use of fixed forward bias, and to prevent injection of minority carriers at high L.O voltage levels. R_s includes contributions from skin effect in the semiconductor and contact wire.

(ii) JUNCTION RESISTANCE (R_j)

The junction resistance R_j can be obtained from the inverse of the slope of equation (4.1) which gives

$$R_j = \left(\frac{dI}{dv}\right)^{-1} = \frac{d}{dv}\left[I_o(\exp av - 1\right]^{-1} = (aI)^{-1} = \frac{\eta KT}{qI} \quad \ldots\ldots\ldots\ldots 4.6$$

or the conductance may be written as

$$g = \frac{dI}{dv} = aI = Iq/\eta KT \quad \text{for } v \gg \frac{KT}{q} \quad \ldots\ldots\ldots\ldots\ldots\ldots 4.7$$

Typical values of η are 1.1 for vacuum-evaporated Schottky-barriers and 1.4 for point contact silicon diodes. From equation (4.6) we can obtain the forward voltage V needed to make $R_j = R_s$. This voltage is the one required to give a diode current $I = \eta KT/qR_s$.

(iii) JUNCTION CAPACITANCE (C_j)

The junction capacitance is given by equation (4.8) below[8].

$$C_j = A\left[\frac{\epsilon q N_d}{2(\phi - v)}\right]^{\gamma} = \frac{C_{jo}}{(1 - v/\phi)^{\gamma}} \quad \ldots\ldots\ldots\ldots\ldots\ldots 4.8$$

where

A = junction area

N_d = donor density

C_{jo} = junction capacitance at zero bias

The other parameters are known from equation (4.5).

In practice, circuit tuning elements are used to match the circuit to the junction resistance R_j so the voltage across C_j and R_j is maximized.

In this case a high diode cut off frequency, $f_c = 1/(2\pi R_s C_j)$ is desired to assure a high voltage across R_j at microwave frequencies.

Other parameters characterizing the mixer diode are: conversion loss, the RF input impedance, the IF output impedance, burnout and noise figure. Impedance mismatch of the RF frequency not only results in signal loss due to reflection, but also affects the IF impedance which is important in determining the coupling circuits between the mixer and IF amplifier. Burnout is a irreversible change in the rectifying and converting properties of the diode as the result of electrical overload. Burnout is a voltage-related rather than power-related phenomenon[9,10]. The most important criterion of mixer diode performance is the noise figure (F_o) which is given by equation (4.9). Germanium or silicon of very low resistivity is used in the fabrication of low noise figure diodes.

$$Fo_{db} = 10 \log_{10}[(S_i/N_i)/(S_o/N_o)] \quad \ldots\ldots\ldots\ldots\ldots\ldots 4.9$$

where

S_i = input signal power

N_i = input noise power = KT_oB

S_o = output signal power

N_o = output noise power = KT_1B

B = effective bandwidth

K = Boltzmann's constant (1.38×10^{-23} joules/Kelvin)

T_o = 290^oK, the standard noise temperature

T_1 = noise temperature of output resistance of the network.

Relative advantages of point contact and Schottky diodes are shown in the table below.

TABLE 4.1 - RELATIVE ADVANTAGES OF POINT CONTACT AND SCHOTTKY DIODES

POINT CONTACT DIODES

a) Higher Burnout capability (C, X, Ku - Band)

b) Higher rectification efficiency at low L.O power levels

c) Excellent as zero bias detector

SCHOTTKY BARRIER DIODES

a) Lower (1/f) noise

b) Lower white noise

c) Bonded Schottky is mechanically more stable

d) Schottky Beam Lead Diodes for Microstrip

e) Schottky chips for MIC's (microwave integrated circuits)

f) Better dynamic range.

4.4 EFFECT OF ELECTRICAL PARAMETERS OF THE CRYSTAL DIODE ON CONVERSION LOSS

In this section the effect on conversion loss of variations in the values of R_j, R_s and C_j will be discussed[6]. The junction resistance R_j in Figure 4.3 represents the desired nonlinear resistance. The elements R_s and C_j are undesirable (parasitic) because they increase the conversion loss above that caused by R_j alone. In order of their importance, the above quantities affecting conversion loss are: 1) R_j, 2) R_s, and 3) C_j. If the equivalent circuit of the diode is represented by R_j only, the conversion loss decreases and approaches asymptotically a constant value as the L.O drive is increased, and utilizes the straight portion of the DC characteristic in the forward direction. In that region, the junction resistance

is minimum or the conductance of the diode is maximum as it is shown in Figure 4.4.

The equivalent circuit at ultra high frequencies (UHF) of crystal diode consists of R_j in series with R_s. The R_s contribute to the conversion loss because of the power dissipated in it at the RF and IF frequencies. The effect of R_s on the overall conversion loss of the mixer is strongly marked at high L.O drive. As the L.O drive is increased the average value of R_j decreases, and at first the conversion loss begins to decrease. Then as the average value of R_j approaches R_s, more power is dissipated in R_s and the coversion loss increases. For high L.O drive, appreciable current flows through the junction during the positive half-cycle and the waveshape of $V_j(t)$ (L.O voltage component) that exists across the nonlinear junction becomes significantly nonsinusoidal. This affects the waveform of the conductance g(t) on which depends the behavior of the diode as a mixer. To find the exact waveshape of $V_j(t)$ we have to solve numerically the voltage loop equation (4.10). This equation is derived from Fig. 4.3 by connecting the L.O voltage source across BB' and neglecting C_j.

$$v_{LO} = V_{LO}\cos\omega_o t = (R_g + R_s)I + V_j(t) \quad \ldots\ldots\ldots\ldots\ldots\ldots 4.10$$

where

$I = I_o[\exp(qv_j(t)/nKT)-1]$

R_g = the L.O generator resistance

R_s = the junction resistance

To obtain the high frequency (X-band, 10 GHz) equivalent circuit, C_j must be added in parallel with R_j. The effect of C_j on the conversion loss is most pronounced at low values of L.O drive. As this drive is decreased, the value of R_j increases, more current is shunted by C_j and therefore,

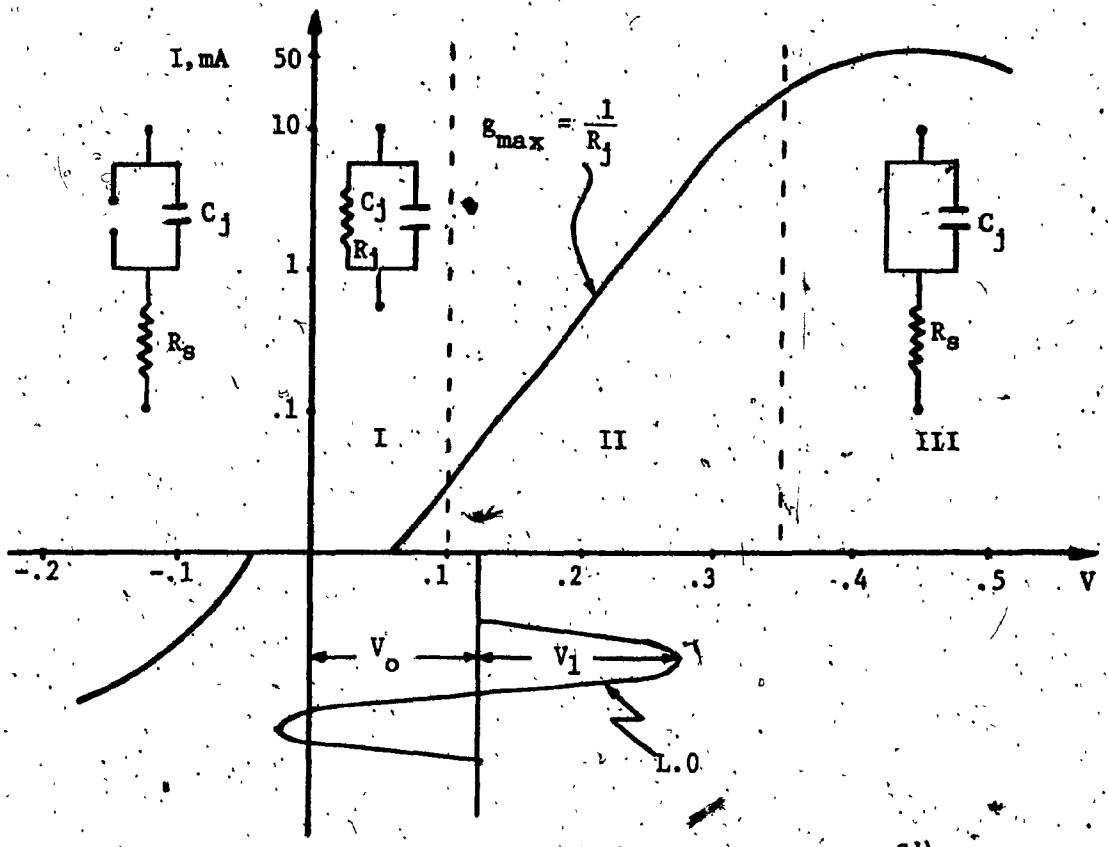

From equation (4.1) for $\upsilon >> \eta KT/q$, $\log I = \text{Log } I_o + .434 \frac{q\upsilon}{\eta KT}$

Fig. 4.4 - Semilogarithmic Volt-Ampere Characteristic of a Mixer Diode.

the conversion loss increases. In that case there is an optimum L.O drive for which the conversion loss is minimum. At this drive, both R_s and C_j decrease the conversion loss by an equal amount. A more general justification of this is readily obtained by using the ratio of the total available input power to the power available to the junction resistance. This ratio is given by equation (4.11)[8] and is derived using Figure 4.3.

$$L_c = \frac{P_T}{P_j} = 1 + R_s/R_j + \omega^2 C_j^2 R_j R_s \quad \ldots\ldots\ldots\ldots\ldots\ldots \quad 4.11$$

From equation (4.11) performing the operation $(\partial L_c/\partial R_j) = 0$ we obtain the value of R_j which minimizes the conversion loss L_c. This value is given by the equation (4.12) below:

$$R_j = 1/\omega C_j \quad \ldots\ldots\ldots\ldots\ldots\ldots \quad 4.12$$

Substituting (4.12) into (4.11) yields

$$(L_c)_{min} = 1 + 2\omega R_s C_j \quad \ldots\ldots\ldots\ldots\ldots\ldots \quad 4.13$$

Both (4.11) and (4.13) illustrate the necessity of minimizing the $R_s C_j$ product. Since R_j is a monotonically decreasing function of the L.O drive, equation (4.12) explains the commonly observed fact that the optimum L.O drive increases with increasing frequency.

The voltage $V_j(t)$ across the junction in this case is given again by solving equation (4.10) but now the current I is given by equation (4.14) which is easy to derive from Figure 4.3.

$$I = I_{R_j} + I_{C_j} = I_o[\exp(qv_j(t)/n KT) - 1] + C_j(V_j)\frac{dV_j(t)}{dt} \quad \ldots\ldots \quad 4.14$$

The volt-ampere characteristic of Figure 4.4 has been divided into three sections. In section I, R_j is greater than the reactance of C_j, $X_{C_j} = 1/j\omega C_j$. In Section II, R_j is much smaller than X_{C_j} and much greater than R_s. In

Section III, the junction resistance R_j is less than R_s. Therefore, if the bias were too low, the L.O power would bypass R_j through C_j and if it were too high, the L.O and signal power would be dissipated in R_s. For the diode to act primarily as a nonlinear junction resistance it should be biased between these two extremes. In practice, silicon diodes are used without bias while germanium diodes are biased about 0.15 volt forward. Germanium mixer diodes have a slightly lower conversion loss than silicon diodes because the spreading resistance R_s is about three times lower.

4.5 Diode Packages

Microwave mixer diodes, in order to be compatible with microwave circuits come in different cartridges. Some typical microwave diodes are shown in Figure 4.5. All the diodes shown can be used in both waveguide and coaxial applications. Other types of diodes developed for stripline circuit applications are too small to be shown in Figure. 4.5. The encapsulations in Figure 4.5a and b are useful up to about 10 GHz, and the types (c) and (d) are useful up to about 30 GHz.

Most of the devices use an n-type Gallium Arsenide (GaAs) crystal (high mobility and relatively low dielectric constant) and a phosphor bronze whisker or a more reliable thermocompression bond. A method of forming these diodes while observing the RF performance has been developed to provide high uniformity from diode to diode. Since the degree of systems performance improvement depends on diode characteristics improvement, a lot of research and development work has been done and goes on toward the perfection of these units. For example, with the perfection of high quality GaAs Schottky-barrier mixer diodes a low average noise figure of 5.6 dB and

greater than 50 percent 3dB bandwidth have been obtained in the 11GHz range.[20] Before the invention of the Schottky-barrier diode, noise figures below about 7dB could only be obtained by using tunnel diode or parametric amplifiers with sacrifice in receiver simplicity, stability, and dynamic range.

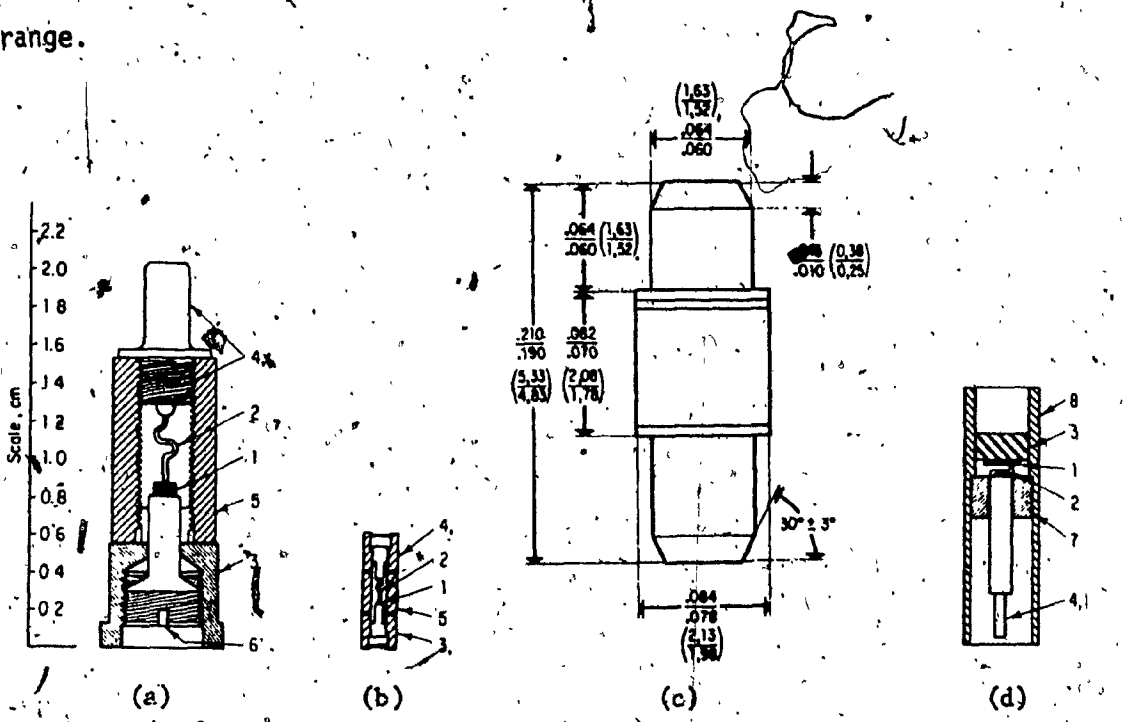

Fig. 4.5 - Typical microwave mixer diodes (1) semiconductor; (2) metal contact whisker; (3) wafer contact; (4) external whisker contact; (5) ceramic case; (6) adjustment screw; (7) insulating spacer; (8) outer conductor.

4.6 The Frequency Translator (Mixer)

The definition and generation of microwave mixing given in the previous sections is applicable to those devices that are usually referred to as up-converter, down-converter, modulators, demodulators, and microwave IF mixers. In this section we will use the non-linear impedance

of the diode to operate as a mixer or down converter by incorporating it into a circuit such as that shown in Figure 4.6. F_s, F_i and F_L are selective filters that have infinite impedance at the signal frequency, ω_s, at the intermediate frequency, ω_{IF}, and at the L.O (pump) frequency, ω_o, respectively, and zero impedance at all other frequencies.

The following terminology, commonly in use for the down converter (mixer), results from the location of the intermediate frequency spectrum relative to the signal spectrum. In down conversion we have $\omega_s > \omega_{IF}$ and if ω_{IF} is defined by the relation $\omega_{IF} = \omega_s - \omega_o$, the down converter is said to be a noninverting mixer, also called noninverting down-converter or upper single-side band mixer, since $\omega_s > \omega_o$. On the other hand, if ω_{IF} is defined by the relation $\omega_{IF} = \omega_o - \omega_s$ then the down converter is an inverting mixer, also called a lower single side band mixer.

In addition to the frequencies involved, the noise figure, conversion loss, voltage standing wave ratio (VSWR), isolation, spurious response, and third order intermodulation product (linearity), describe the mixer performance. The definition of the noise figure and conversion loss was given earlier in this chapter. For the conversion loss a general expression in terms of the elements of a linear equivalent network of the mixer is given in references[12,13]. The input and output ports require minimum VSWR or equivalently maximum return loss to minimize mismatching problems. The matching of the L.O port to the mixer port is also very important for a good conversion loss and frequency response. High isolation between the three ports of the mixer is required so that no one of the three frequencies (ω_s, ω_o, ω_{IF}) is coupled directly to any one of the other two ports. We call spurious frequencies the unwanted frequencies generated into the mixer and they appear in the output frequency band.

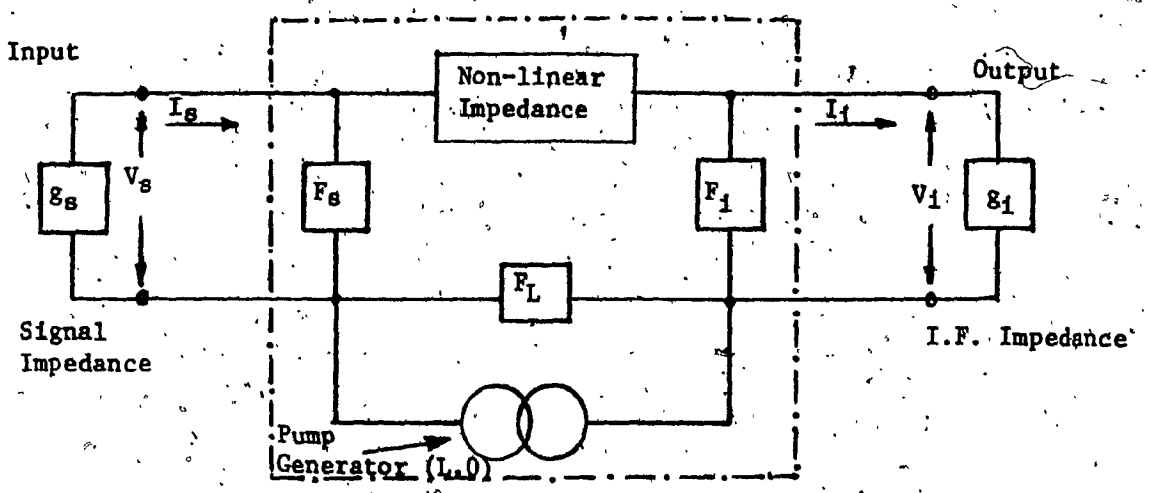

Fig. 4.6 - Nonlineal impedance down converter.

4.6.1 Single Diode Down Converter

The first microwave mixer, called single-ended or unbalanced mixer, utilized a single diode. The schematic of this mixer is shown in Figure 4.7. This basic mixer consists of the input and output BP filters, the L.O low pass filter, the coupling mechanism where the two signals (RF and L.O) are fed into a single line, and the diode holder with the diode where the mixing of the two signals generates all the frequencies mentioned in Sections 4.1 and 4.2.

In the mixer of Figure 4.7a the IF output power is derived from the principal frequency transformation $\omega_s - \omega_o$. All other side bands are either absorbed by the isolator or lost in the waveguide walls because of multimoding. A mixer of this type, where the signal and image termination are equal, is termed broadband mixer. The mixer of Figure 4.7b gives lower conversion loss because the useful signal power contained in the image frequency ω_I, is reflected back into the mixer by the input filter, where it beats with L.O frequency to produce current at intermediate frequency ω_{IF}. The phase of this current is adjusted to be the same as that derived from the principal frequency transformation, by varying the distance L

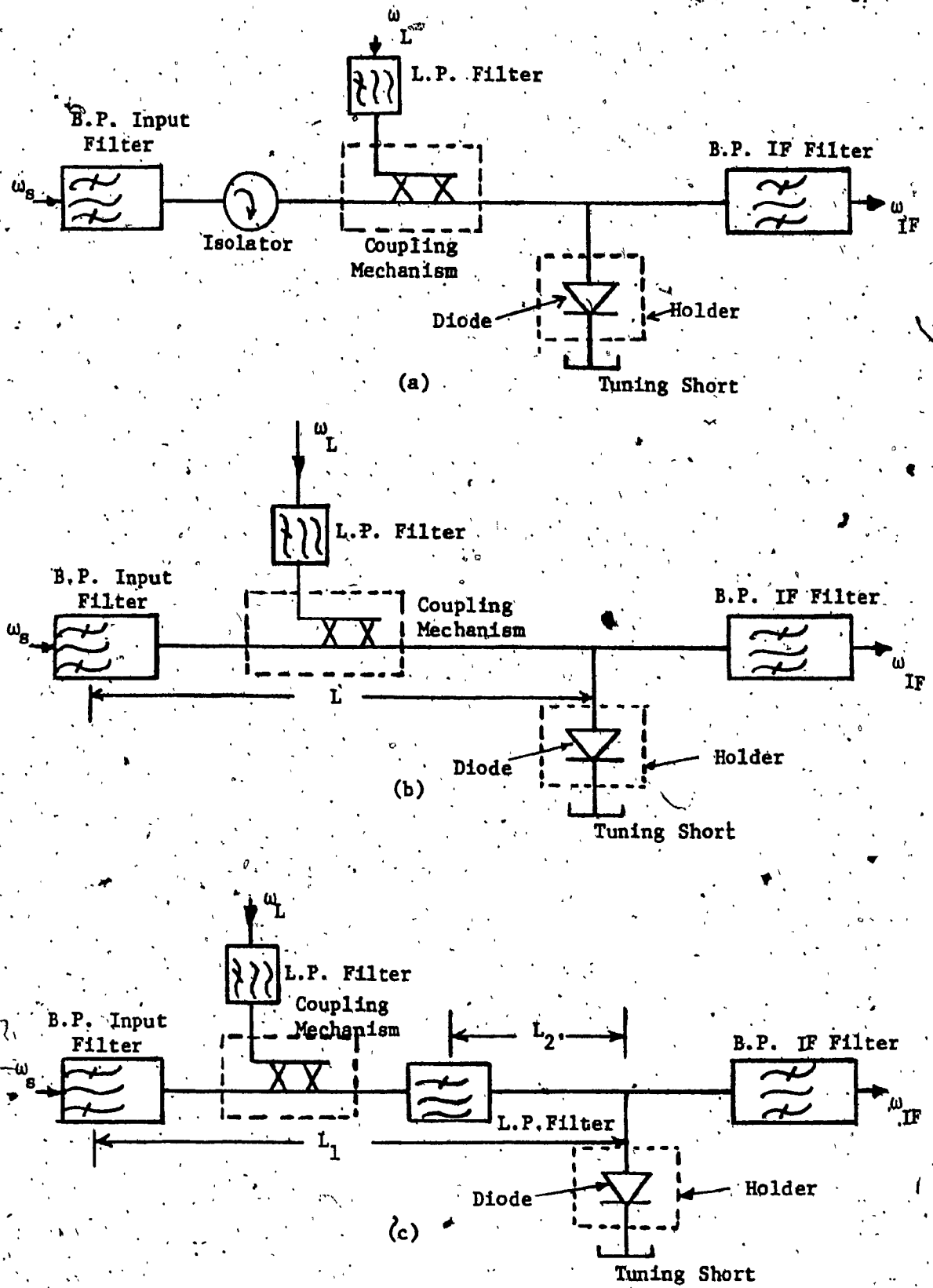

Fig. 4.7 - Schematic of single diode mixers.

between the input filter and the diode. Finally, with the mixer shown in Figure 4.7c even smaller conversion loss is achieved by reflecting back to the diode both the image ω_I and sum ω_Σ frequencies. The sum frequency is reflected back by the low pass filter, beats with $2\omega_o$ to produce current at the intermediate frequency $\omega_{IF} = \omega_\Sigma - 2\omega_o$. Its phase is adjusted by the length L_2 between the low pass filter and the diode.

Open circuit termination of the image frequency gives the lowest conversion loss but also the highest IF impedance. For lower IF impedance the short-circuited image termination has to be chosen. This can be achieved by using for the length L_1 slightly shorter than half wavelength. It can be shown[14], that when the sum and harmonic frequencies are open circuit terminated, the short-circuited image mixer becomes significantly better than the open-circuited image mixer.

In Figure 4.8 some typical coupling mechanisms for single diode mixers are shown[10]. The capacitive probe is practical in coaxial line mixers and the inductive loop is used when the diode is mounted in waveguide and the L.O is coupled by means of a coaxial line. The T section and resistive T section are the simplest but the directional coupler is probably the most practical coupling mechanism for optimum performance. It provides flat coupling with low VSWR over broad frequency ranges and good isolation between signal and L.O ports.

The advantages of the single diode mixers are their simplicity of construction, the design and the need for only one diode. The disadvantages are that highly sensitive single ended mixers tend to be narrow band and that there is no provision for eliminating the L.O amplitude modulated noise at the IF output port.

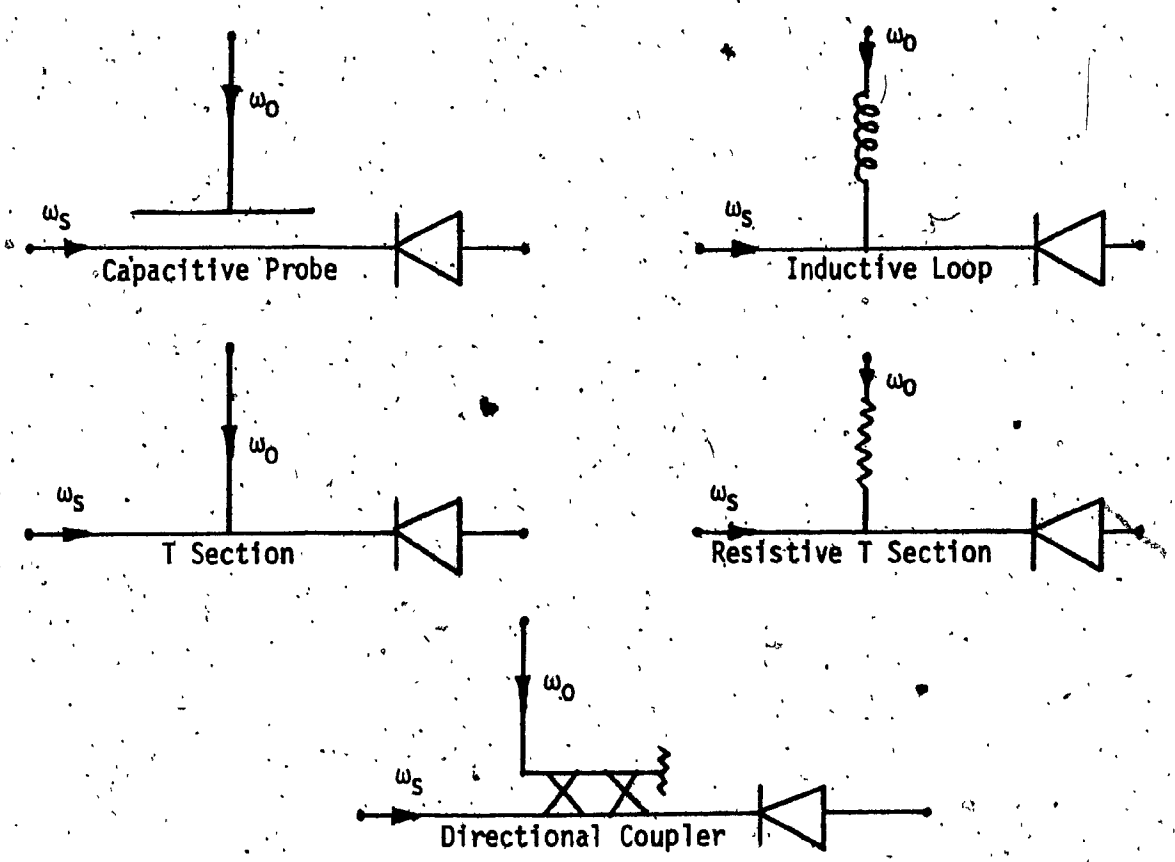

Fig. 4.8 - Schematics of typical coupling mechanisms for single diode mixers.

4.6.2 The Balanced Mixer

To cancel some of the problems of the single diode mixer, especially the suppression of the L.O amplitude modulated noise, the microwave balanced mixer was developed [15,16]. A balanced mixer uses two separate mixer units driven in shunt by the L.O signal and in push-pull by the RF signal, or vice versa. A schematic of a balanced mixer is shown in Figure 4.9. Since only half of the input RF signal and L.O power is applied to each diode a special coupling mechanism must be used. Some typical coupling mechanisms for balanced mixers are shown in Figure 4.10. Any of these has the property that an input signal, to any one of the input ports, will be divided to two equal output components with relative phase of 90^0 for the 3 dB coupler and 0^0 or 180^0 for the magic T or rat-race, depending upon the input port chosen. The 3 dB coupler gives good

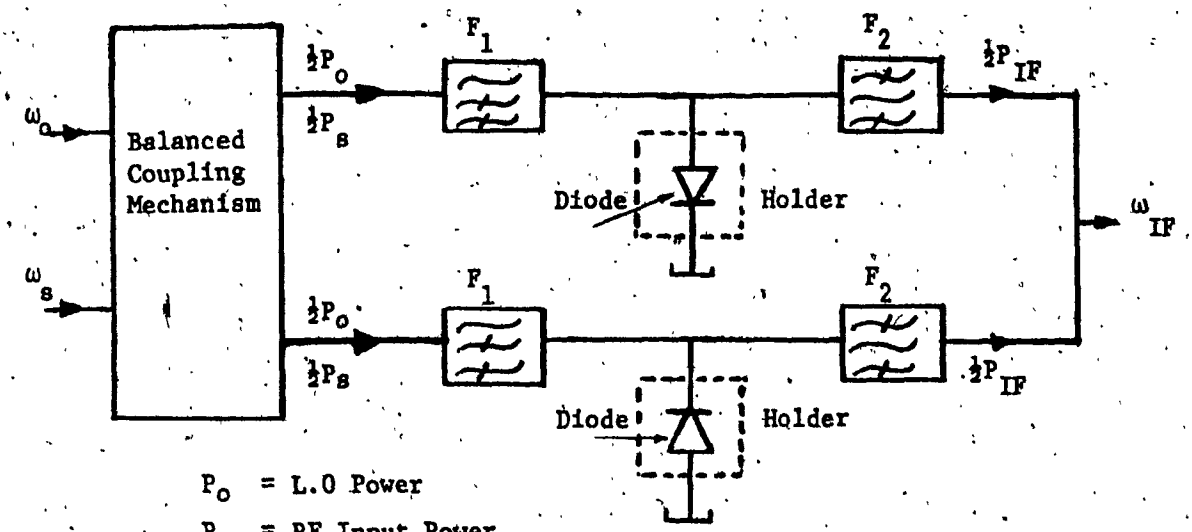

P_o = L.O Power

P_s = RF Input Power

Fig. 4.9 - Schematic of a Balanced Mixer.

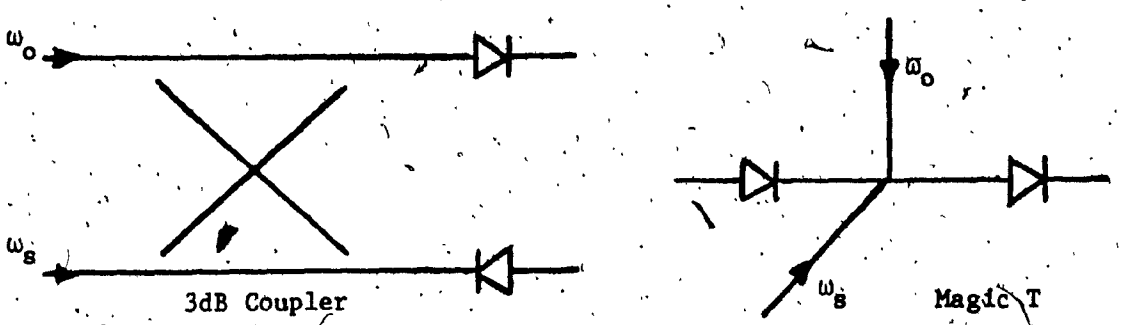

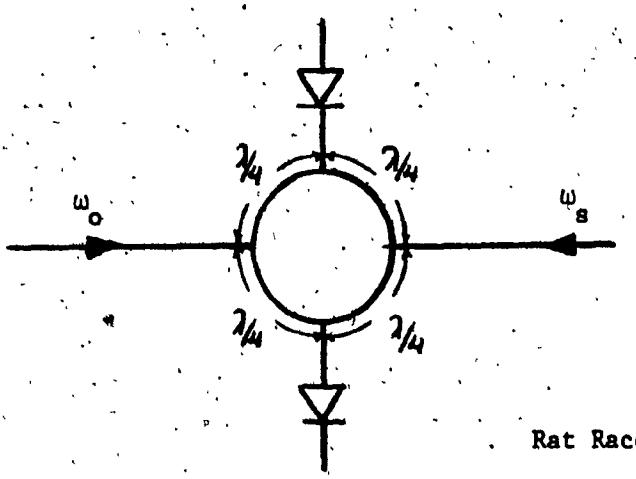

Fig. 4.10 - Schematics of Coupling Mechanisms for Balanced Mixers.

(low) VSWR but poor isolation and the other two give high isolation but poor VSWR. The solution in both cases is to match the individual diode holders. For different applications there are several different types of diode holders, both coaxial and waveguide.

The main purpose of filters F_1 is to pass both frequencies ω_s and ω_o, and to stop the ω_{IF} frequency, and for the filters F_2 is to pass ω_{IF} but at the same time to stop ω_s and ω_o. The individual filters must have low VSWR's for the pass band frequencies and to appear as short circuits to the stop band frequencies. Thus, each frequency has only one path of entry and exit to the diode. Since the RF admittance of the diode is the more serious source of unbalance in this mixer, diodes are selected in balanced pairs on the basis of RF admittance measurements.

The mathematical explanation of the L.O noise suppression is given by Chacran and Tenenholtz[17]. A simple explanation is that because the polarity of one diode is reversed the two IF noise voltages at the output terminals will be 180^0 out of phase and hence cancel. In some applications, where two foreward diodes are used, the noise cancellation is achieved by using a balanced transformer to recombine the two, on phase, outputs from the diodes. Another advantage of the balanced mixer is the efficient use of RF and L.O power, in all coupling mechanisms, which improves the overall mixer efficiency.

At the higher, millimeter wave, frequencies where reliable stable L.O sources are either unavailable or very expensive, harmonic mixing is used. An antiparallel diode pair has the following unique and advantageous characteristics as a harmonic mixer[18]: i) reduced conversion loss by suppressing fundamental mixing products; ii) lower noise figure through suppression of L.O noise sidebands iii) suppression of direct video detection; iv) inherent self protection against large peak inverse volt-

age burnout. These results are obtained without the use of either filters or balanced circuits employing hybrid junctions.

CHAPTER V

THE FREQUENCY TRANSLATOR (MIXER) OF THE CTS TRANSPONDER

The objective of this chapter is to present the design technique and the performance test data of the 14/12 GHz microwave frequency translator of the CTS SHF transponder. In Section 5.1 the design specifications are given and in Section 5.2 the circuitry (filters and diode mount) of the translator is described. Section 5.3 presents the selection of the optimum diode. In Section 5.4 and subsections the tuning, measurements and test results for the electrical parameters VSWR, conversion loss, gain flatness, inband spurious, intermodulation, noise figure and group delay for the translator are presented. The parameters: conversion loss, gain flatness and spurious also ware measured under the required operational temperature range (to determine the ability of the translator to survive in the launch and space environment). Sinusoidal and random vibration tests were performed on the Engineering model of the translator to qualify it for the Delta 2914 launch vehicle. Finally, the test results are summarized and discussed.

5.1 Design Specifications

The wideband frequency-translator of the SHF transponder is an integral part of the low noise receiver as shown in Figure 3.1a. It is a single diode image rejection (for better noise and conversion loss per-

formance) down converter, and its function is to provide frequency translation of the received signal without frequency inversion. A single-ended mixer was used because it has the advantages of a lighter and more compact physical structure and higher reliability. It is a three port network where the input port carries the RF signal at 14 GHz, the output port carries the IF frequency at 12 GHz and in the third port is the L.O drive at 2.1667 GHz. The mixer is capable of accepting and translating both receive bands (RB1, RB2) together. A 14 GHz TDA is used in front of the mixer as preamplifier and a 12 GHz TDA in the output as an IF amplifier.

Noise figure, conversion loss, gain flatness and group delay characteristics are the key design parameters of the unit. The main design specifications of the mixer are listed in Table 5.1. The mixer shall meet all the performance requirements under the operational temperature range of $0^{o}C$ to $+55^{o}C$. The electrical schematic diagram of the mixer is shown in Figure 5.1a and the mechanical configuration is illustrated in Figure 5.1b. The final assembly of the mixer with the input and output waveguide to coaxial adaptors is shown in Figure 5.2.

TABLE 5.1 - DESIGN SPECIFICATIONS FOR THE FREQUENCY TRANSLATOR OF THE CTS SHF TRANSPONDER

PARAMETER	SPECIFICATION
Input Frequency Band	13.974 to 14.324 GHz, BW = 350 MHz
Output Frequency Band	11.807 to 12.157 GHz, BW = 350 MHz
Conversion Loss	5dB
Gain Flatness	$\pm$.15 dB over 85 MHz
Noise Figure	8dB
Output Intercept Point	-6 dBm
Group Delay	1 nsec over 85 MHz
RF Input, Output VSWR	1.5:1
Continuous RF overdrive	+30dB
Nominal RF input power	-35 dBm
Required L.O drive	+ 9 dBm
Weight	0.5 lb (two waveguide to coaxial transitions included)

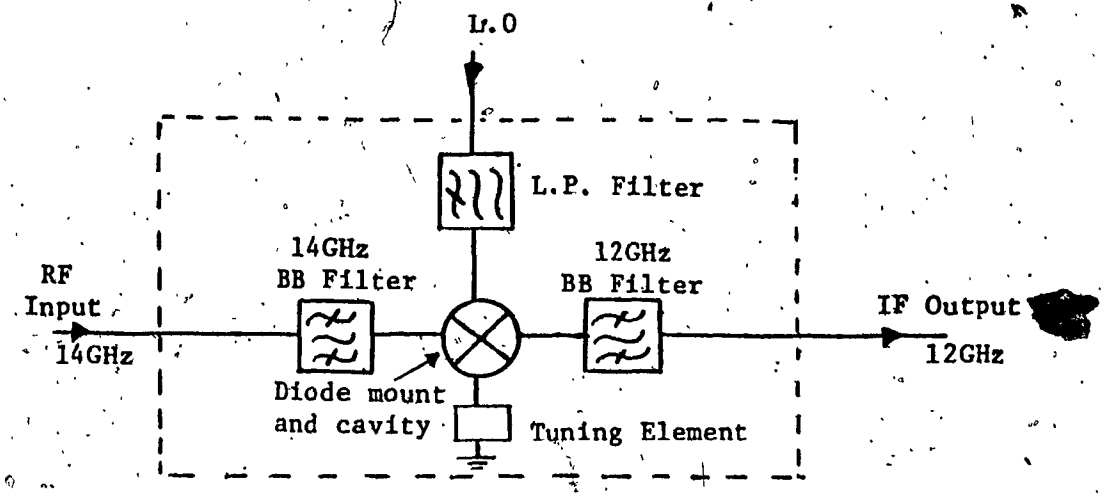

Fig. 5.1a - Electrical Schematic Diagram of the Mixer.

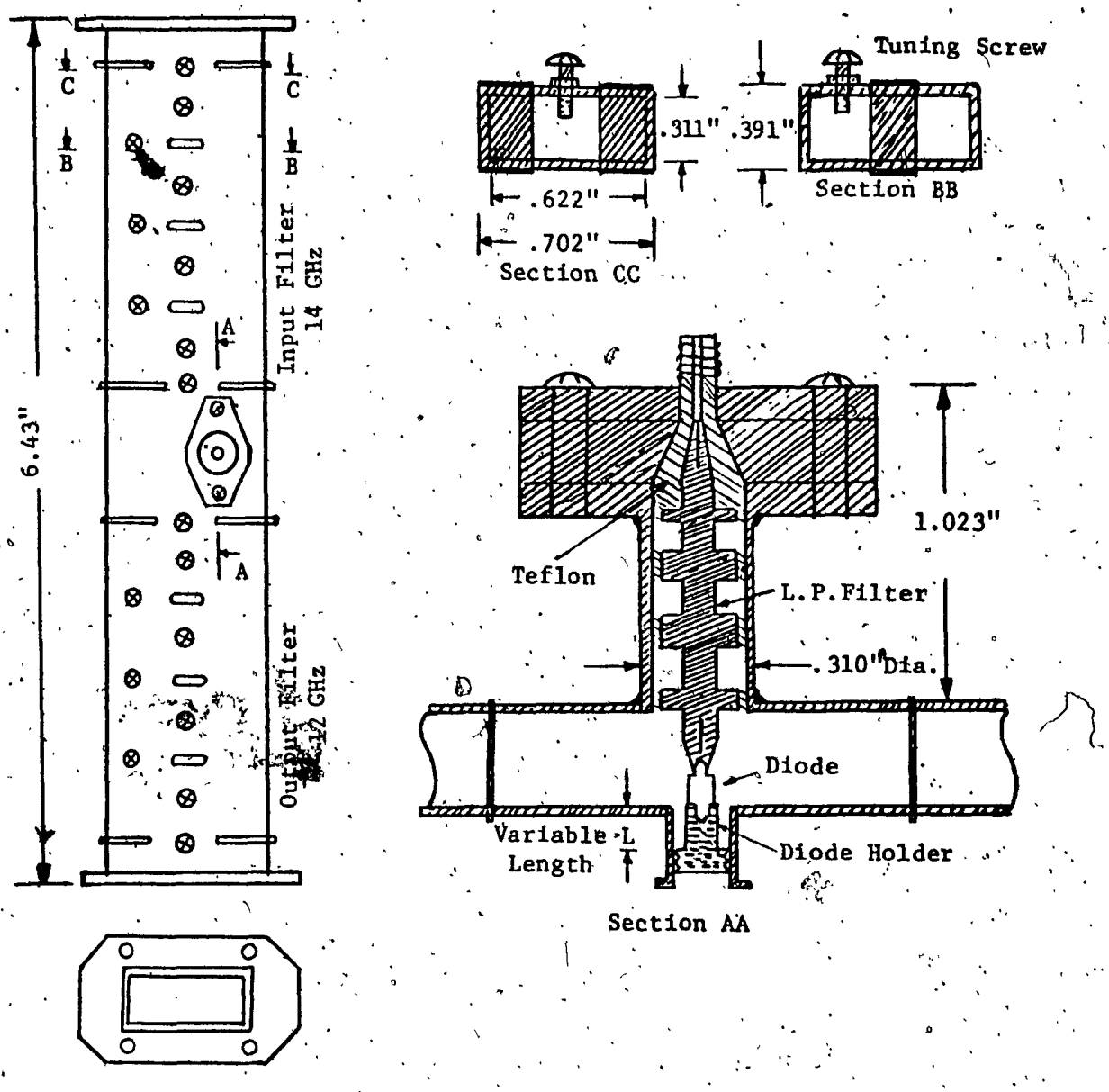

Fig. 5.1b - Mechanical Configuration of the Mixer.

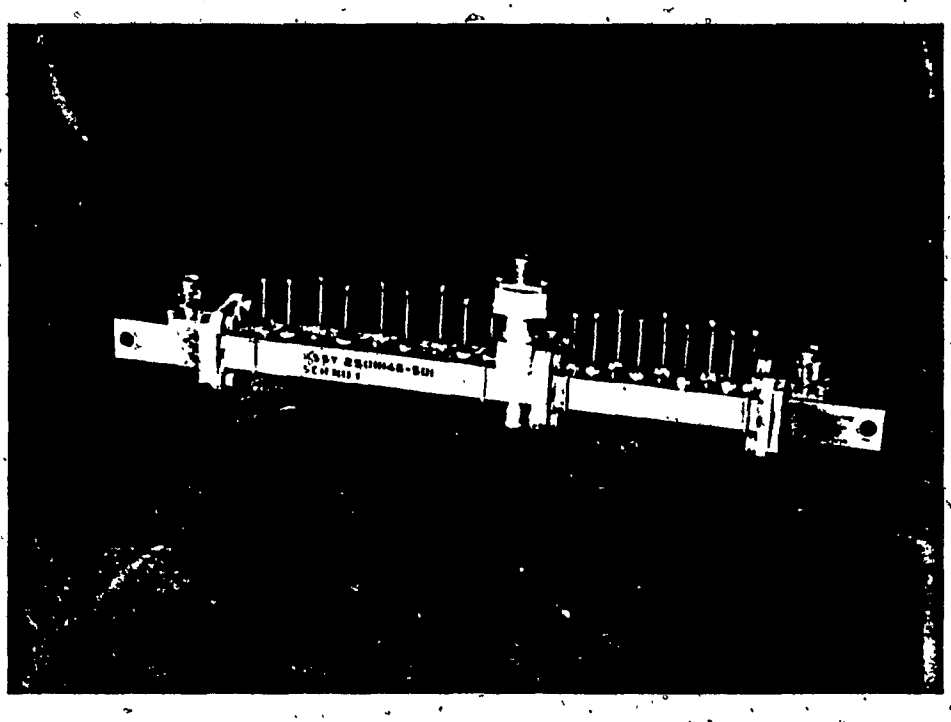

Fig. 5.2 – Final mixer assembly.

5.2 Circuit Description of the Frequency Translator

To obtain low conversion loss and noise figure, image rejection techniques are used by mounting the diode between three filters. To achieve high performance in the frequency ranges of interest, a waveguide construction was selected. At these frequencies (14 and 12 GHz), waveguides are small enough to be compatible in size and weight with satellite requirements. Standard WR 62 waveguides were used to construct the input and output filters and the coaxial line for the low pass filter in the L.O port of the mixer. Due to the intrinsic mode properties of the rectangular waveguide, filters made from WR 62 waveguides offer spurious free isolation up to about 19.0 GHz. Such an isolation characteristic provides good rejection for all the significant image and sum frequencies at the respective short circuit planes of the filters.

1) INPUT FILTER

The input signal BP filter is designed in the WR 62 waveguide with a minimum bandwidth of about 380 MHz and in-band return loss of -26 dB (VSWR = 1.1). Fourth order Chebyscheff filter response was used in the design and a minimum isolation of 50 dB between the input and output frequencies of the mixer was obtainable[22]. The midband insertion loss is about 0.3 dB. This filter rejects input signals at the image frequency, reactively terminates the diode at the image frequency, and prevents leakage of the L.O power to the antenna. Thus, low insertion loss (for a low conversion loss of the mixer) and at the same time good selectivity (to provide the image frequency termination) are the characteristics of the input filter.

ii) OUTPUT FILTER

The output BP filter also is a fourth order Chebysheff filter designed in WR 62 waveguide[21], with 380 MHz bandwidth and in-band return loss of -26 dB. Thus, the IF passes through the output filter, which rejects all other frequencies. The output filter is also used as the matching network at the IF port. Its midband insertion loss is also 0.3 dB.

The input and output BP filters are designed with a passband larger than the required signal band to avoid the need of phase equalization. Because the signal band occupies only 76 percent of the equiripple bandwidth, the group delay variation does not exceed the specified requirements.

iii) THE L.O BANDPASS FILTER

A third filter for the L.O frequency was necessary to complete the design. This filter has to provide adequate rejection at the input and output frequencies of the mixer and image bands and in addition, to stop undesired harmonics generated in the L.O multiplier chain. These harmonics otherwise could enter the mixer at a higher level than the received signal.

Most band pass filters exhibit spurious responses in the upper stop band, and the monotonic out of band characteristic of the insersion loss function is disrupted because of mode problems. For the mixer, the two RF frequency bands are at 12 and 14 GHz while the L.O frequency is 2.1667 GHz. Such a wide gap in frequency practically rules out the use of a bandpass filter for the L.O port of the mixer. However, a properly designed coaxial low pass filter has a very wide stop band[22]. In addi-

tion, the coaxial low pass filter can be made very compact to save weight.

For the mixer, a seven section Chebysheff coaxial low pass filter was designed to have a cut-off frequency of 7.0 GHz and a passband return loss of -10 dB. The predicted spurious in the stop band is around 22 GHz, while measurements indicate that the isolation is better than 30 dB up to at least 18 GHz. This gives a clean monotonic stop band with an insertion loss of 30 dB in the 12/14 GHz bands.

(iv) DIODE MOUNT (matching)

Physically the three filters are joined together as shown in Figure 5.1, with the diode at the junction. The electrical distance from the input filter to the diode determines the admittance which terminates the diode at the image frequency. For a good impedance match to produce a good VSWR and low conversion loss, the diode position was carefully optimized with respect to the three short circuit planes of the three filters. Figure 5.3 shows the six dimensional parameters which, together with frequency, form the set of independent variables which characterizes the impedance of this microwave structure, commonly called the waveguide mount[23]. The microwave diode is located at the gap of the post. The major effects that each of the six parameters has on the characteristics of the waveguide mount are given below:

a) 'a' Waveguide width - is a primary parameter and establishes the frequency range for the dominant mode.

b) 'b' Waveguide width - directly scales the magnitude of all mode impedances and is a factor in higher mode cut-off frequency determination.

c) 'W' Post width - normalized to 'a' determines the m* index convergence.

*m,n = Transfer Electric (TE) and Transfer Magnetic (TM) mode indices with
m = field variations in the X-direction
n = field variations in the Y-direction.

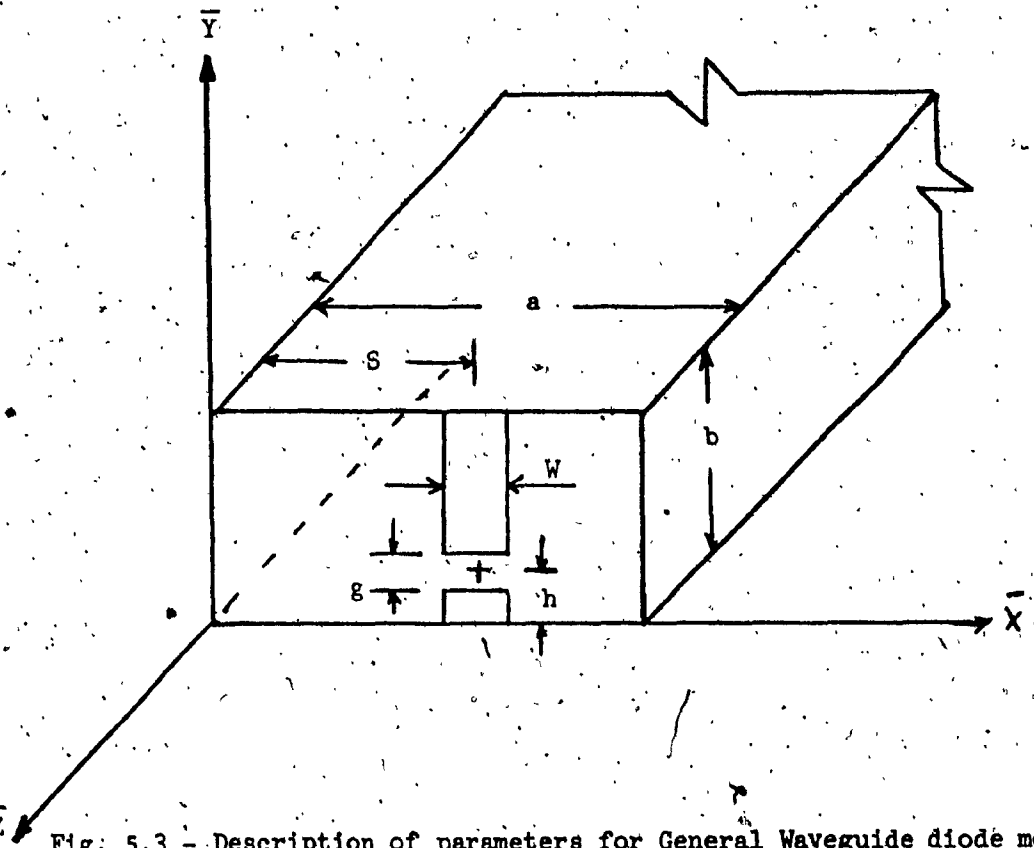

Fig. 5.3 - Description of parameters for General Waveguide diode mount.

d) 'g' Gap size - Normalized to 'b' determines the n* index convergence.

e) 'S' Post position - determines coupling between the post and the modes.

f) 'h' Gap position - determines coupling between the gap and the modes.

A theoretical and experimental analysis of these parameters is given by Eisenhart and Khan[23].

5.3 Diode Selection for the Frequency Translator

Different Schottky Barrier (silicon hot carrier) diodes from the Hewlett Packard 5082 series were tried. Each diode was individually optimized for the sake of selection. For mechanical reasons, package 49 in the HP catalogue was chosen for the diode. Extensive measurements were carried out to discover the optimum diode for this application. It was finally decided that diode No. 2713 gave the best results. Details of the diode characteristics are given in Appendix A.

The diode operates with self bias and eliminates the need of an extra bias and circuit complexity. Also, when DC bias is added, there is a tendency to increase the noise figure of the diode. In self biased operation, the bias is furnished by the DC voltage drop across a bias resistor resulting from the small rectified current occuring when the diode voltage swings into the forward direction.

5.4 Measurements and Test Results of the CTS Frequency Translator

This section will deal with the electrical test and test results of the frequency translator. To understand the meaning of each test, the basic theory, the test set-up and its operation is given before the test

*See footnote on page 70.

results. Because the frequency translator comes in separable parts, before we perform any electrical test, it has to be assembled and tuned first. Thus, the tune-up procedure is given first in the following subsections.

5.4.1 Tune Up Procedure of the Frequency Translator

The frequency translator comes in two separable waveguide parts with the low pass coaxial filter and the output BP filter as one part, and the input BP filter as the other part. There is no tuning involved with the low pass filter. The two waveguide BP filters are tuned separately to produce equi-ripple passband with passband return loss of -26 dB as it is shown in Figure 5.4. After the tuning the two filters are joined together. With the low pass filter and the diode, with its holder, inserted in place, final tuning is achieved by the frequency and coupling tuning screws of the input and output waveguide filters. The L.O drive level is adjusted by using two pad attenuators, between L.O and mixer, to achieve optimum results. Also the length L of the diode holder is very critical and has to be optimized. The variable position of the short, created by this length, located below the diode (Figure 5.1b) tunes the diode and its holder at approximately 12 GHz.

With nominal RF input power to the mixer of -30 dBm and optimum L.O drive level of +5 dBm and diode holder length of 0.247 inches, the mixer was tuned to meet all the specifications. The test set-up used for all these tuning operations is shown in Figure 5.7.

5.4.2 VSWR, Conversion Loss and Gain Flatness Measurements

All these parameters can be measured by using the same test set-up which is shown in Figure 5.7. This set-up is calibrated as follows:

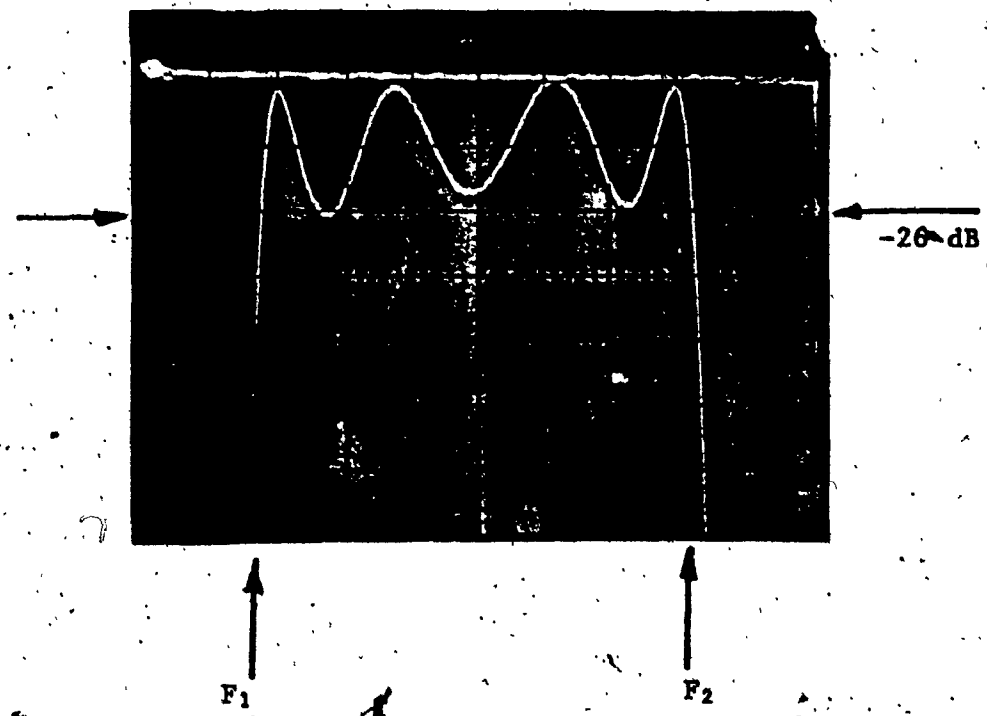

Fig. 5.4 - Return Loss of the Input and Output Filter.

Input Filter: F_1= 13.970 GHz
F_2= 14.320 GHz
Output Filter: F_1= 11.800 GHz
F_2= 12.150 GHz

with a power output of about zero dBm from the sweep generator and sweeping over the entire band from 13.970 to 14.620 GHz, a short circuit is presented to the point A and the oscilloscope is calibrated for total reflection with a particular setting on the variable attenuators. Next the set-up is connected up with the mixer removed. For the same power output from the sweep generator, the second beam of the scope is calibrated for conversion loss by means of the variable attenuators. Calibration reference lines are necessary to determine the conversion loss and gain flatness response of the mixer.

With the set-up properly calibrated the mixer is inserted into and inband VSWR, conversion loss and gain flatness are read off against the calibration lines. These parameters can also be recorded on an X-Y recorder. The results are shown in Figure 5.5.

If it is desired to measure the conversion loss of the mixer in a single frequency (IF mid band frequency) for more accurate measurements, Figure 5.8 can be used. The signal generator one (1) and L.O are set at the proper frequencies and power levels and the height of the output signal is marked on the Spectrum Analyser (S.A.). Now the S.A. is connected to the second signal generator (2), which is set at the desired output frequency and its power is adjusted to give the same signal height, on the S.A., as that given by the mixer output. By comparing the input power to the mixer to the output power from the generator two (2) we can determine the conversion loss of the mixer in dB. The conversion efficiency of the mixer as a function of L.O power is shown in Figure 5.6. As was explained in Section 4.4, the conversion efficiency is less (higher conversion loss) with small L.O amplitudes than with large amplitudes where the straight portion of the DC characteristic in the forward direction is utilized.

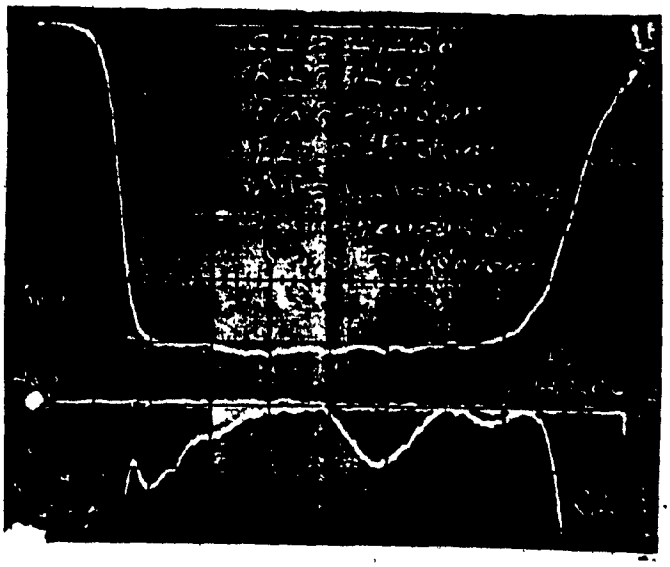

Fig. 5.5 - Conversion Loss, Gain Flatness and Return Loss of the Mixer.

Power Input = -30 dBm

F_1 = 13.970 GHz)
F_2 = 14.320 GHz) $\Delta F = F_2 - F_1 = 350$ MHz

L.O Power = +5 dBm

$F_{L.O}$ = 7.1667 GHz

Conversion Loss = 4.4 dB

Gain Flatness = .2 dB peak-to-peak

Return Loss = 14 dB (VSWR = 1.5)

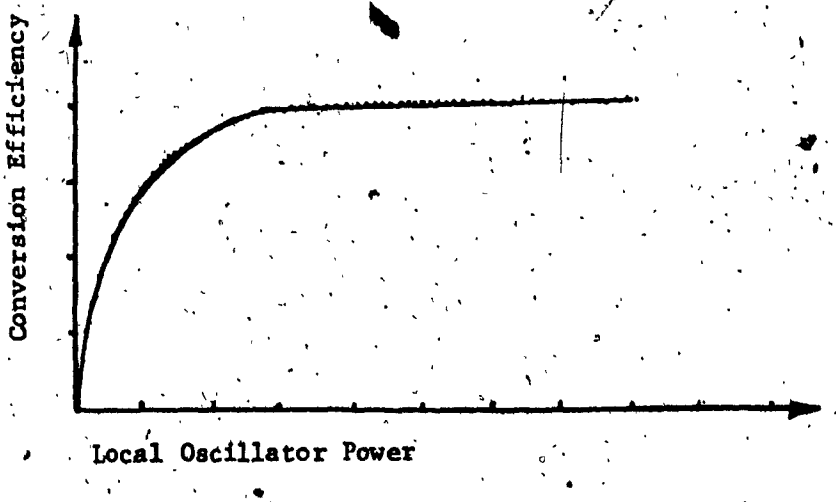

Fig. 5.6 - Typical curve for conversion efficiency vs local oscillator drive.

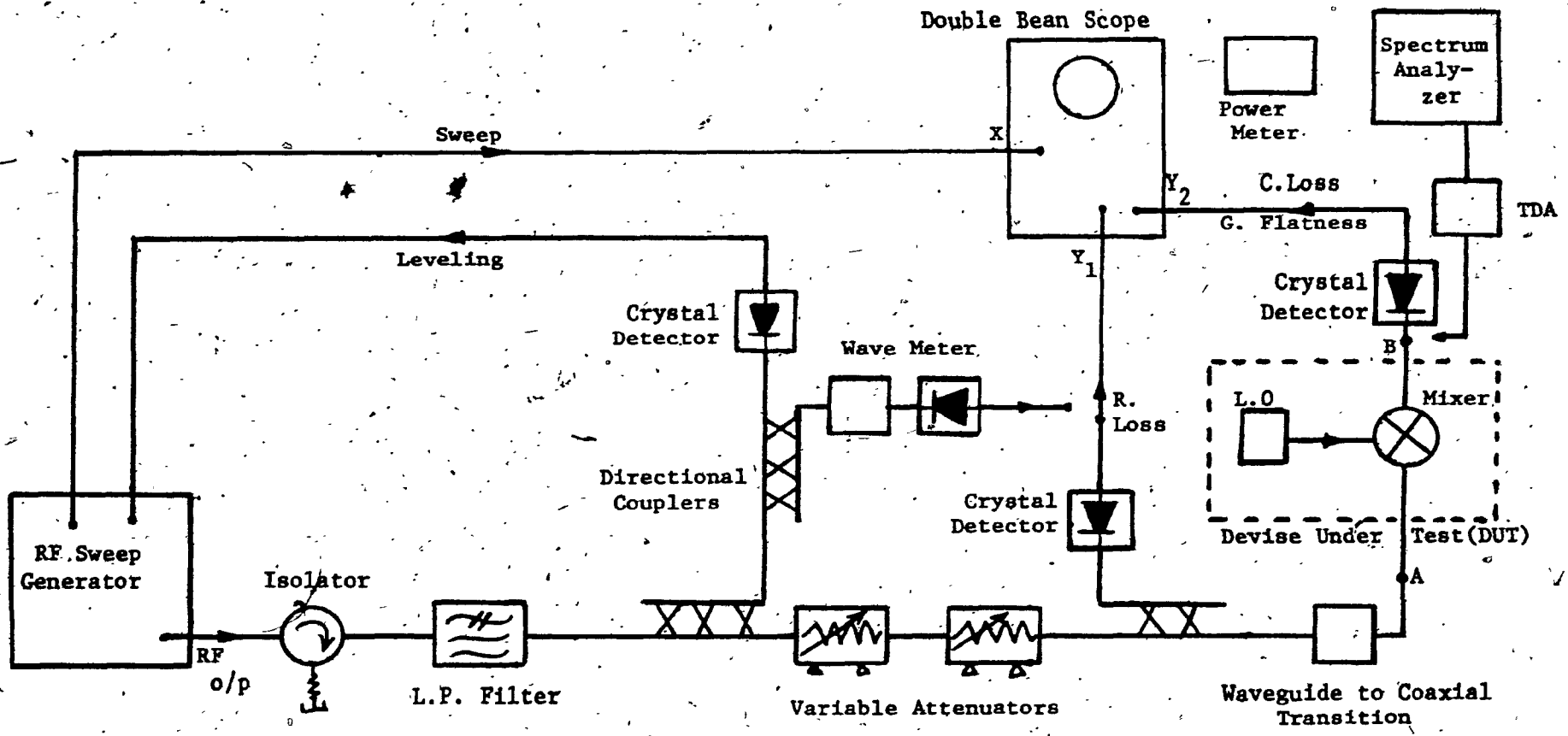

Fig. 5.7 - Test Set-up (with WR-62 waveguides) for Tuning and VSWR (Return Loss), Conversion Loss, Gain Flatness and In-Band Spurious Measurements of the Mixer.

Since the mixer is, for all practical purposes, reciprocal we can use it in reverse (12/14 GHz up converter) and have the same results for the conversion loss, return loss (VSWR) and gain flatness. That is, if an IF signal (12 GHz) were impressed upon the IF port, then an RF signal (14 GHz) will be produced at the signal port.

5.4.3 In-Band Spurious Response of the Frequency Translator

An in-band spurious frequency was discovered in the output of the mixer during the test of the bread-board model transponder. This spurious was found to be the mixing product of the twelfth harmonic of the L.O frequency and the input RF signal. It was clear that the spurious could be suppressed by discouraging the generation of the harmonics of the L.O frequency in the mixer diode. One difficulty encountered was the non-linearity of the diode impedance with respect to the L.O drive level and the bias.

An effort was made to match the diode, its mount and cavity, to the L.O source by altering the design of the low pass coaxial filter. The reactive part of the diode and cavity impedance has to be absorbed in the first section of the low pass filter and the resistive part has to be transformed through the filter to 50 ohms. Using Matthaei's design procedure[25], it turned out that the value of the first capacitor of the filter becomes negative. Partial matching achieved by altering the first section of the filter and fairly good results were obtained. Also an alternative solution was found by adjusting the length of the transmission line between the L.O output and the mixer and the L.O power drive. This did not involve any increase in weight and the spurious level under matched conditions was 45 dB below the carrier level.

The test set-up for in-band spurious measurements is shown in

Figure 5.7. The spectrum analyzer with the TDA is connected in the output of the mixer at the point B of the set up. The TDA is used to amplify the signal for better signal to noise resolution. The spurious level is checked by sweeping the CW RF signal manually. Since by sweeping the input carrier across the input band the spurious most of the time is outside of the output band to check the spurious the carrier frequency was at 14.095 GHz and -30 dBm. The results are shown in Figure 5.9.

5.4.4 Third Order Intermodulation Product of the Frequency Translator (intercept point)

i) Theory

In general, all mixers have a signal level limitation, beyond which the input and output powers are no longer proportional to each other. The point at which the output level drops 1 dB from following the input on one-to-one basis is the -1 dB compression point. If one operates the mixer too close to this compression point, the RF signal will begin to generate harmonics due to the nonlinearity in the mixer conversion loss curve. Harmonics of the RF signal can then combine with existing stronger harmonics of the L.O source and produce unwanted interfering signals or single-tone intermodulation products of the form:

$$M(F_{RF}) \pm N(F_{LO}) = \text{Output Frequency (IF)}$$

where M and N are integers.

In other applications of mixers, where more than one RF signal is applied, it is possible for harmonics of each RF signal to combine and form unwanted two-tone intermodulation products. The most important two-tone product is the third order because it is usually larger than any other combination of the two inputs. The two tone intermodulation products are

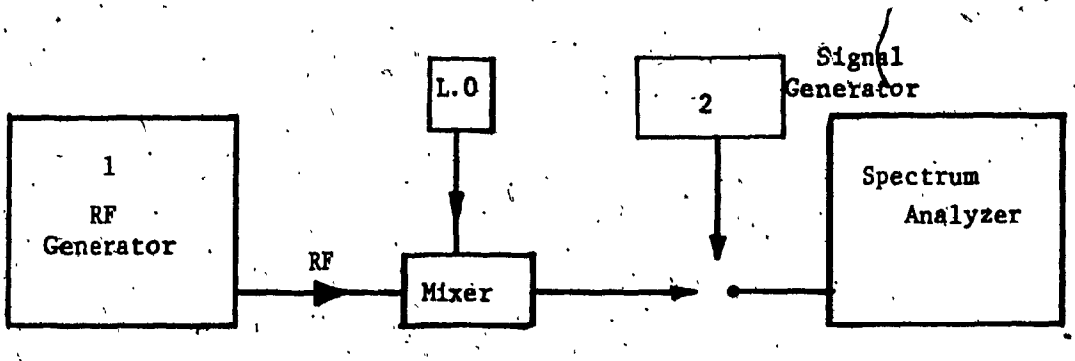

Fig. 5.8 - Test set-up for single point conversion loss measurements.

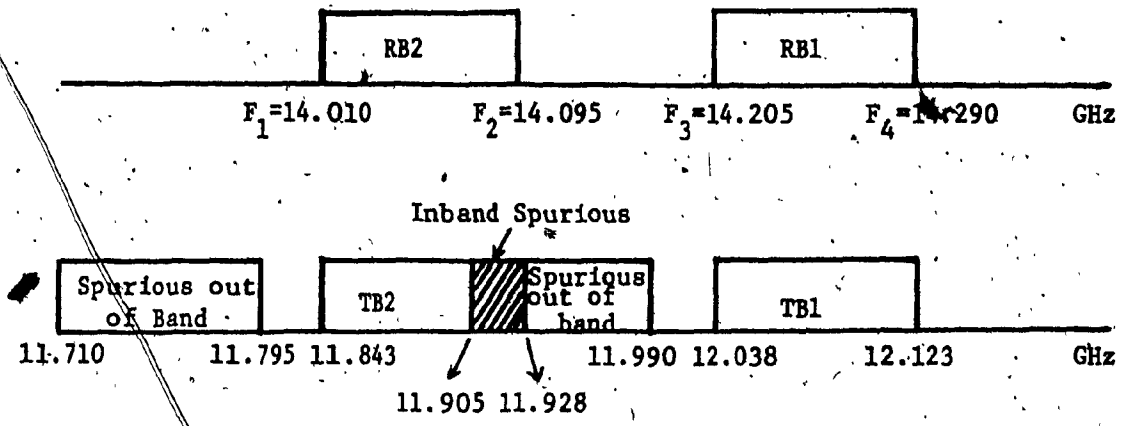

12 L.O - F_1 = 26.000 - 14.010 = 11.990 GHz

12 L.O - F_2 = 26.000 - 14.095 = 11.905 GHz

12 L.O - F_3 = 26.000 - 14.205 = 11.795 GHz

12 L.O - F_4 = 26.000 - 14.290 = 11.710 GHz

Inband spurious region from 11.905 GHz to 11.928 GHz

P_{1N} = -30 dBm

P_{LO} = +50 dBm

F_{1N} = 14.095 GHz

F_{LO} = 2.1667 GHz

Spurious level 44 dB below the carrier.

Fig. 5.9 - Spurious response of the mixer.

of the form:

$$F_{LO} \pm (NF_1 \pm MF_2)$$

When $N \pm M = 3$ the two tone/third order intermodulation products are:

$$(2F_1 \pm F_2) - F_{LO} = \text{Output Frequency (IF)}$$

or

$$(F_1 \pm 2F_2) - F_{LO} = \text{Output Frequency (IF)}$$

Figure 5.10 shows the intermodulation spectrum for 2 and 3 input carriers. The level of the input signal relative to the saturation or -1 dB compression point of the mixer is the first important consideration that determines the absolute level of various intermodulation products. Also, the local oscillator switching characteristics (determined by the L.O frequency) of the mixer are very important for the absolute level of various intermodulation products (IMD).

Furthermore, if one were to plot the output (IMD) products versus the input RF signal on a log/log scale, each product would appear as a straight line having a slope equal to the order of the RF harmonic. For example, the RF level-dependent single-tone product $2F_{RF} \pm F_{LO}$ would have a slope of 2, whereas the RF level independent $F_{RF} \pm 2F_{LO}$ product would be linear with a slope of 1. The two tone products $(2F_1 \pm F_2)-F_{LO}$ and $(F_1 \pm 2F_2)-F_{LO}$ each would have a slope of 3. Knowing an absolute RF input power and measuring the third order IMD products ratio in dB, at that power level, we can extrapolate the RF input power that will cause the IMD products and the desired products to become equal. This power level is defined as the third order intercept point. The intercept point is a fictitious point but is an effective means of evaluating mixer linearity and spurious suppression. The intercept concept is most easily understood if we consider a mixer whose IMD products vary as shown in Figure 5.11. If two RF

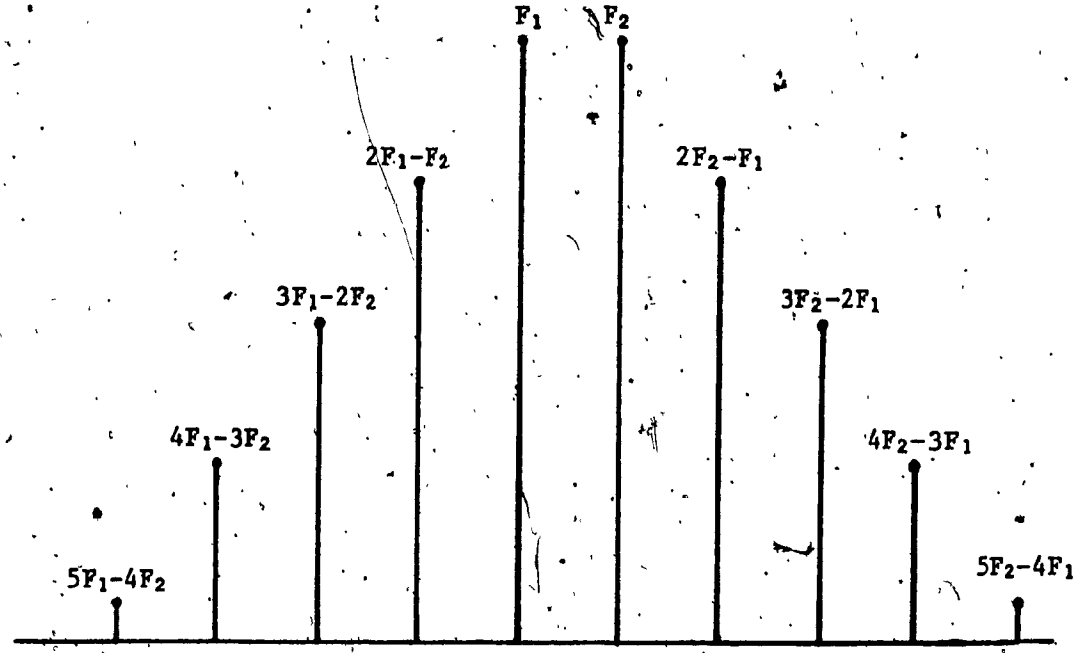

(a)

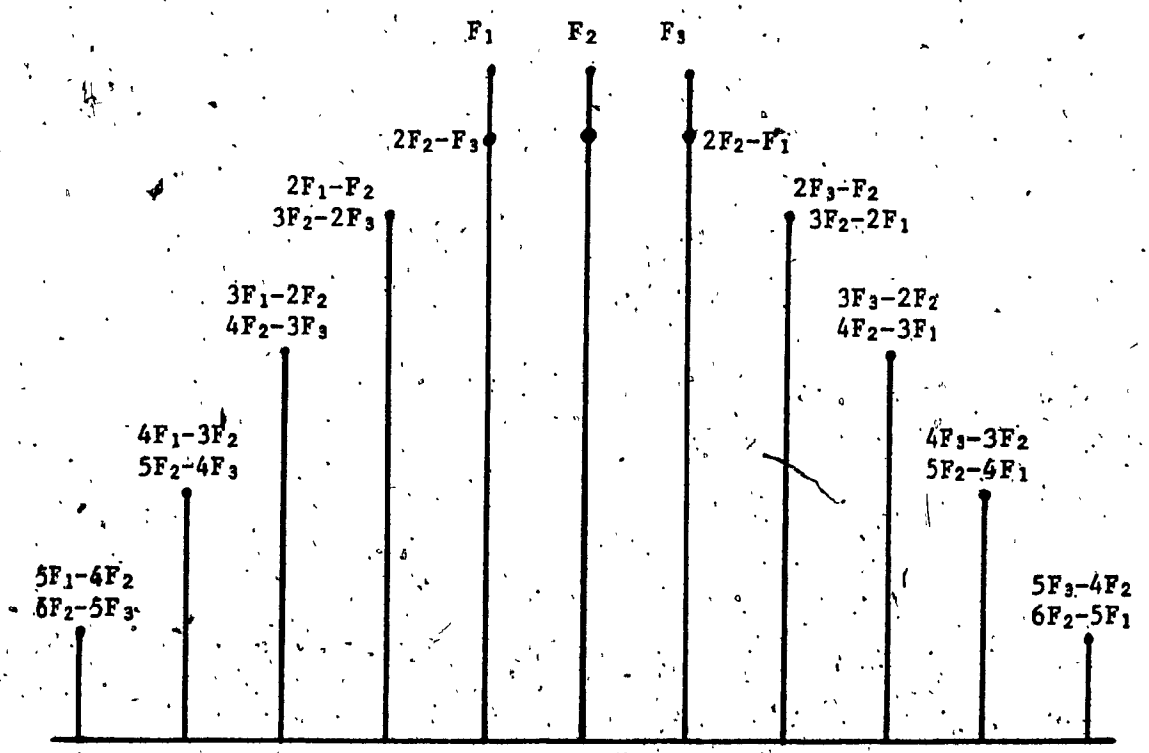

(b)

Figure 5.10 - Intermodulation (IMD) spectrum. (a) for two input carriers; (b) for three input carriers.

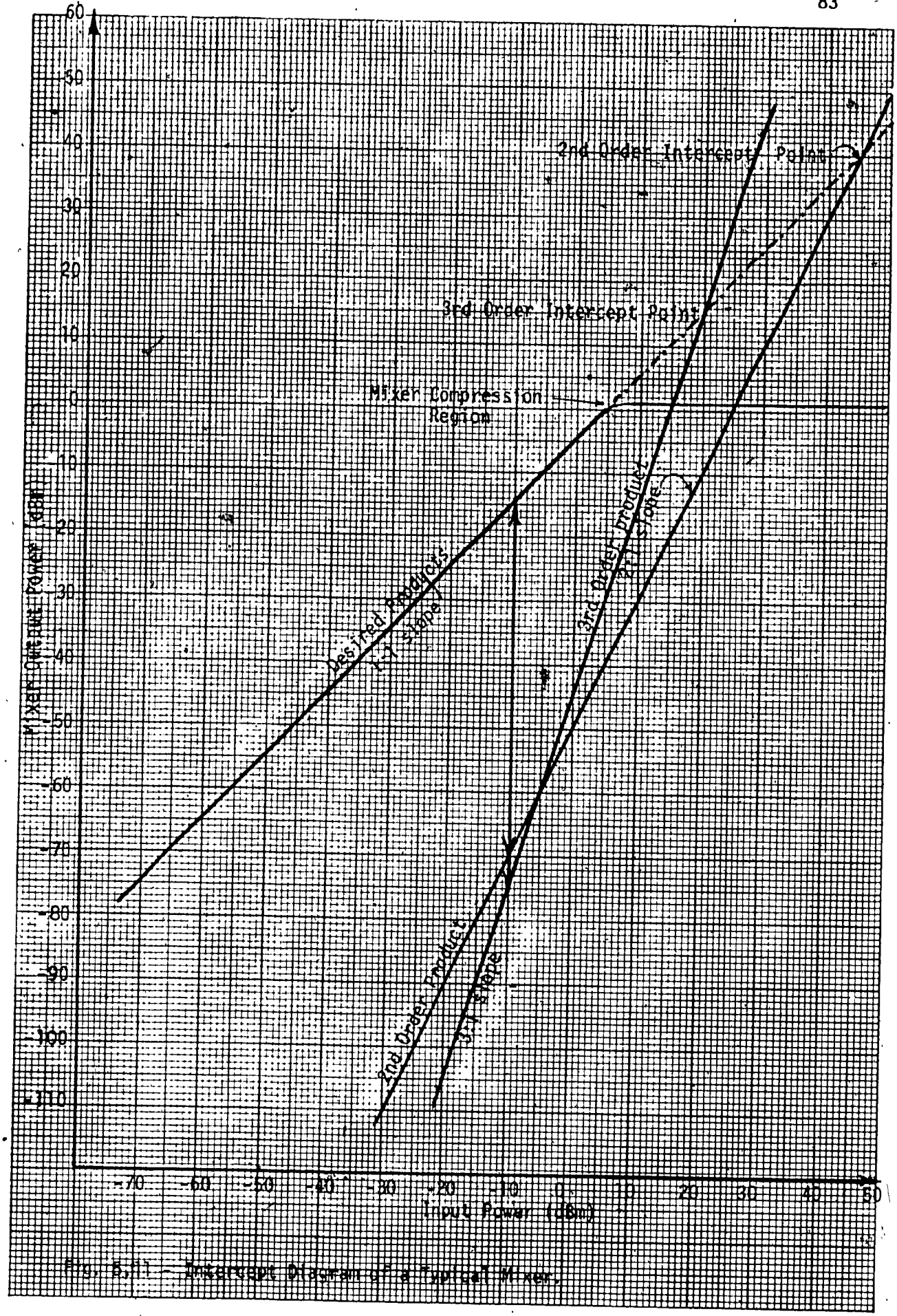

Fig. 5.11 — Intercept Diagram of a Typical Mixer.

inputs are present at, say, -10 dBm then the second and third order IMD products will be found at 55 and 60 dB, respectively, below the desired output. In other words, the IMD ratio is 55 dB and 60 dB respectively. The IMD product levels are -70 dBm and -75 dBm respectively. If both inputs are changed, then the desired products will change on a 1:1 slope; the second order products will change on a 2:1 slope and the third order products on a 3:1 slope on a dB scale as shown. If the mixer exhibited no compression, there would be a point at which the desired output levels would be equal to the second or third order product. This point is defined as the output intercept point for the product order. In the example shown, the third order intercept is at +15 dBm and the second order intercept is at +40 dBm. The third order intercept for the mixer in Figure 5.11, occurs at an RF input of +20 dBm, approximately 15 dB above the 1 dB compression point of the mixer. To have better IMD ratio and product levels the intercept point is desired to occur at an RF input level as high as possible.

ii) TEST AND TEST RESULTS OF THE CTS MIXER

The test set-up for this measurement is as shown in Fig. 5.12. Two equal CW signals spaced 50 MHz apart situated in the middle of the input frequency band are fed into the mixer. The input power to the mixer is varied from the nominal maximum input level (-30 dBm) to +5 dBm in 5 dB steps by using the variable attenuator in the input of the mixer. Signs of saturation showed up when the mixer was overdriven by about 30 dB. The intermodulation products become indentifiable from the noise when the power level of either carrier was approximately -20 dBm. Figure 5.13 are photographic recordings of the spectrum analyzer displays for the

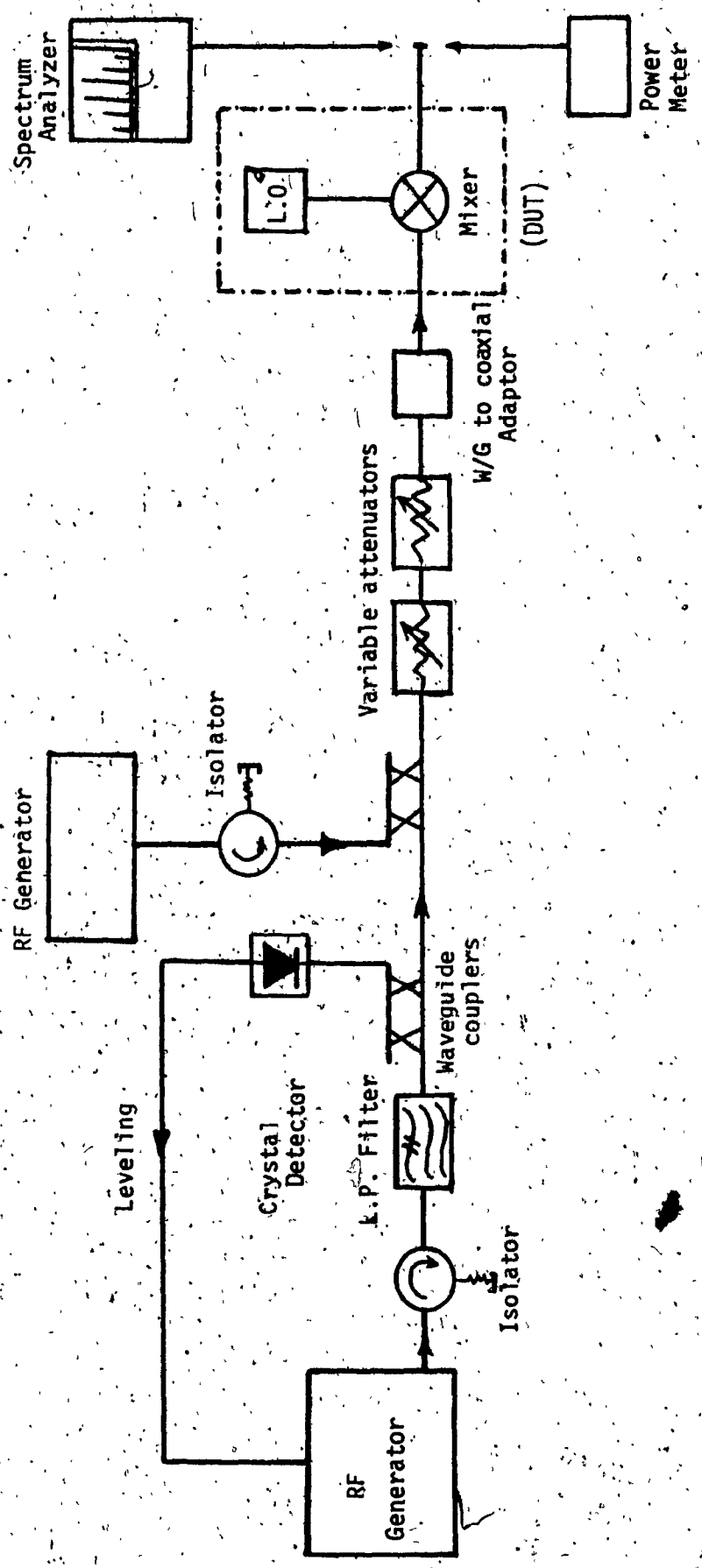

Fig. 5.12 - Test Set-Up (WR-62 waveguides) for Intermodulation Measurement of the Mixer.

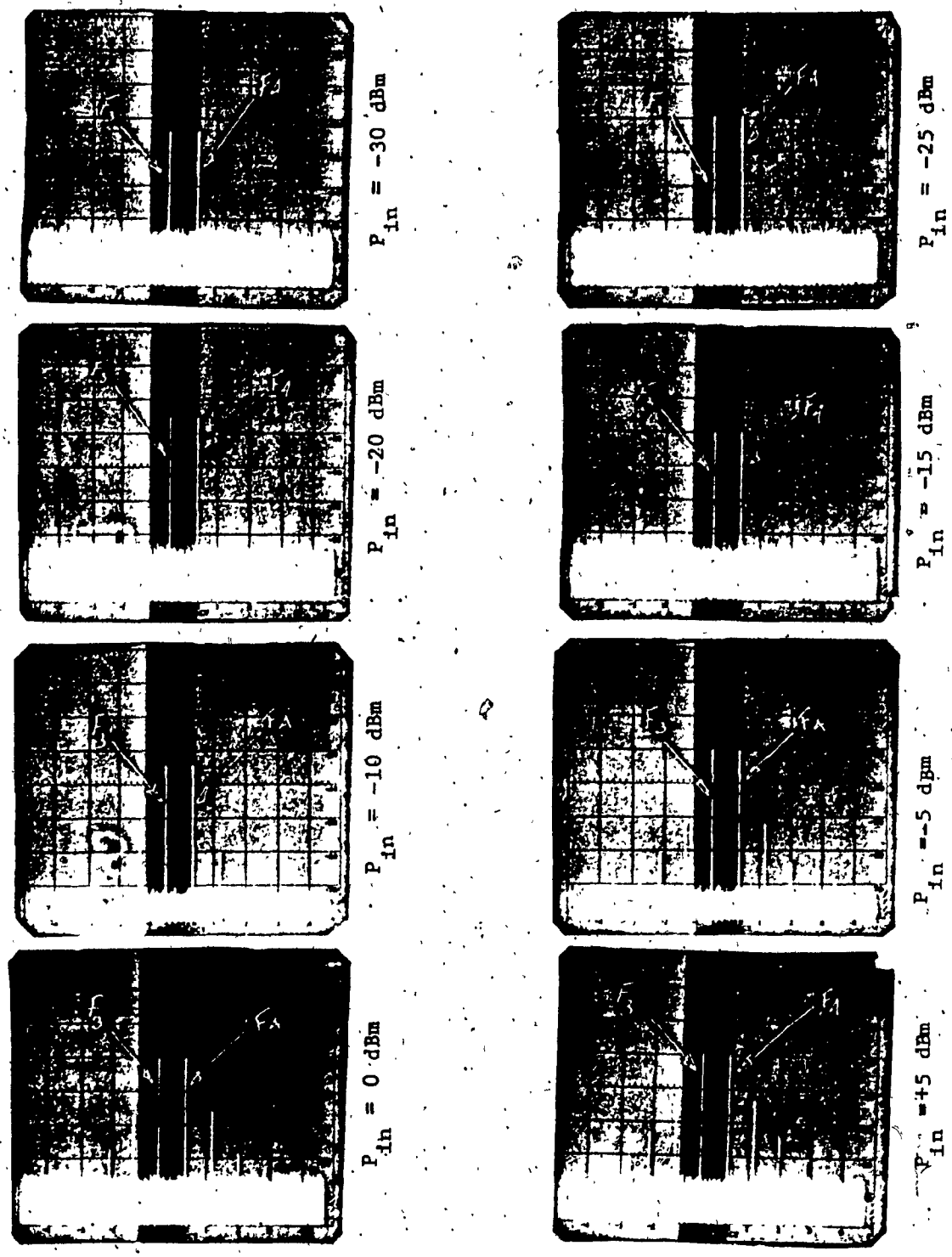

Fig. 5.13 - Photos of 3rd order I.M. Products of the Mixer

P_{in} = 2 frequencies in band) Input
F_1 = 14.100 GHz, F_2 = 14.150 GHz)
$F_{L.O}$ = 2.1667 GHz, $P_{L.O}$ = +5 dBm.
F_3 = 11.933 GHz, F_4 = 11.983 GHz) Output

two carriers case. The Table 5.2 was derived from the photographs in Figure 5.13. The absolute power levels were monitored by the power meter in the set-up.

The intercept point is then determined graphically from the results of Table 5.2, where the output carrier levels and the 3rd order IMD product levels are plotted against the input power level of one of the carriers. The intercept point of +8 dBm was determined by the graphical means as shown in Figure 5.14. It can be seen that at nominal maximum input power level of -30 dBm, the mixer is operating in a fairly linear region. The IMD ratio at the input level of -30 dBm (both carriers at nominal maximum level) is approximately 50 dB.

TABLE 5.2 - TWO TONE 3RD ORDER IMD DATA FOR THE CTS MIXER

P_{IN} dBm		P_{out}, dBm		3rd Order IMD Product
P_{F1}	$P_{F1} + P_{F3}$	P_{IN}=1 CARRIER	P_{IN}=2 CAR.	dBm
-35	-32	-38.50	-35.90	< -80
-30	-27	-34.30	-31.35	< -71.35
-25	-22	-29.45	-26.45	< -66.45
-20	-17	-24.70	-21.65	-63.65
-15	-12	-19.70	-16.40	-52.90
-10	-7	-15.30	-12.50	-43.50
-5	-2	-10.90	-8.10	-34.00
0	3	-6.75	-5.00	-23.00
+5	8	-3.8	-3.00	-16.00

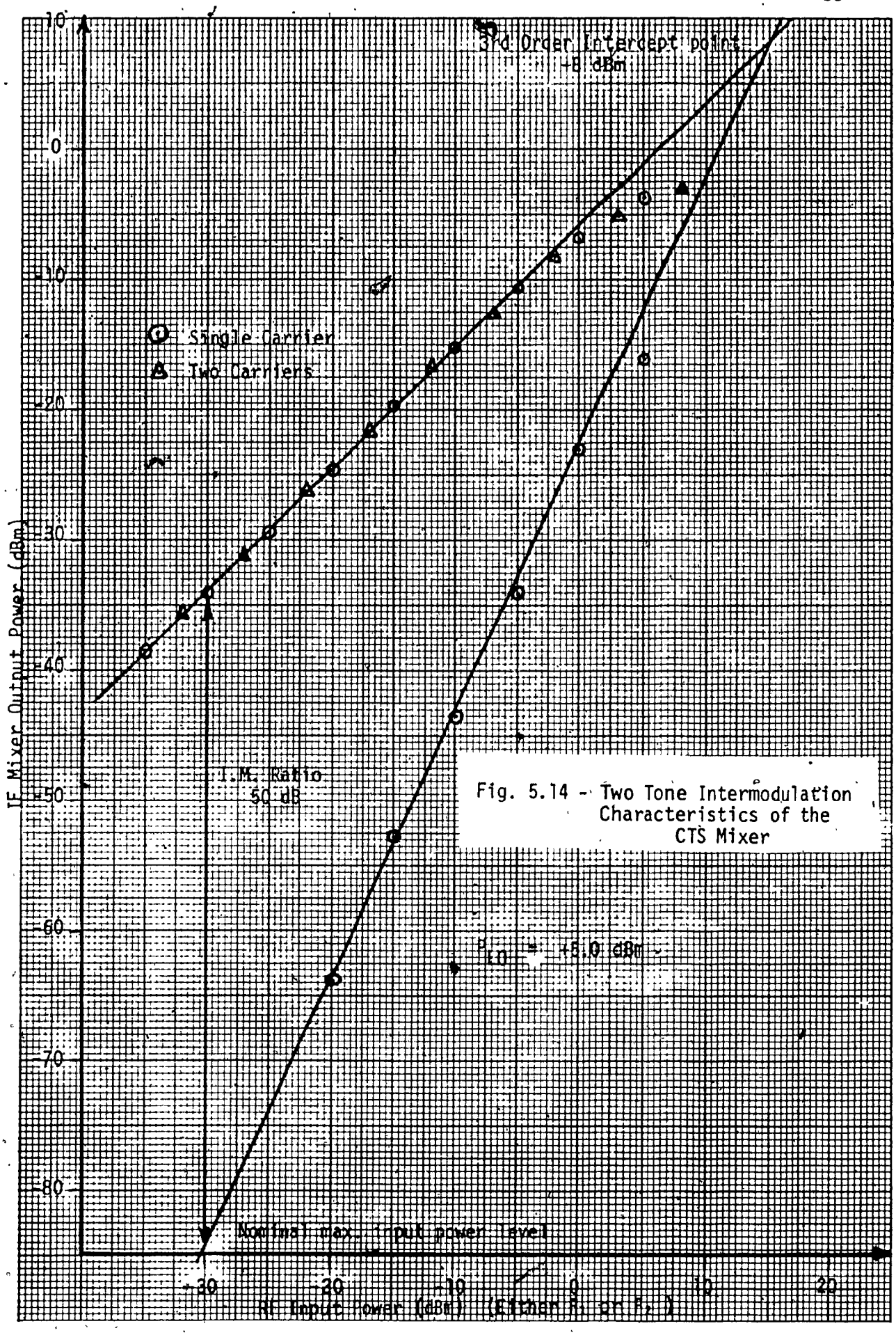

Fig. 5.14 - Two Tone Intermodulation Characteristics of the CTS Mixer

5.4.5 Noise Figure Measurements of the Frequency Translator

1) THEORY

The basic consideration in the design of the mixer and preamplifier is the receiver noise figure (F_0). The F_0 of a receiver is a measure of the sensitivity of the receiver. The lower the F_0, the lower the signal input power can be and still generates a meaningful output signal power. The equation that relates the CW receiver sensitivity to the F_0 and band width B of the receiver is given by equation (5.1) below[26].

$$S_n = KT_0F_0B \Longrightarrow S_n = [-174 + 10\log_{10}B + F_{0\,DB}]\ \text{dBm} \quad \ldots\ldots \quad 5.1$$

where F_0 = noise figure

B = bandwidth

$T_0 = 290^0$K, the standard noise temperature

K = Boltzmann's constant (1.38×10^{-23} joules/Kelvin).

A receiver with F_0 = 8 dB and B = 2 MHz would have a sensitivity of -103 dBm.

The definition of noise figure was given by equation 4.9 in Section 4.3, which we rewrite below in equation 5.2:

$$F_0 = (S_i/N_i)/(S_0/N_0) = (1/Ga)\cdot(N_0/N_i) = (1/Ga)\cdot(KT_1B/KT_0B) \quad \ldots \quad 5.2$$

where Ga = available power gain of the network = S_0/S_i.

The noise figure is a function of the frequency and hence is sometimes referred to as the spectral noise figure or noise factor. For a perfect device, F_0 equals unity. The closeness of F_0 to unity is the measure of superiority of the device from the noise point of view. However it should be emphasized here that the noise figure measures not the absolute but the relative quality of the device under test. It indicates the noisy-

ness of the device relative to the noisyness of the source. It is evident from the definition that the noise figure of the mixer can be made as close to unity as possible, merely by adding extra noise in the source. This obviously is not the proper solution for improving the performance of the mixer, since this approach merely makes the source so noisy that the mixer, in comparison, appears almost noise free.

The application of the noise figure expression for an attenuator or a filter operating at a temperature of $290^{o}K$, gives a noise figure equal to their loss. If the temperature is not $290^{o}K$ then the noise figure can be expressed as LT/T_o, where T is the actual temperature and L is the loss expressed as a ratio greater than unity. For the mixer which is an active network the effective noise temperature is different from the environment temperature. Thus, the noise figure of the mixer, is given by $F_m = L_c T_e/T_o = L_c N_R$ where L_c is the conversion loss of the mixer and N_R is its noise temperature (ratio) which is defined as the ratio of the effective noise temperature (T_e) to the standard noise temperature (T_o).

The overall noise figure of mixer and IF amplifier commonly used in a receiver is given by the following expression:

$$F_o = L_c(N_R + F_{IF} - 1)$$

or

$$(F_o)_{DB} = (L_c)_{DB} + 10\log_{10}(N_R + F_{IF} - 1) \quad \ldots\ldots\ldots\ldots\ 5.3$$

where F_{IF} is the noise figure of the IF amplifier. N_R and F_{IF} are numerical ratios, not expressed in decibels. The desired result is a low noise figure. Therefore $F_o = L_c(N_R + F_{IF} - 1)$ must be minimized by choice of bias, local oscillator power, and operating intermediate frequency. Figure

5.18 shows a typical curve of the overall noise figure versus L.O power resulting from the combination of the three quantities in equation (5.3). We can observe that the noise figure decreases in about the same way as the conversion efficiency increases for small L.O power drive (Fig. 5.6). For high L.O power, the conversion efficiency no longer increases so rapidly but the noise temperature (N_R) continues to increase. Therefore the overall noise figure goes through a minimum value and then increases again.

(ii) NOISE FIGURE MEASUREMENT PROCEDURES

From equation (5.2) we have

$$N_o = KT_oBFG$$

Expansion of this relation yields

$$N_o = [KT_oB + (F - 1)KT_oB]G = [KT_oB + KT_eB]\,G. \quad \ldots\ldots\ 5.4$$

where T_e is the effective input noise temperature - a measure of the internal noise of the transducer.

Equation (5.4) provides the basis for an indirect, but convenient, method of measuring noise figure. Figure 5.16a is a representation of equation (5.4). The actual transducer is replaced by its noiseless equivalent, i.e. one exhibiting the same gain-bandwidth characteristics. Noise source A is the input termination and noise source B is a fictitious source that represents the network's contribution to the noise output, referred to the input.

Figure 5.16a can be modified as indicated in Figure 5.16b, where a second input termination source C at a temperature T_2 is added. The available output power of the network for this termination will be given

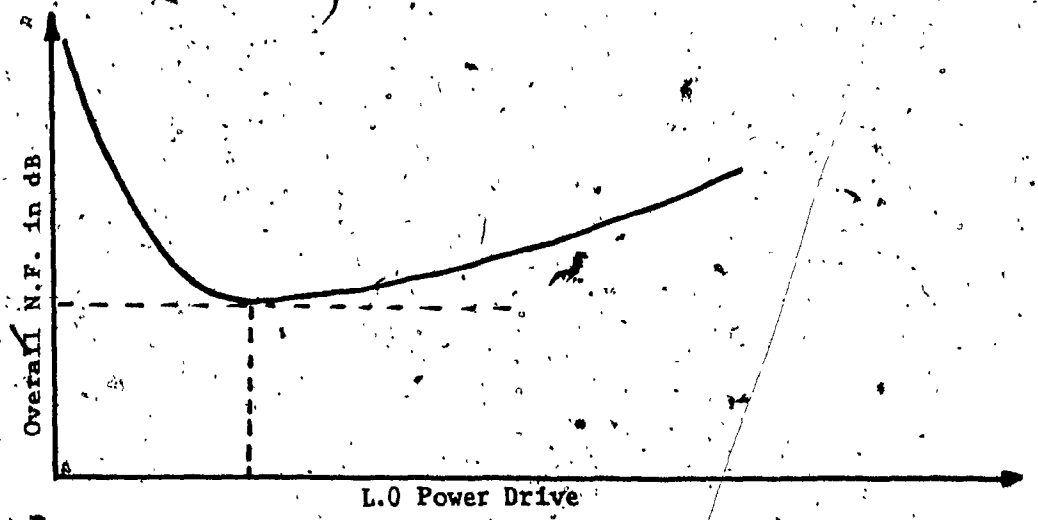

Fig. 5.15 - Overall noise figure vs local oscillator drive (typical)

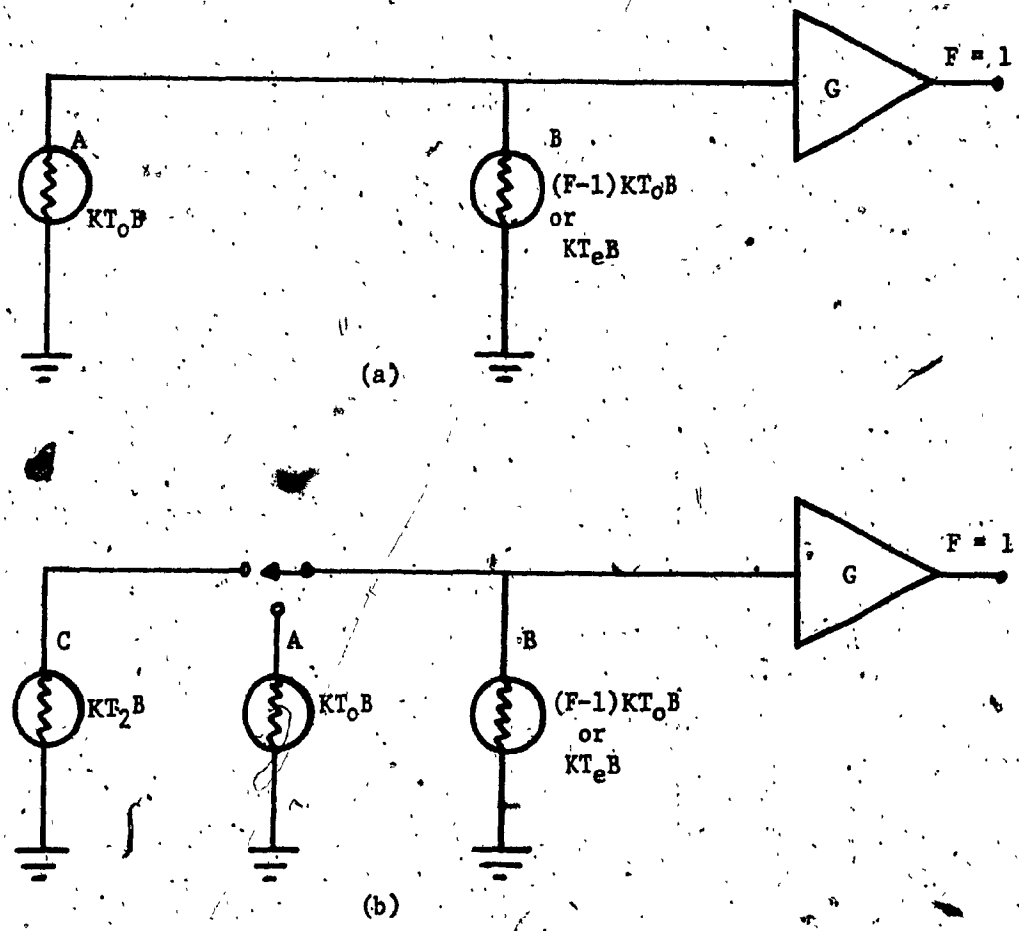

Fig. 5.16 - Equivalent noise representation of a noisy network.

by

$$N_o = [KT_2B + KT_oB(F - 1)]\,G \quad \ldots\ldots\ldots\ldots\ldots\ldots \quad 5.5$$

From equations (5.4) and (5.5) we have

$$\frac{N_{02}}{N_{01}} = \frac{[KT_2B + KT_oB(F - 1)]G}{KT_oBFG} = \frac{T_2 + T_o(F - 1)}{T_oF} \quad \ldots\ldots\ldots \quad 5.6$$

or

$$F = \frac{(T_2/T_o) - 1}{(N_{02}/N_{01}) - 1} = \frac{T_{ex}}{Y - 1} \quad \ldots\ldots\ldots\ldots\ldots\ldots \quad 5.7$$

where $T_{ex} = T_2/T_o - 1$ = ENR called "excess noise ratio"

and $Y = N_{02}/N_{01}$ is called "Y-factor".

Equation (5.7) is the basic relation for determining noise figure. If T_{ex} is known, which is a measure of the output capability of the noise generator (source), the ratio N_{02}/N_{01} can be measured and the noise figure can be computed from equation (5.7). This method of measuring the noise-figure is known as the manual Y-factor method. In the Y-factor method is allowed only single frequency measuements and the noise figure of the devise under test across the band has to be found point by point. When the highest level of accuracy is required, the Y-factor method should be used. Where many measurements must be performed or where determining the noise figure-frequency characteristic of a device, and ease of operation and measurement speed are of importance, another method must be used which is known as the "automatic" method. This method requires a direct reading indicator, such as a precision automatic noise figure indicator (PANFI), which electronically implements the Y-factor measurement and displays the results directly in noise figure. The direct reading indicator also provides the operator with the unique capability of observing changes in noise performance while the system is being tuned or set up.

iii) NOISE FIGURE TEST AND TEST RESULTS OF THE CTS MIXER

The test set-up for the noise figure (NF) measurements using the automatic method is shown in Figure 5.17. The basic elements are: the AILTECH 75 precision automatic noise figure indicator (PANFI), the AILTECH 76 solid state noise source of 15.5 dB ENR at 12.4 GHz to 15 GHz, and the AILTECH mixer and preamplifier. The PANFI sends a signal (square wave) of low audio frequency which periodically turns the noise source ON and OFF. The output of the mixer consists of square wave modulated noise. The two levels of this square wave represent the mixer and the mixer plus noise source noise. The AILTECH 75 PANFI is a 30 MHz instrument and an external AILTECH mixer is required. The local oscillator (RF sweep generator) is set to f_o + 30 MHz, where f_o is the midband output frequency of the mixer under test and 30 MHz is the IF frequency of the AILTECH mixer. The output of the AILTECH mixer is amplified by the preamplifier and then is applied to the noise indicator where we read the noise figure in dB on the meter. The RF level (L.O) is adjusted by using the variable attenuator for minimum reading of noise figure on the PANFI which is calibrated for the known ENR = 15.5 dB of the noise source. Then we set the RF generator (L.O) to sweep across the output bandwidth of the mixer under test, 11.8 to 12.15 GHz, and we read the noise figure on the noise indicator. A second output from the PANFI unit is available which can be applied to an oscilloscope or X-Y recorder in order to obtain a display or plot of the noise figure versus frequency characteristic of the mixer under test.

The measurement philosophy is that of substitution, i.e. with and without the mixer in the set-up. The test results for the noise figure of the test set-up alone and set-up plus the mixer under test are shown in Figs. 5.18, 5.19 respectively. To calculate the noise figure of the mixer we will use the equation (5.8) which gives the overall noise figure of a two stage device.

$$F_{12} = F_1 + \frac{F_2 - 1}{G_1} \quad \ldots\ldots\ldots\ldots\ldots\ldots\ldots\ldots\ldots\ldots\ldots\ldots (5.8)$$

$$\text{from which} \quad F_1 = F_{12} - \frac{F_2 - 1}{G_1} \quad \ldots\ldots\ldots\ldots\ldots\ldots\ldots\ldots\ldots\ldots (5.9)$$

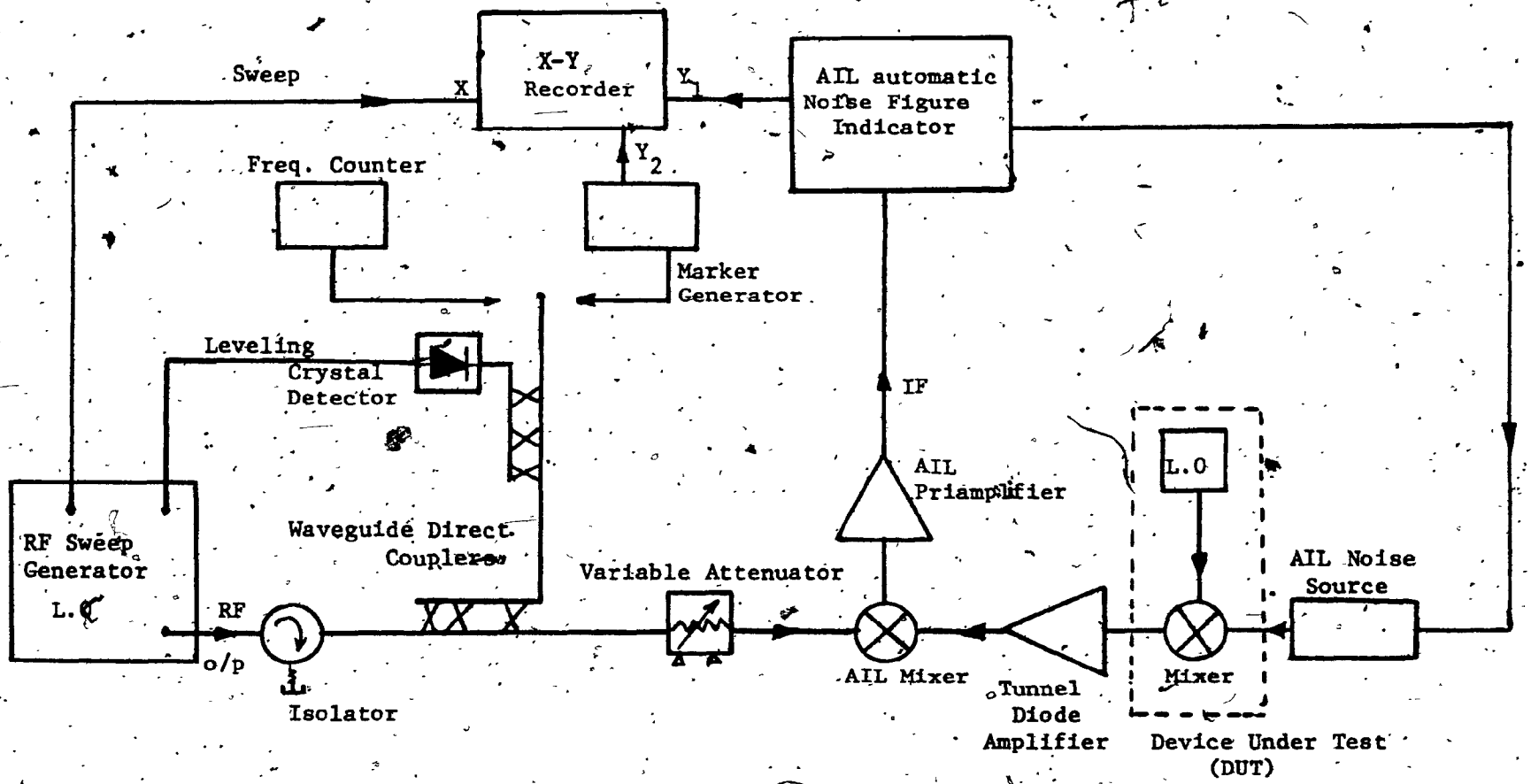

Fig. 5.17 - Test Set-Up for Noise Figure Measurement of the Mixer.

where all terms are in power ratios, and

F_1 = noise figure of the mixer under test

F_2 = noise figure of the rest of the test set-up

F_{12} = overall noise figure (mixer plus test set-up)

G_1 = is the gain (conversion loss) of the mixer under test.

In general, the overall noise figure for many stages is given by substituting the noise figure and gain of each stage into the cascade noise figure equation (5.10).

$$F_T = F_1 + \sum_{n=2}^{N} \frac{F_n - 1}{G_{in}} \quad \ldots\ldots\ldots\ldots\ldots\ldots\ldots\ldots \quad 5.10$$

where $G_{in} = \prod_{j=1}^{n-1} G_j$ represents the total gain preceding the n^{th} stage.

If F_{12}, F_2 and G_1 are known, F_1 the noise figure of the mixer can be calculated from equation (5.9). The conversion loss of the mixer is a very sensitive factor in the noise calculation since it is equivalent to a gain less than unity. Thus, the conversion loss has to be known accurately before a noise figure can be calculated from the noise measurement. Noise figure measurments of amplifiers are somewhat easier because G_1 is usually very much greater than unity and the second term of the RHS of the equation (5.9) has lesser effect on the accuracy of the measurement. In some cases, the second term can be totally ignored. However, such is not the case in this particular measurement.

From equation (5.9) with the value G_1 well established and the values of F_{12} and F_2 taken from Figure 5.18 and 5.19 (taking in consideration the 30 MHz IF frequency of the AILTECH mixer), the noise figure of the mixer is calculated. The calculation is done only for three frequencies (lower end, midband and upper end) but because the G_1, F_{12}, F_2 are flat,

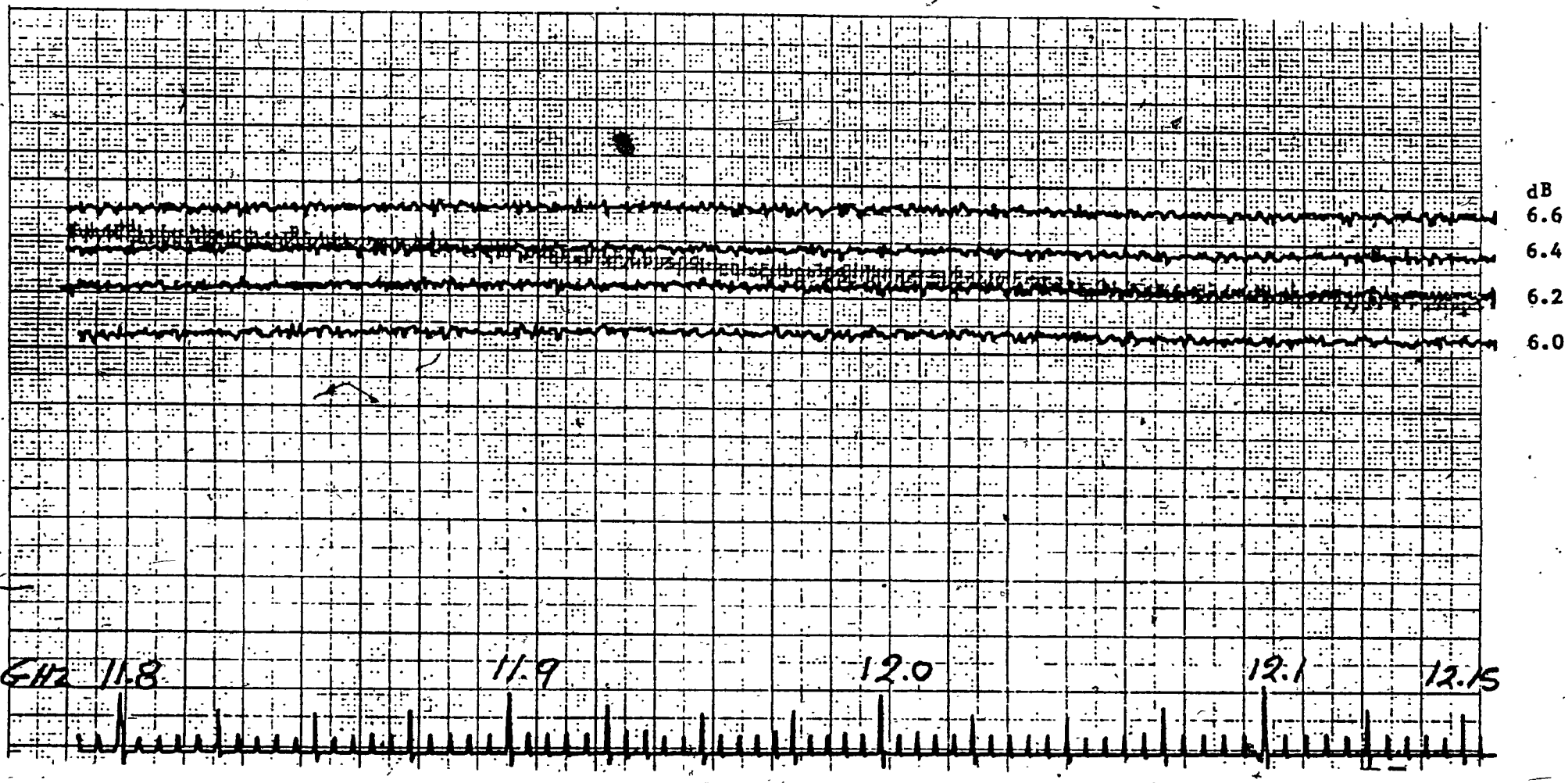

Fig. 5.18 – Noise Figure of the Test Set-Up.

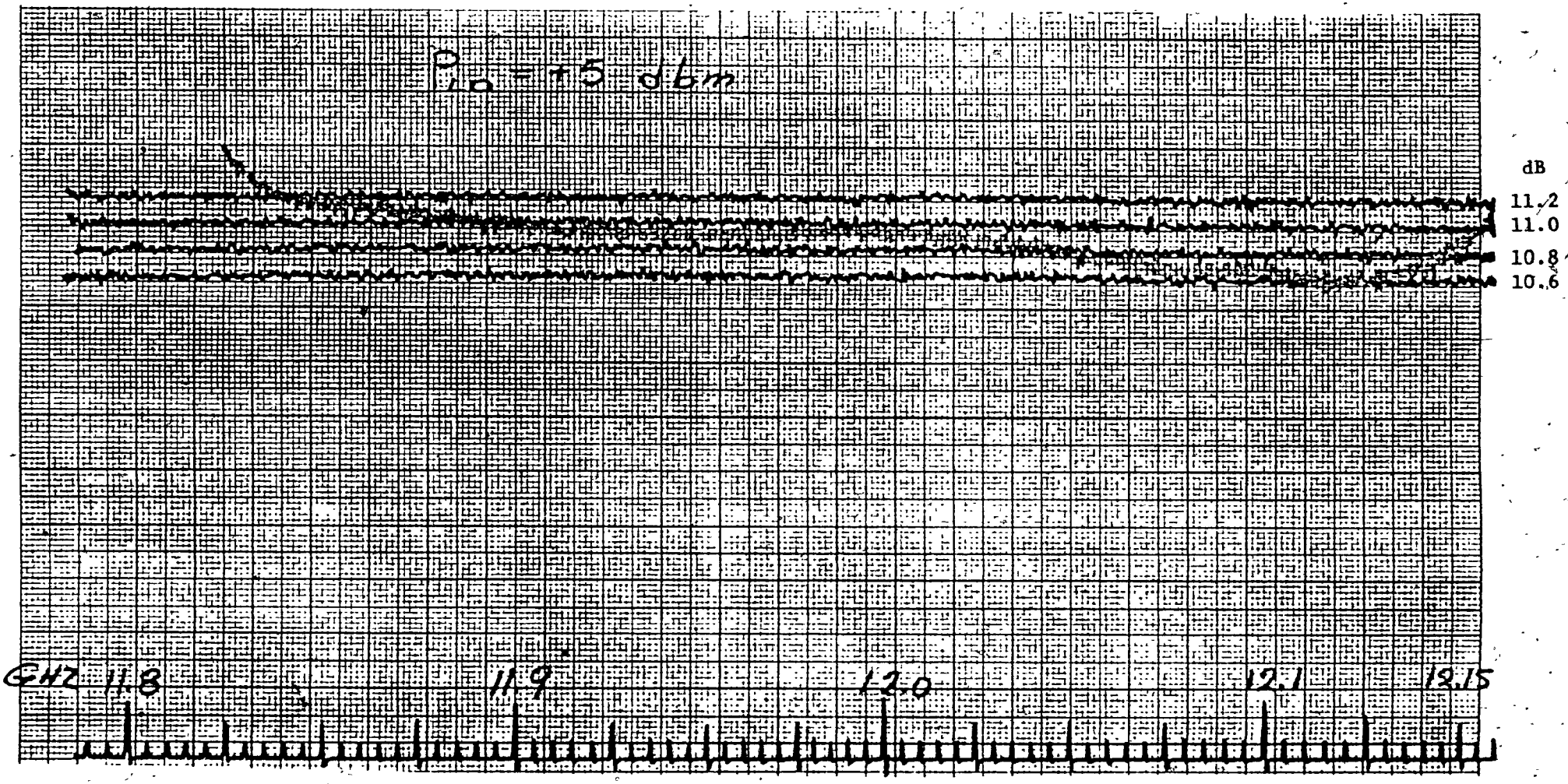

Fig. 5.19 - Noise Figure of the Flight Mixer S/N 2 and the Test Set-Up.

there will not be large variations from the calculated values for other frequencies. The results are shown below in Table 5.3.

TABLE 5.3 - NOISE FIGURE TEST DATA OF THE MIXER

FREQUENCY	F_{12}		F_2		G_1		F_1 Mixer N. Figure
GHz	dB	Linear	dB	Linear	dB	Linear	dB
Lower end of the band 11.813	11.2	13.18	6.45	4.42	-4.6	.346	5.18
Midband 11.983	10.95	12.45	6.3	4.27	-4.5	.354	5.06
Upper end of the Band 12.093	10.7	11.75	6.2	4.17	-4.4	.363	4.8

5.4.6 GROUP DELAY MEASUREMENTS

i) THEORY

The term, group delay, is used to describe the delay of a signal f(t) as it passes through a system. This delay can cause problems like crosstalk or intersymbol interference between baseband channels. With the system function given by equation (5.11), its group and phase delay t_{gr} and t_{ph} are defined by equation (5.12) and (5.13), respectively.[27] Thus, the t_{gr} is the slope of $\theta(\omega)$ at a given frequency ω, and t_{ph} is the slope of the line from the origin to a point $[\omega,\theta(\omega)]$ of the phase curve.

$$H(\omega) = A(\omega)_e^{-j\theta(\omega)} \quad \ldots\ldots\ldots\ldots\ldots\ldots\ldots\ldots \quad 5.11$$

$$t_{gr} = d\theta(\omega)/d\omega = .d(2\pi\frac{\theta}{360})/d(2\Pi f) = d\theta/df(360) \quad \ldots\ldots\ldots \quad 5.12$$

$$t_{ph} = \theta(\omega)/\omega \quad \ldots\ldots\ldots\ldots\ldots\ldots\ldots\ldots \quad 5.13$$

where θ = degrees, f = (Hz), t_{gr} = (seconds).

The terms, group and phase delay, are applied to inputs that are narrow-band in the following sense: suppose that the input to our system is amplitude modulated given by equation (5.14).

$$f(t) = f_m(t)\cos\omega_o t \quad \ldots\ldots\ldots\ldots\ldots\ldots\ldots \quad 5.14$$

We assume for the Fourier transform of the envelope $f_m(t)$ that

$$|F_m(\omega)| = 0 \quad \text{for } |\omega| > \Omega \quad \ldots\ldots\ldots\ldots\ldots\ldots \quad 5.15$$

where Ω constant, and that in the $(\omega_o - \Omega, \omega_o + \Omega)$ interval the ampltidue of $H(\omega)$ is constant and its phase linear:

$$A(\omega) = A(\omega_o) \qquad \omega_o - \Omega \leq \omega < \omega_o + \Omega \quad \ldots\ldots\ldots\ldots\ldots\ldots \quad 5.16$$

$$\theta(\omega) = \theta(\omega_o) + \theta'(\omega_o)(\omega - \omega_o) = \omega_o t_{ph} + (\omega - \omega_o)t_{gr}$$

Thus, the Fourier integral $F(\omega) = \mathcal{F}[f(t)] = 1/2\,[F_m(\omega + \omega_o) + F_m(\omega - \omega_o)]$ of the input f(t) is zero outside the band $(\omega_o - \Omega, \omega_o + \Omega)$ and its image, and in this band the system acts as an ideal symmetrical bandpass filter. Therefore the response (output) $f_o(t)$ is given by equation 5.17.

$$f_o(t) = f_m(t - t_{gr})\cos\omega_o(t - t_{ph}) \text{ for } A(\omega_o) = 1. \quad \ldots\ldots \quad 5.17$$

From equation (5.17) we see that the group delay t_{gr}, evaluated at the carrier frequencey $\omega = \omega_o$, is equal to the delay of the envelope $f_m(t)$ of the input and the phase delay t_{ph}, is equal to the delay of the carrier (Figure 5.20).

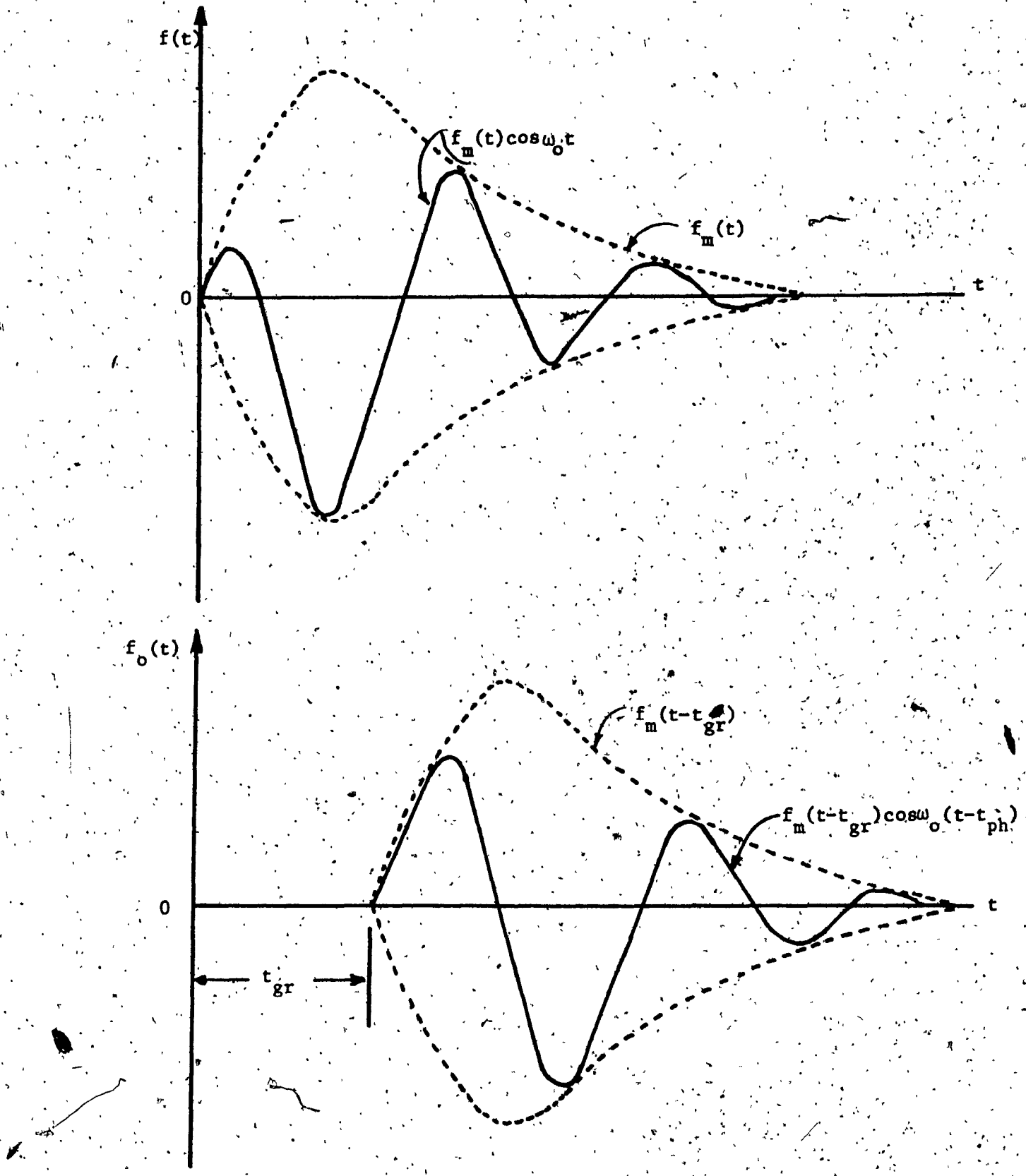

Fig. 5.20 - Group and Phase Delay Representation.

ii) GROUP DELAY MEASUREMENT

The theory just discussed is applied for measuring the group delay using the test set-up shown in Figure 5.21. The group delay indicator measures the envelope delay encountered as an RF signal, modulated at either a 1 MHz or 200 KHz rate and it is passed through the device under test (DUT). The external RF generator provides a continuous wave RF signal to the modulator unit where it is modulated either by 1 MHz or 200 KHz. The selected modulating frequency is obtained from the frequency generator of the group delay indicator. The modulated RF signal from the modulator unit is applied to the input of the DUT and the output of the DUT is applied to the detector unit. The detector recovers the 1 MHz or 200 KHz envelope that has been shifted in phase (time) in passing through the DUT. The output of the detector unit is applied to the group delay indicator where we read the group delay on the meter. A second output from the group delay indicator is available which can be applied to an oscilloscope or recorder in order to obtain a display or plot of the group delay when the RF generator is operated in the swept frequency mode. The RF signal power to modulator is set to + 5 dBm (+10 dBm max.) and the variable attenuator is used to adjust the signal level until it is within the specified range.

The group delay measurement of the mixer was performed with the whole receiver assembly and the results are shown in Figure 5.22. Since, in the receiver, only the filters of the mixer affect the group delay the results would be the same if the mixer was tested alone. We can see from Figure 5.22 that the group delay variation is less than 0.5 nsec for TB1 and 1.5 nsec for TB2 band for both receivers.

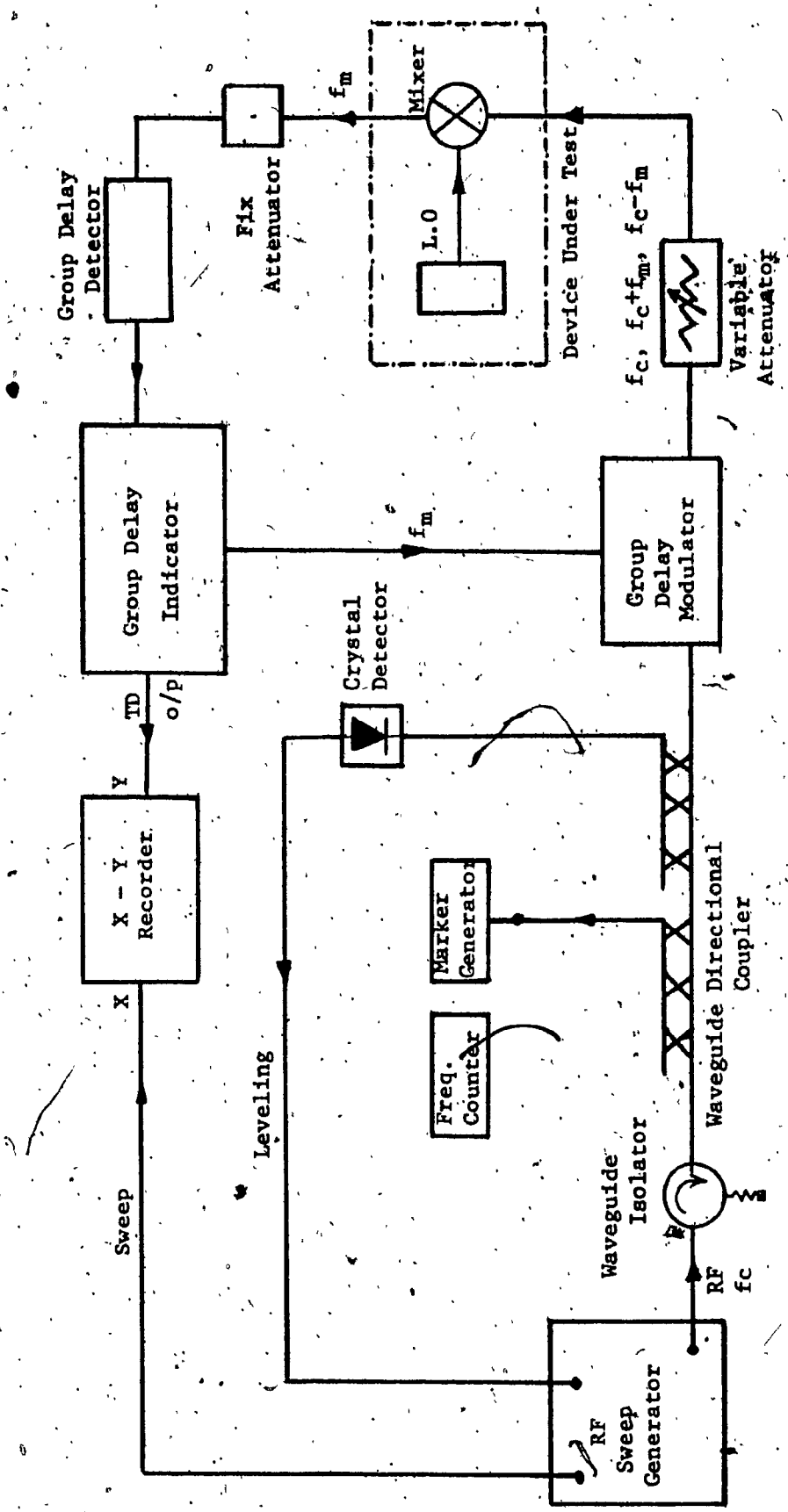

Fig. 5.21 - Test Set-up for Group Delay Measurement.

Fig. 5.22 - Group Delay for RCVR No. 1 and RCVR No. 2

Sensitivity = .5ns/div

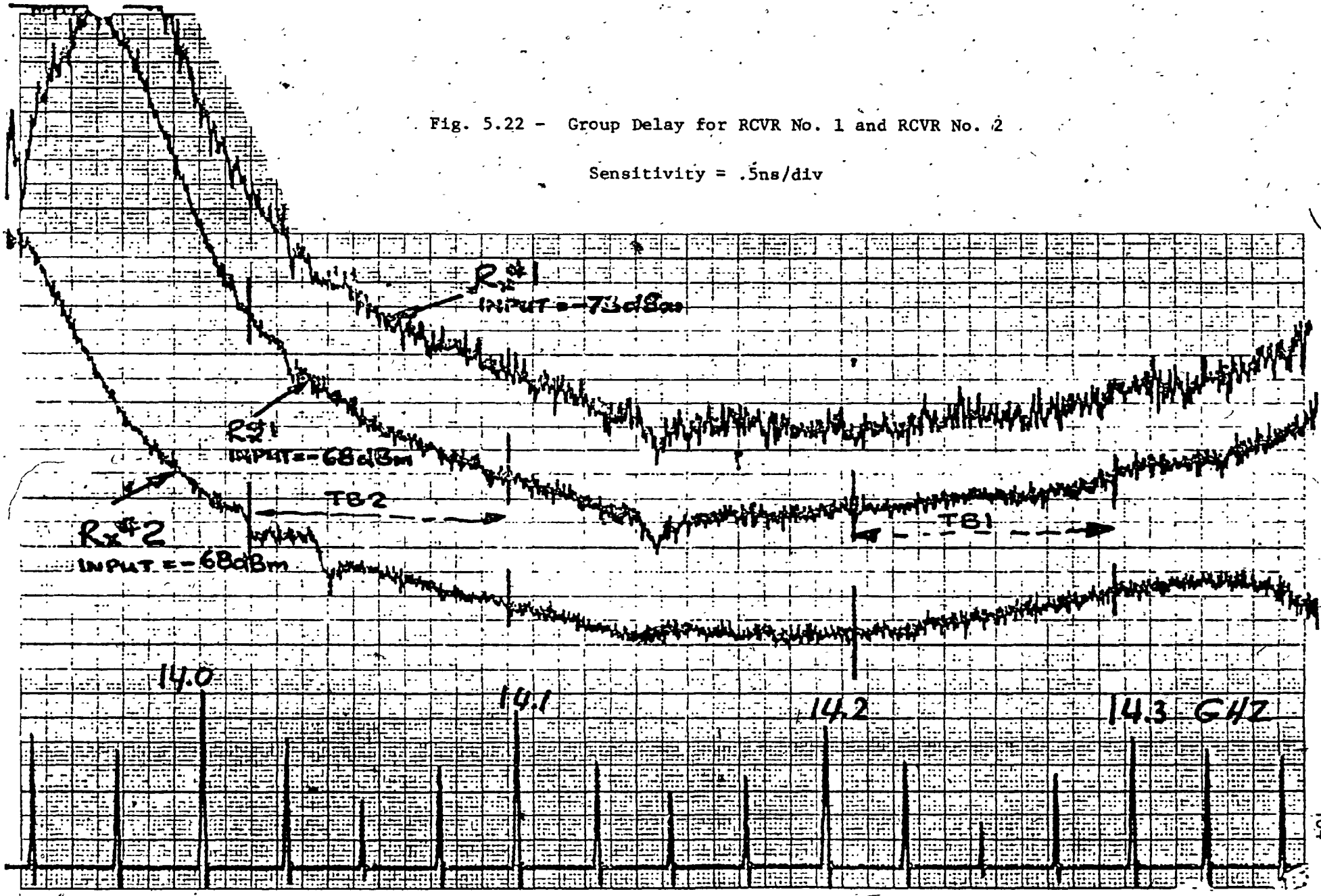

5.4.7 Effects of L.O Power Variations on Mixer Parameters

All the tests so far have been run with the mixer driven by a constant local oscillator (L.O) power and frequency. In actual practice a change in L.O power level of ± 0.3 dB within the specified temperature range is possible. The present section deals with the effects of a L.O power variation on the mixer performance.

The critical parameters of the mixer that have to be monitored while the L.O power level is being varied are: conversion loss, gain flatness, and the spurious level. The return loss of the mixer was not greately affected by the L.O power level variation, especially with a variation of the order of ±0.5 dB. Thus the return loss was not monitored during the experiment. The mixer was tuned for best performance with a L.O power drive of +5.6 dBm. The L.O power was then varied on either side of +5.6 dBm. The results are summarized in the Table 5.4 and Figure 5.23 is a graphic representation of the results obtained in this test. It appeared that the conversion loss and gain flatness actually improved when the L.O drive was reduced. The spurious level, on the other hand, is rising sharply on either side of the optimum L.O level. For a ± 0.5 dB excursion of L.O level the spurious degradation is 9.5 dB. In the actual case, the spurious level should at most degrade 7 dB since the expected L.O level fluctuation is ±0.3 dB or less.

TABLE 5.4 - DATA ON VARIATIONS OF CONVERSION LOSS, GAIN FLATNESS AND SPURIOUS LEVEL VS L.O POWER OF THE MIXER

L.O Power dBm	Conversion Loss dB	Gain Flatness dB Peak-to-Peak	Spurious Level dB below carrier
5.2	4.2	.19	35
5.3	4.23	.20	38
5.4	4.26	.20	40
5.5	4.30	.20	42
5.6	4.30	.20	44
5.7	4.30	.235	44
5.8	4.33	.24	42
5.9	4.37	.26	37
6.0	4.40	.29	35
6.1	4.45	.30	34.5
6.2	4.50	.33	32.5

5.4.8 TEMPERATURE CYCLING TEST OF THE FREQUENCY TRANSLATOR

This test was an attempt to demonstrate the ability of the mixer to function within specifications under the allowable temperature variations. The specified temperature range is from $0^{o}C$ to $+55^{o}C$ and the survival and storage range is from $-50^{o}C$ to $+75^{o}C$. For this particular test, it was decided that parameters such as conversion loss, gain flatness and spurious level be measured but not the VSWR of the mixer. Because of

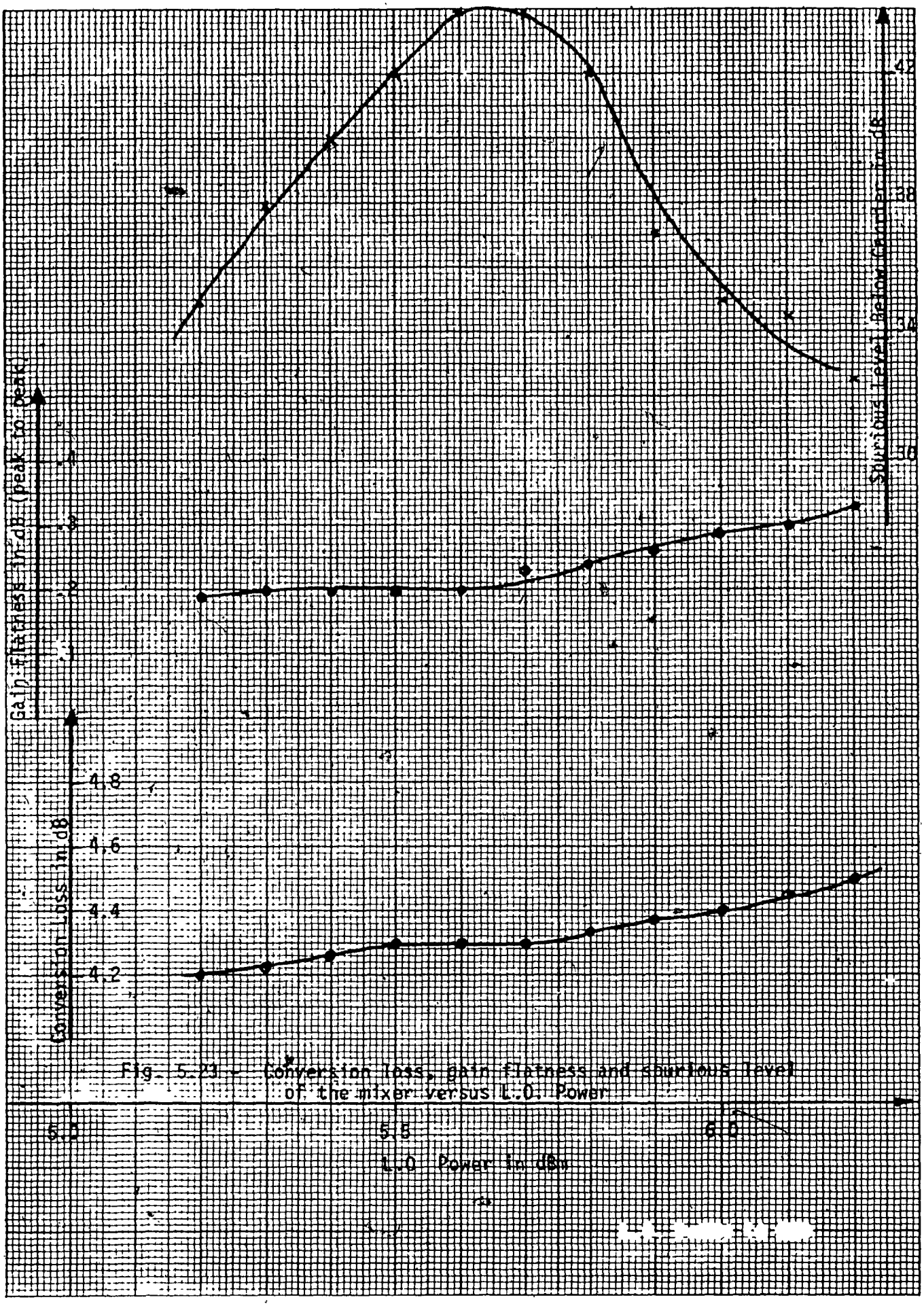

Fig. 5.23 - Conversion loss, gain flatness and spurious level of the mixer versus L.O. Power

the temperature chamber the mixer had to be connected to the outside test equipment through waveguide bends and runs developing a certain amount of mismatch. Under such conditions, the temperature cycling test should demonstrate only the change or degradation in performance due to temperature variations.

At low temperatures, there was a noticeable degradation of the spurious level, but the mixer performance was more susceptable to high temperatures. Input return loss degradation over the specified temperature range was 0.5 dB. Similar degradation was expected had the mixer been tuned into a matched system to meet the return loss specification. The results of the temperature cycling test are summarized in Table 5.5. It can be safely concluded that under temperature cycling conditions and for constant L.O drive and RF input, the mixer meets the return loss, gain flatness, conversion loss and spurious specifications.

TABLE 5.5 - DATA ON VARIATIONS OF CONVERSION LOSS, GAIN FLATNESS AND INBAND SPURIOUS LEVEL OF THE FREQUENCY TRANSLATOR VS TEMPERATURE CHANGE

Temperature °C	Conversion Loss dB	Gain Flatness dB Peak-to-Peak	Spurious Level dB below carrier
25 ambient	4.40	.2	34
0	4.35	.3	32
-5	4.30	.4	32
25 from ~~-5°C~~	4.40	.2	35
55	4.75	.25	40
60	4.80	.25	39
Specifications	5	.3	-

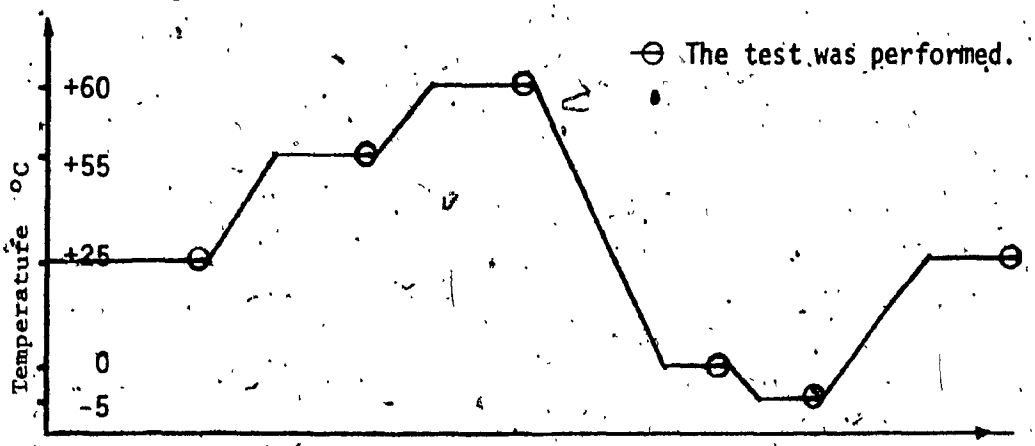

Fig. 5.24 - Temperature Cycle

5.5 Summary of Test Results

The results obtained from the previous tests carried out on the CTS frequency translator are summarized in the Table 5.6. The following notes should be made concerning this table.

The parameters: noise figure, group delay and output intercept point, were not required to be measured for the mixer itself during thermal cycling but in the next higher assembly, that is the receiver.

The VSWR was not measured during thermal cycling because of the mismatches developed by the waveguide bends and runs, that connect the mixer to the test equipment outside of the temperature chamber. Under such conditions only the changes due to temperature variations were noted. It was found that the VSWR was better at low temperatures.

For the mixer to be connected in the receiver's assembly, two waveguide-to-coaxial adaptors, on either side were required. The use of these adaptors affected mainly the VSWR, conversion loss and the weight of the mixer in the following way. The conversion loss was increased from about 3.80 dB to 4.40 dB and the VSWR to 1.5:1. Finally, the overall weight of the mixer was itself increased to 0.44 lb.

TABLE 5.6 - SUMMARY OF THE TEST RESULTS OF THE FREQUENCY TRANSLATOR

ITEM	VALUE AT AMBIENT	WORST VALUE IN THERMAL CYCLING FROM -5 to + 60°C Temp. Range	SPECIFICATIONS VALUE
Input Frequency band	13.970 - 14.320 GHz	13.970 - 14.320 GHz	13.974 - 14.324 GHz
Output frequency band	11.803 - 12.153 GHz	11.803 - 12.153 GHz	11.807 - 12.157 GHz
Conversion loss	4.40 dB	4.80 dB	5.0 dB
Gain flatness	0.2 dB peak to peak	0.4 dB peak to peak	0.3 dB peak to peak
Noise figure	5 dB average	N/A	8.0 dB
Group delay	1.5 nsec for TB_2, 1 nsec for TB_1	N/A	1 nsec over 85 MHz
Output intercept point	+8 dBm	N/A	-6 dBm
Input & output VSWR	1.5:1	N/A	1.5:1
Local oscillator drive	+5 dBm	+5 dBm	+9 dBm
Continuous RF overdrive	+30 dB	+30 dB	+30 dB
Inband spurious	44dB below carrier	32 dB below carrier	32 dB below carrier
Weight	0.44 lb	0.44 lb	0.5 lb

The small changes demonstrated during the thermal cycling were due mostly to the variations of the crystal diode performance, and to the small changes of dimensions in the filters and tuning screws.

CHAPTER VI

CONCLUSIONS AND RECOMMENDATIONS

The objective of this Technical Report was to demonstrate the importance of the world's most powerful communications technology satellite (CTS) and its 14/12 GHz frequency translator which is one of its advanced technology units.

The CTS realized the dream of using small, simple and low cost earth terminals to provide communications to previously inaccessible northern-areas.

The performance data of the frequency translator summarized in Table 5.6, have shown that the unit's performance exceed the design requirements.

Although the downconverter (mixer) reported here is characterized as having low noise and low conversion loss, which are the most important factors in setting the entire system performance, it is still far above those theoretically possible with Schottky-barrier diode mixers. Theoretically, the conversion loss can be as small as a few tenths of a dB[24]. The practical problems which are involved in achieving very low conversion loss, center around the terminating impedances at the different frequencies involved. Therefore, careful attention of the RF circuit construction is required.

Since every communication system uses a mixer at the front end, it is desirable to have mixers with gain rather than loss, because

of the low signal power available at that stage. By using crystal diode mixers we can reduce the conversion loss to a few tenths of a dB but we can not get any gain. If we use a transistor, instead of a crystal diode as the nonlinear element for the mixer, we can have conversion gain instead of losses. For example, a square-low or exponential, voltage in-current out, characteristic is approximated quite closely by many field effect transistors (FET) and bipolar transistors respectively, operating in their "constant current" region. In this case one applies the incoming signal and the local oscillator voltages so that they effectively add to the dc bias voltage to produce the total gate-source or base-emitter voltage. This signal is then passed through the device nonlinearity to create the desired sum and difference frequencies.

Microwave FET transistors have been designed and successfully fabricated, and a lot of development work goes on to build microwave FET mixers. In the never-ending drive toward better performance, the microwave FET transistors in combination with integrated circuit techniques are making possible the design of microwave mixers with conversion gain and greatly reduced size and cost. As in the past, the user's necessities will prove to be the mother of invention.

It is hoped that this report has shown a general view of the operation of CTS satellite and its capabilities.

REFERENCES

1. C.A. Franklin and E. H. Davison, "A High Power Communications Technology Satellite for the 12 and 14 GHz Bands", American Institute of Aeronautics and Astronautics (AIAA), Paper No. 72-580, 4th Communications Satellite Systems Conference, Washington, D.C., April 24-26, 1972.

2. "Communications Technology Satellite", Communications Research Centre (CRC) serial document 06-RI & PS-1, March 1972. Revised May 1973.

3. V. O'Donova, G. Lo and A. Bell, L. Braun, "Design of a 14/12 GHz Transponder for the Communications Technology Satellite", American Institute of Aeronautics and Astronautics (AIAA) paper No. 72-734, CASI/AIAA Meeting: Space-1972 Assessment, Ottawa, Canada, July 10-11, 1972.

4. RCA Second Intermediate Design Review of the Super High Frequency (SHF) Transponder, Volume II, IIa. July 1973.

5. "Requirements, SHF Communications Transponder", Communication Research Centre (CRC) Document Ref. No. SS01-06, May 1973.

6. H.C. Torrey and C.A. Whitmer, "Crystal Rectifiers", McGraw Hill Book Co., New York, 1948, Chapter 5.

7. H.A. Watson, "Microwave Semiconductor Devices and Their Circuit Applications", McGraw-Hill Book Co., New York, 1969, Chapter 11, Equation 11.12.

8. H. A. Watson, "Microwave Semiconductor Devices and Their Circuit Applications", McGraw-Hill Book Co., New York, 1969, Chapters 11 and 12.

9. Microwave Associates, Inc., "High RF Burnout Resistance Mixer Diodes", Microwave Journal, Vol. 13, pp. 26, 1970.

10. H.C. Torrey and C.A. Whitmer, "Crystal Rectifiers", McGraw-Hill Book Co., New York, 1948, Chapter 8.

11. M. R. Barber, "Noise Figure and Conversion Loss of Schottky Barrier Mixer Diode", IEEE Tran. Microwave Theory Tech. vol. MTT-15, pp. 629-635, Nov. 1967.

12. H. C. Torrey and C. A. Whitmer, "Crystal Rectifiers", McGraw-Hill Book Co., New York, 1948, Chapter 5, equation 105.

13. R. Y. Pound, "Microwave Mixers", McGraw-Hill Book Co., 1948, Chapter 2, Section 2.6.

14. K.M. Johnson, "X-Band Integrated Mixer with Reactively Terminated Image," IEEE Tran. on Electron Devices, July 1968.

15. T. S. Saad, "The Microwave Mixer", Sage Laboratories, Incorporated, pp. 1-35, 1966.

16. R. V. Pound, "Microwave Mixers", McGraw-Hill Book Co., New York, 1948, Chapter 6.

17. J. Chacran and R. Tenenholtz, "Recent Advances in Microwave Mixers", The Institute of Radio Engineers (IRE) Convention Record, 1961, part 3, pp. 139-146.

18. M. Cohn, J.E. Degenford and B.A. Newman, "Harmonic Mixing with an Antiparallel Diode Pair", IEEE Transactions on MTT, Vol. MTT-23, No. 8, August 1975.

19. H.C. Torrey and C. Whitmer, "Crystal Rectifiers", McGraw-Hill Book Co., New York, 1948, Chapter 10.

20. T. L. Osborne, L.V. Kibler and W.W. Snell, "Low Noise Receiving Down Converter", Bell Syst. Techn. J., Vol. 48, pp. 1651-1663, July-August, 1969.

21. N.K.M. Chitre and M.V. O'Donovan, "Computer Aided Design of Waveguide Filters", RCA Engineer, Vol. 12, No. 1, June 1966.

22. G.L. Matthaei, L. Young and E.M.T. Jones, "Microwave Filters, Impedance Matching Networks and Coupling Structures", McGraw-Hill Book Co., New York, 1964, Chapter 7.

23. R. L. Eisenhart and P. J. Khan, "Theoretical and Experimental Analysis of a Waveguide Mounting Structure", IEEE Transactions on Microwave Theory and Techniques, Vol. MTT-19, No. 8, August 1971, pp. 706-719.

24. C. Dragone, "Amplitude and Phase Modulations in Resistive Diode Mixers", B.S.T.J., July-August 1969, pp. 1967-1998.

25. G.L. Matthaei, "Tables of Chebyshev Impedance-Transforming Networks of Low-Pass Filter Form", Proceedings of the IEEE Vol. 52, pp. 939-963, August 1964.

26. Anazac Electronics "Application Notes", March 1970, pp. 248-249.

27. A. Papoulis, "The Fourier Integral and Its Applications". McGraw-Hill Book Company, Inc., 1962, Chapter 7, pp. 134.

APPENDIX A

DETAILS OF THE DIODE CHARACTERISTICS

HEWLETT hp PACKARD

COMPONENTS

MICROWAVE MIXER HOT CARRIER DIODES 6-18 GHz

5082-2234
5082-2235
5082-2701 thru 2703
5082-2706 thru 2708
5082-2711 thru 2714
5082-2721 thru 2724

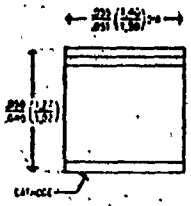

PACKAGE 44

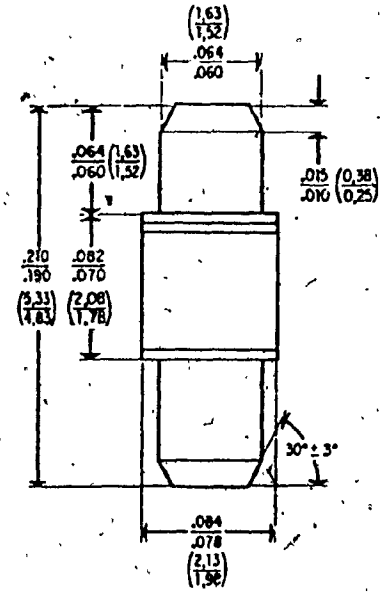

PACKAGE 49

Dimensions In Inches & Millimeters
Cathode End Indicated
By Color Code

Features

- Low and Stable Noise Figure
  - Less than 6.0 dB at 10 GHz
  - Less than 6.5 dB at 16 GHz
- High Burnout Rating
  - 1 W RF Pulse Power Dissipation
- High Uniformity
  - VSWR of 1.5:1 Assures Repeatable RF Impedance
- Rugged Design
  - Two Hermetically Sealed Package Styles Available
- Excellent Environmental Capabilities

Description

These mixer diodes are silicon hot carrier (Schottky barrier) diodes of planar, epitaxial passivated chip design. The processing technique used produces a diode family with extremely uniform electrical characteristics. A very tight tolerance in junction capacitance and a minimized series resistance provide a uniform RF impedance from diode to diode and low and stable noise figure characteristics. In the rugged and hermetically sealed metal, ceramic packages, the conventional cat whisker has been replaced by the more reliable thermocompression bond. This construction allows the device to be used in environments requiring reliable performance during high shock and vibration.

Applications

The hot carrier diodes described in this data sheet are optimized for use in broad and narrow band stripline, coaxial, or waveguide mixer assemblies operating from 6 to 18 GHz and above, where low noise and high reliability are of importance. This excellent uniformity of the hot carrier diode RF characteristics allows the design of mixer assemblies with predictable performance characteristics and makes the devices field replaceable with no circuit adjustments. Typical equipment applications include telecommunication receivers, ECM/radar front ends, and OEM mixer assemblies where sensitivity and high burnout power are required.

Devices with relaxed specifications (i.e. NF less than 7.0 dB and VSWR less than 2:1 in X-Band) are provided for high level frequency conversion applications required in microwave frequency synthesizers and low power up-converters.

Absolute Maximum Ratings

T_{OPR}		— Operating Junction Temperature Range	−60° C to +150° C
T_{STG}		— Storage Temperature Range	−60° C to +150° C
P_{DISS}	(Pulse)	— Pulse Power Dissipation at T_A = 25° C (Notes 1, 2, 3)	1W
P_{DISS}	(CW)	— CW Power Dissipation at T_A = 25° C (Notes 2,3)	200 mW
I_F		— DC Forward Current at T_A = 25° C (Note 3)	100 mA

Electrical Specifications at T_A=25°C

FREQUENCY RANGE, GHz	PART NUMBER 5082-	CONFIGURATION	PACKAGE OUTLINE	NOISE FIGURE dB TYP.	NOISE FIGURE dB MAX.	IF IMPEDANCE Ω MIN.	IF IMPEDANCE Ω MAX.	VSWR
6-14 (TEST FREQUENCY 9.375 GHz)	2713	SINGLE	49	5.8	6.0	200	400	1.5:1
	2714	MATCHED PAIR						
	2701	SINGLE	44	5.8	6.0	200	400	1.5:1
	2706	MATCHED PAIR						
	2711	SINGLE	49	6.3	6.5	200	400	2.0:1
	2712	MATCHED PAIR						
	2702	SINGLE	44	6.3	6.5	200	400	1.5:1
	2707	MATCHED PAIR						
	2234	SINGLE	49	6.8	7.0	200	400	2.0:1
	2235	MATCHED PAIR						
	2703	SINGLE	44	6.8	7.0	200	400	1.5:1
	2708	MATCHED PAIR						
10-18 (TEST FREQUENCY 16.0 GHz)	2723	SINGLE	49	6.3	6.5	200	400	1.5:1
	2724	MATCHED PAIR						
	2721	SINGLE	49	6.8	7.0	200	400	2.0:1
	2722	MATCHED PAIR						
TEST CONDITIONS	—	—	—	(NOTES 4,5)		(NOTE 7)		(NOTE 4)

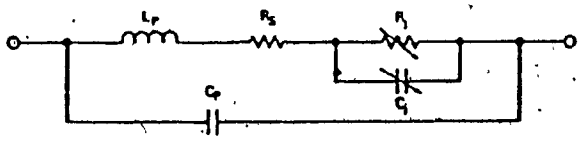

Figure 1. Equivalent Circuit of Packaged Diode.

Typical Equivalent Circuit Parameters at T_A=25°C

PART NUMBER 5082-	PACKAGE OUTLINE	L_P	C_P	R_S	R_j	C_j
2701–2703 2706–2708	44	0.4	0.13	9	100	0.15
2711–2714 2234 2235	49	1.0	0.15	9	100	0.15
2721–2724	49	1.0	0.15	9	100	0.13
UNITS	—	nH	pF	Ω	Ω	pF
TEST CONDITIONS	—	NOTE 6	—	—	NOTE 4	NOTE 4

NOTES:

1. 1 μs pulse, Du = .001.
2. Power absorbed by the diode. Frequency range: X- or Ku-Band, DC load resistance <1 Ω. Cathode stud is connected to infinite heat sink.
3. Derate linearly to zero at 150°C.
4. Measurements are performed on the diode in a fixed tuned mount.

Local Oscillator Power . . . . . 1 mW
Local Oscillator Frequency . . . (See Diode Test Frequency)
IF Frequency . . . . . 30 MHz
DC Load Resistance . . . . . <1.0 Ω

For matched pairs, the following additional specifications apply:

Noise Figure Match . . . . . $\Delta NF \leq 0.3$ dB
IF Impedance Match . . . . . $\Delta Z_{IF} \leq 25\ \Omega$

5. Single sideband receiver noise figure including an IF amplifier noise figure of 1.5 dB.
6. Series inductance of a coaxial line consisting of the diode with short circuited chip as inner conductor and an outer conductor of 0.18 inch diameter. The ends of the coaxial line are defined by the ends of the diode (for package outline 44) or by the steps to .083 in diameter (for package outline 49).
7. Same conditions as Note 4, except IF frequency is 10 KHz.

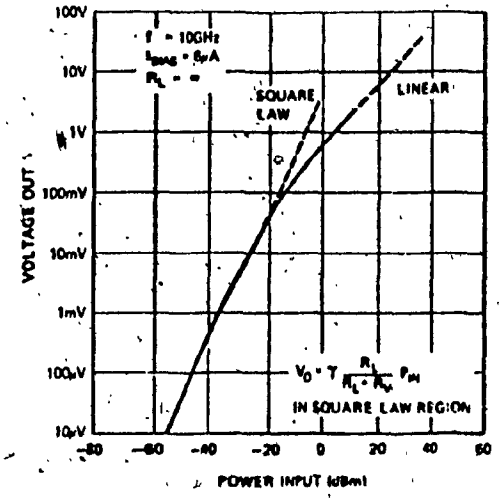

Figure 2. Typical Detected Voltage vs. Input Power. Voltage Sensitivity = 3 mV/μW Typical.

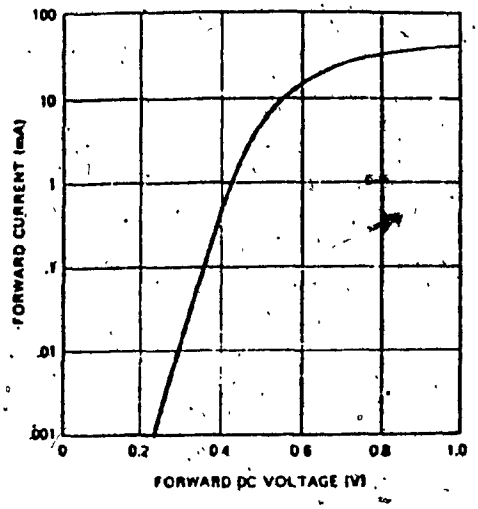

Figure 3. Typical Forward Characteristics.

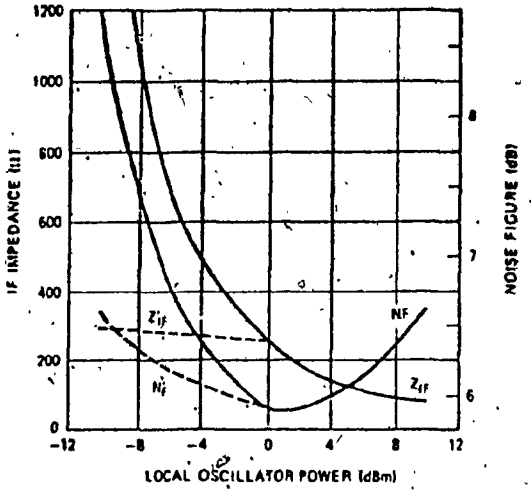

Figure 4. Typical Noise Figure and IF Impedance for 5082-2702 and 2711 vs. Local Oscillator Power. Note the improved performance at low levels of L.O. power when d.c. bias is superimposed (dashed curves).

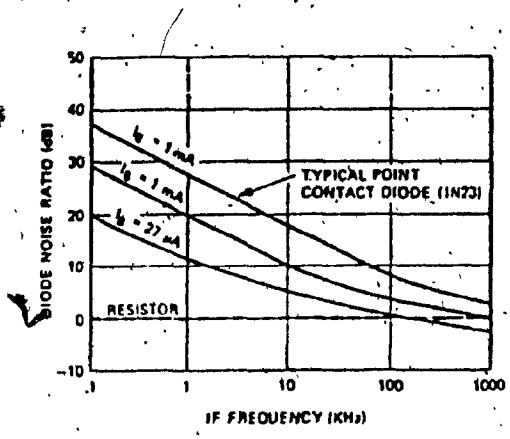

Figure 5. Typical Noise Ratio vs. IF Frequency and Bias Current Showing Typical Hot Carrier and Point Contact Diodes.

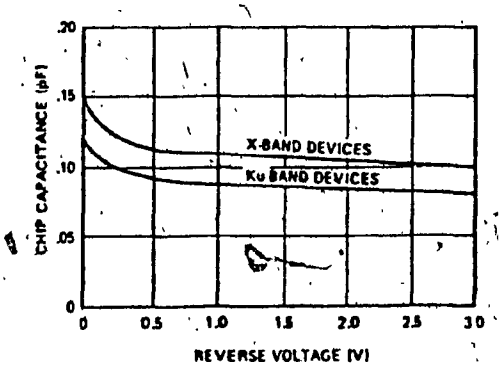

Figure 6. Typical Chip Capacitance vs. Reverse Voltage.

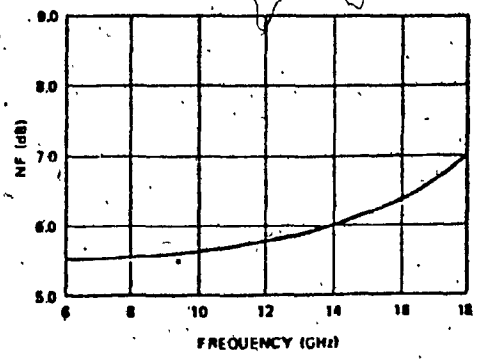

Figure 7. Typical Single Sideband Noise Figure vs. Frequency, 5082-2723, IF = 30 MHz, NF_{IF} = 1.5 dB, P_{LO} = 1 mW.

Mechanical Specifications

The HP outline 44 is a symmetrical, microminiature, hermetically sealed ceramic package. Both flanges are gold plated kovar. The anode contact is made by a thermocompression bonded gold wire or mesh. The maximum soldering temperature is 230°C for 5 seconds.

The HP package 49 is a hermetically sealed double stud ceramic package. The anode and cathode stud are gold plated kovar. Stud-stud TIR is 0.010 inch maximum.

Environmental Capabilities

The HP packages 44 and 49 have been designed to have the environmental capabilities as outlined in MIL-STD-750 with the following conditions:

TEST	METHOD	CONDITIONS
Temperature, Storage	1031	See maximum ratings
Temperature, Operating	1026	See maximum ratings
Temperature, Cycling	1051	5 cycles, −65°C to +125°C
Thermal Shock	1056	5 cycles, 0°C to +100°C
Moisture Resistance	1021	10 days, 90-98% RH, −10°C to +65°C
Shock	2016	5 blows, X_1, Y_1, Y_2 at 1500 G
Vibration Fatigue	2046	32 hours each X, Y, Z at 1500 G
Vibration Variable Frequency	2056	Four 4 minute cycles, X, Y, Z at 20 G min 100 - 200 Hz
Constant Acceleration	2006	1 minute each X_1, Y_1, Y_2 at 20,000 G